JAERI-Review
97-010

JAERI TANDEM & V.D.G. ANNUAL REPORT 1996

(April 1, 1996 - March 31, 1997)

September 1997

Department of Reactor Engineering

日本原子力研究所
Japan Atomic Energy Research Institute

本レポートは，日本原子力研究所が不定期に公刊している研究報告書です。
入手の問合わせは，日本原子力研究所研究情報部研究情報課（〒319-11 茨城県那珂郡東海村）あて，お申し越しください。なお，このほかに財団法人原子力弘済会資料センター（〒319-11 茨城県那珂郡東海村日本原子力研究所内）で複写による実費領布をおこなっております。

This report is issued irregularly.
Inquiries about availability of the reports should be addressed to Research Information Division, Department of Intellectual Resources, Japan Atomic Energy Research Institute, Tokai-mura, Naka-gun, Ibarakiken 319-11, Japan.

編集兼発行　日本原子力研究所
印　　刷　ニッセイエブロ株式会社

JAERI-Review 97-010

JAERI TANDEM & V.D.G.
Annual Report
1996
April 1, 1996 - March 31, 1997

Department of Reactor Engineering※

Tokai Research Establishment
Japan Atomic Energy Research Institute
Tokai-mura, Naka-gun, Ibaraki-ken

(Received August 19, 1997)

This annual report describes research activities which have been performed with the JAERI tandem accelerator and the Van de Graaf accelerator from April 1, 1996 to March 31, 1997. Summary reports of 48 papers, and list of publications, personnel and cooperative researches with universities are contained.

Keywords: JAERI tandem, V.D.G., Nuclear Structures, Nuclear Reaction, Nuclear Theory, Atomic Physics, Solid State Physics, Radiation Effects in Materials, Progress Report

---

※Editors : Suehiro TAKEUCHI, Hiroshi IKEZOE, Akira IWAMOTO, Masao SATAKA, Yuichiro NAGAME, Tokio SHOJI, Takashi OKABE and Hiroshi MAEKAWA

原研タンデム、バンデグラフ加速器
１９９６年度年次報告

日本原子力研究所東海研究所
原子炉工学部※

(1997年８月19日受理)

本年次報告は、原研タンデム及びバンデグラフ加速器で、1996年４月１日から1997年３月31日までの間に東海研で行われた研究活動をとりまとめたものである。

(1) 加速器の運転と開発研究 (2) 核構造 (3) 核反応 (4) 核理論 (5) 原子分子物理・固体物理及び材料の放射線効果の５部門にまたがる48編の研究報告、公表された文献、関与した職員及び大学等との協力研究のリストを収録している。

東海研究所：〒319-11 茨城県那珂郡東海村白方白根2-4
※（編集者）竹内末広・池添 博・岩本 昭・左高正雄・永目諭一郎・荘司時雄・岡部 隆
前川 洋

PREFACE

This report covers research and development activities using the tandem accelcrator and its superconducting booster at JAERI, Tokai, during the period from April 1, 1996 to March 31, 1997. During this period, the tandem accelerator was operated over 5200 hours and delivered stable beams to the experiments in the fields of accelerator development, nuclear structures, nuclear reactions, atomic physics, solid state physics and radiation effects in materials. For 35 days out of the beam time of over 230 days, the superconducting booster was used for experiments. Nineteen research programs have been carried out in collaboration with a hundred researchers from universities and national research institutes.

A result obtained out of the experiments was an identification of neutron-rich rare-earth nucleides ^{165}Gd (10.3 ± 1.6 s) and ^{161}Sm (4.8 ± 0.8 s) and neutron-deficient americium nucleide ^{236}Am (4.4 ± 0.8 min), for which the gas-jet coupled JAERI-ISOL was used. In addition, a new isotope ^{212}Pa (5.1 +6.1/-1.9 ms) was synthesized using the JAERI recoil mass separator. Heavy ion irradiation experiments with high Tc superconducting materials started in the booster target room for a study of pinning effects on magnetic flux, as an irradiation chamber was completed.

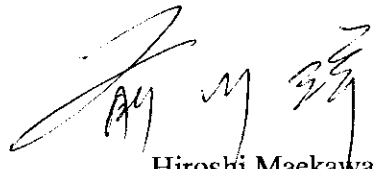

Hiroshi Maekawa
Deputy Director
Department of Reactor Engineering

Contents

1. Accelerator Operation and Development

I. 1 TANDEM ACCELERATOR AND BOOSTER OPERATION

ACCELERATORS OPERATION GROUP

Tandem Accelerator and Booster: The scheduled operations of the tandem accelerator for experiments were performed through the past one year. There were two short periods of scheduled maintenance. The running time was 5260.4 hours. The summary of the operation from April 1, 1996 to March 31, 1997 is as follows.

1) Time distribution in terms of terminal voltages (Tandem accelerator)

>16 MV	26 days	11.3 %
15-16	100	43.3
14-15	20	8.7
13-14	21	9.1
11-12	19	8.2
11-12	19	8.2
10-11	22	9.5
9-10	1	0.4
8-9	0	
<8	6	2.6

Booster operation

^{33}S	600 MeV	2 days
^{58}Ni	281	7
^{74,76}Ge	550-651	14
^{90}Zr	340-430	10
^{127}I	510-650	2

2) Time distribution in terms of projectiles

^{1}H (2H,3H)	52 days		^{35,37}Cl	11days	
^{6,7}Li	28		^{54,56}Fe	2	
^{11}B	4		^{58,60}Ni	32	
^{12,13}C	2		^{74}Ge	15	
^{16,18}O	5		^{79,81}Br	1	
^{19}F	4		^{90}Zr	10	
^{27}Al	5		^{107}Ag	2	
^{28,30}Si	23		^{127}I	8	
^{31}P	9		^{197}Au	5	
^{32,33}S	11				

3) Time distribution in terms of activities

Operation for research		231 days
Atomic and solid state physics	(39.7)	

Radiation effects in materials	(13.8)	
Nuclear chemistry	(35)	
Nuclear physics	(116)	
Fast neutron physics	(22)	
Radiation chemistry	(0)	
Detector development	(2	
Accelerator test operation	(2.5)	
Voltage conditioning		2
Scheduled maintenance(2 tank openings)		77
Unexpected repair with tank opening		9
Training of operation		2

The tandem accelerator had an unexpected tank opening at the end of August due to a trouble of the power generator in the shorted section. After 9 days cancellation of the scheduled-experiments, the accelerator was operated until 24th in October. The tandem booster and the helium refrigeration system were operated 3 periods during 3 scheduled machine time periods. There are some small troubles on the control computer system, SattCon 31 computer manufactured in Sweden, which is a module type small computer. The control system was recovered immediately by exchanging a control circuit board. Some control valves for liquid helium distribution to the cryostats sometimes ran in the wrong. The trouble of the distribution valves was a little bit serious, because it was due to lack of reliability of electronic circuits and piezo electric valves. Before resuming refrigerator operation, we always checked up all the valves of the cold boxes and the liquid helium distribution lines.

The helium refrigeration systems were in operation for 22 days from May 23 in 1996, 31 days from August 13 and for 76 days from January 14 in 1997. During these times, the super-conducting booster was utilized for 35 days for 12 experimental subjects. The booster ran steadily in every operation. The accelerating field gradients of the super-conducting resonators were between 2.9MV/m and 4.2MV/m.

An irradiation chamber for solid-state physics was installed in the middle of this fiscal year, and irradiation experiments for the super-conducting materials were carried out with high energy heavy ions from the tandem booster.

2MV Van de Graaff accelerator: The 2MV Van de Graaff accelerator was operated for 285.3 hours from April 1,1996 to March 31,1997. The main research subjects were solid state physics, atomic and molecular physics, and material science.

1. 2 IMPROVEMENTS FOR THE JAERI TANDEM SUPERCONDUCTING BOOSTER

S. TAKEUCHI and M. MATSUDA

The superconducting booster for the JAERI tandem accelerator has been running well without serious troubles since its completion in 1994. There are, however, some points which we want to improve.
1) Some resonators are suffering from *Q-disease*(resonator Q degradation due to an increase of rf surface resistance with niobium hydride precipitation)
2) Beam transmission was frequently much lower than the expected value of 60%(the bunching efficiency).
3) A low-β resonator section is necessary to accept and boost efficiently very heavy ions from the tandem accelerator.
The point 3) is a big improvement project we want to do for the booster, which is to instal low-β(v/c=0.06) superconducting resonators into the entrance part of the booster linac. The low-beta section allows to accelerate very heavy ions like Pb without multiple steps of electron stripping in the tandem accelerator. There are strong demands for such very heavy ions, such as from a group of gamma-ray spectroscopy. We, however, postponed a fabrication plan of a prototype resonator in FY 1996 for some reasons. We rather decided to concentrate ourselves to the intallation project of a compact ECR(electron cycrotron resonance) ion source into the high voltage terminal of the tandem accelerator. This project is reported elsewhere in this annual report. several kinds of very heavy ions can be boosted without the low-beta section. several kinds of very heavy ions can be boosted without the low-beta section. Several kinds of very heavy ions can be boosted without the low-β section, if their charge states are higher than those after an electron stripper at the high voltage terminal in the usual tandem acceleration mode.

Following are the improvements we did in the fiscal year of 1996:
1) *Q-disease problem* : The Q degradation is due to hydrogen absorption in their chemical surface treatment and niobium-hydride precipitation which occurs approximately between 130 K and 90 K in the precooling process. Two of the 40 resonators in the booster linac were severely damaged in their on-line performance with this problem. We were forced to operate them at a field gradient of 2.0-2.5 MV/m. About 14 resonators could be operated at 3.5-5.0 MV/m. Those are installed in the first four cryo-modules. The rest 24 resonators are not affected by the Q-degradation, fortunately. There are two methods of recovering high Q; (a) One is to precool the resonators as fast as possible over the temperature range of 130K to 90K. The fast cooling is effective in preventing absorbed hydrogen from precipitating as a form of niobium-hydride on the niobium resonator surface; that is, in preventing a large increase of rf surface resistance. (b) The other one is to extract hydrogen out of the niobium.
(a) The cryogenic system of the booster is composed of two identical refrigerators. Cooled helium gas parallely flows into six or seven cryo-modules, in each of which four resonators are housed and cooled in series. Cooling rate can be improved if all the cooled helium gas flow is limited to a group of fewer number of cryo-modules. All the resonators can be cooled fast over the temperature region of 130 K to 90 K by switching the flow group after group. Such a sequential cooling method was carried out for the first five cryo-modules of the booster linac. The cooling rate (in average) was, as a result, improved to -20 K/h for 3 cryo-modules and to -28.5 K/h for 2 cryo-modules, from -12K/h for the normal cooling. Averaged resonator Q values except the severely damaged two resonators were, respectively, recovered to 64% and 74% of those obtained at a rapid cooling rate as fast as or faster than - 40 K/h in off-line testing. With respect to the field gradients, a clear result was not obtained because electron field emission at high field gradients has been increasing with increasing particles on the resonator surfaces as time elapsed.
(b) Various trials except heat treatments were made to extract hydrogen from hydrogen polluted niobium using a spare resonator and niobium samples, but resulted in no effect. A heat

treatment above 600 C is not applicable for our resonators because their outer cans are made of niobium and copper composite materials. The next or the last trial would be to partially heat the center conductor part in vacuum without heating the outer can.

2) *Beam transmission* : Misalignment was most likely to worsen the beam transmission from our experimental result that beams were steered away from the axis by quadrupole lenses and resonators. After improving the alignment set of laser beams and position detectors, the positions of the quadrupole lenses and cryo-modules(resonators) were carefully measured and many of them were found to be misplaced as much as 2 mm. After correcting them, the beam transmission was improved to more than 80% of the theoretically expected value.

3)*RF power increase* : A hundred watts rf power amplifires which have been placed by the resonator control stations in the rf control room are not powerfull enough to control the resonators stable in case of loosing helium pressure stability. Their output power were increased to more than150W by tuning them up. The amplifires were also made remote controllable in order to change their position to the sides of the cryo-modules. These changes can increase allowable forwarding rf power at input couplers from 80W to 135 W to widen a phase control band width. There is an additional advantage that a loud noise from the amplifire's cooling fans vanishes from the rf control room.

4)*Beam/Resonator phase prediction* : Beam and resonator phases for different heavy ions can be predicted from calculation, if field gradients, resonator positions, rf signal propagation times and respective linearity of amplitudes and phases to their setting values of the controllers have been accurately measured. It is not so easy to keep accurate values for all the parameters. We, however, dared start trying such a prediction, because from the work we could extract some useful knowledge about the beam dynamics and the rf system of the booster. For example, we learned that velocity changes in the resonators and beam spread in the longitudinal phase space have to be taken into account in the beam phase calculation at an incident velocity much smaller than the optimum beam velocity of 0.1c for the booster resonators. The work is developping as a theoretical and experimental program.

5) *Others* : Problems in the cryogenic system and rf control stations were routinely cared for by S. Kanazawa et al, and I. Ohuchi et al, respectively. The systems were improving and running well. There were no serious troubles to report. A satellite control station of the tandem accelerator was developed by S. Hanashima, which was to be placed next to the resonator control stations. Resonator operation including conditioning was done mainly by N. Ishizaki and H. Tayama.

1. 3 ECR ION SOURCE FOR THE JAERI TANDEM ACCELERATOR

M. MATSUDA, S. TAKEUCHI and C. KOBAYASHI*

We have pushed forward a plan of an electron cyclotron resonance(ECR) ion source in the terminal of the JAERI tandem accelerator in order to increase beam intensity, beam energy and beam species. A compact ECR ion source, so called "NANOGAN" source [1], with a permanent magnet structure has been developed at GANIL, France, for accelerating the radio active ions. Its size and reliability are quite fitted to our plan. A way for stable acceleration of high intensity beams is expected to be opened by the use of the ECR ion source, since the beams from the source are in high charge states and with high intensity, and the operation without foil-strippers bring us no influence of a change of the terminal voltage on the charge state of the beams. In addition, it is possible to accelerate noble gas ions, which are impossible for conventional negative ion sources.

However, many difficulties have to be solved to install the source in the tandem terminal, such as the problems of the limited space, power supply, cooling system, RF source, vacuum system, control system, beam optics and so on. Some measures should be taken into consideration against electronic discharges and high pressure, because the source environment is on a high voltage of 16 MV and at the high pressure gas of 4.5 kg/cm^2·G. In spite of these difficulties, we could find some steps for solving above problems. The problems with the space, power supply and control system will be solved by the replacement of the Duo-plasmatron type ion source, which has been used, so far to the ECR ion source with some modifications. A TWT-type amplifier made for airplane is applied for the 10GHz RF source, and is set in the airtight vessel at the atmospheric pressure, for the vacuum system an ion pump encloses a gas flow. With an ion pump, ion extractions from the source were successfully examined for noble gases in accord with a small gas flow.

Several experiments with the ion source until now have proved the performance as expected. The optimum condition and the simplification of the operational parameters were searched on the assumption of installing the ion source in the tandem accelerator. The results of this experiment enabled us to reduce the six operational parameters to the three, which were the gas flow, bias voltage and the RF power. In this experiment, the gases used was previously mixed in the optimum and the RF tuner was fixed. This experimental procedure was brought from the experimental purpose, which was not to obtain maximum performance of the ion source, but to obtain stable intensity of ion beams against a change in the operational parameters. The gas flow, or, the vacuum of the system was the critical parameter for the stable operation. The results of the experiment for three gases, Ar, Kr and Xe, mixed with N_2 or O_2, are shown in Fig.1. The emittance for Ar ions from the above experiment was about 10mm·mrad·MeV$^{1/2}$ (80%) and its form profile was very complicate.

The arrangement of the ion source is planned as is shown in Fig.2. The ion beams extracted by 30kV from the ion source are focused by an einzel lens, and then the mass and charge of

* Nihon Advanced Technology. Co.

them are roughly selected by the 45° pre-analyzing magnet. The pre-analyzing magnet is used to reduce the load of the pre-acceleration, since the beams from the ion source amount to 2mA. The beams are accelerated again by a 80 kV pre-acceleration tube, and are finally led to the tandem accelerator tube after the desired beams are selected by the 45° analyzing magnet. Only a small part of beams are injected into the tandem after reducing the large emittance by several apertures.

Comprehensive examinations including the beam optics and the control system will be made in the near future prior to the installation in the high voltage terminal. The installation and the experiments with the ECR ion source will be carried out at the end of the next fiscal year. Acceleration of heavy metal ions is also considered as our future plan.

Reference

[1] P. Sortais et al., Proc. 12th Int. Work. on ECR ion sources, RIKEN, 1995, p.44.
[2] D. K. Olsen et al., Proc. 10th Int. Work. on ECR ion sources, Oak Ridge, 1990, p.1.

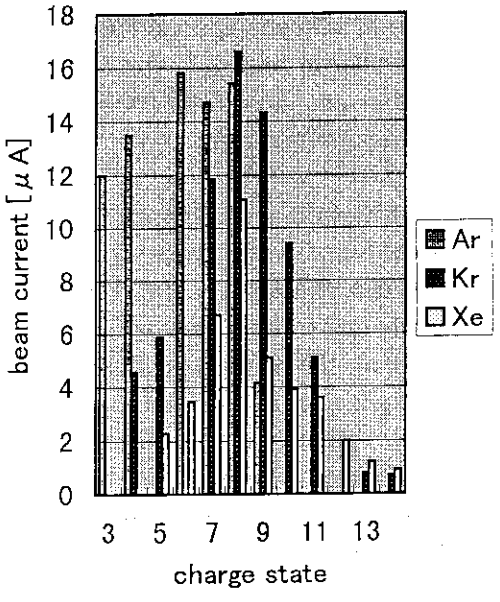

Fig. 1 Charge state distribution for three gases, Ar, Kr and Xe, mixed with N_2 or O_2.

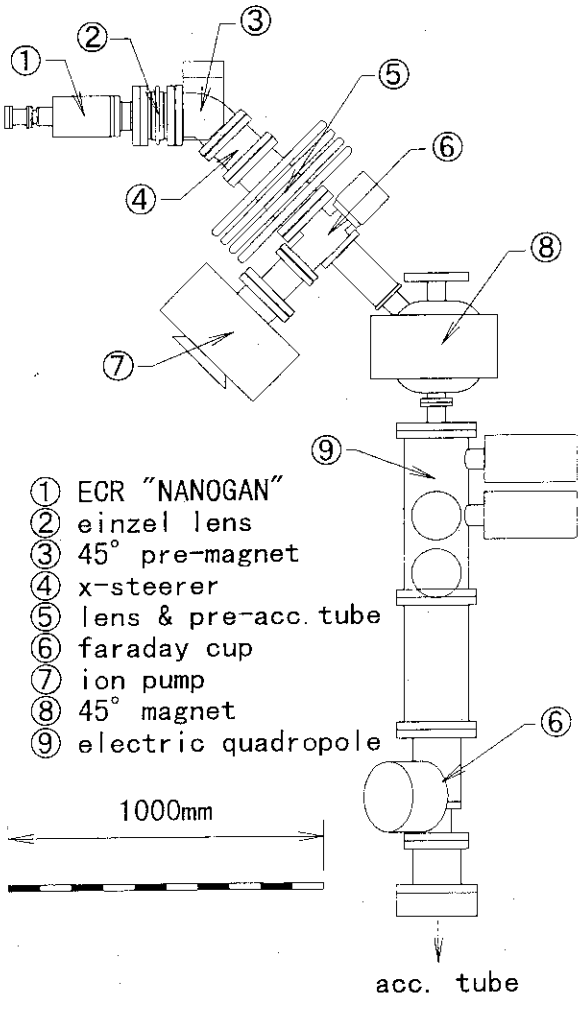

Fig. 2 Installation arrangement of the ion source.

1. 4 CONTROL SYSTEM FOR THE JAERI TANDEM ACCELERATOR

S.HANASHIMA

A control system of JAERI tandem accelerator is a concurrent processing system using several transputers[1,2]. In this fiscal year, we have made several improvements on the system. They are installation of the second control console, replacement of CAMAC serial highway drivers, an improvement of valuators on the control console, replacement of processor modules of the central multi processor etc. Figure 1 shows the configuration of the system.

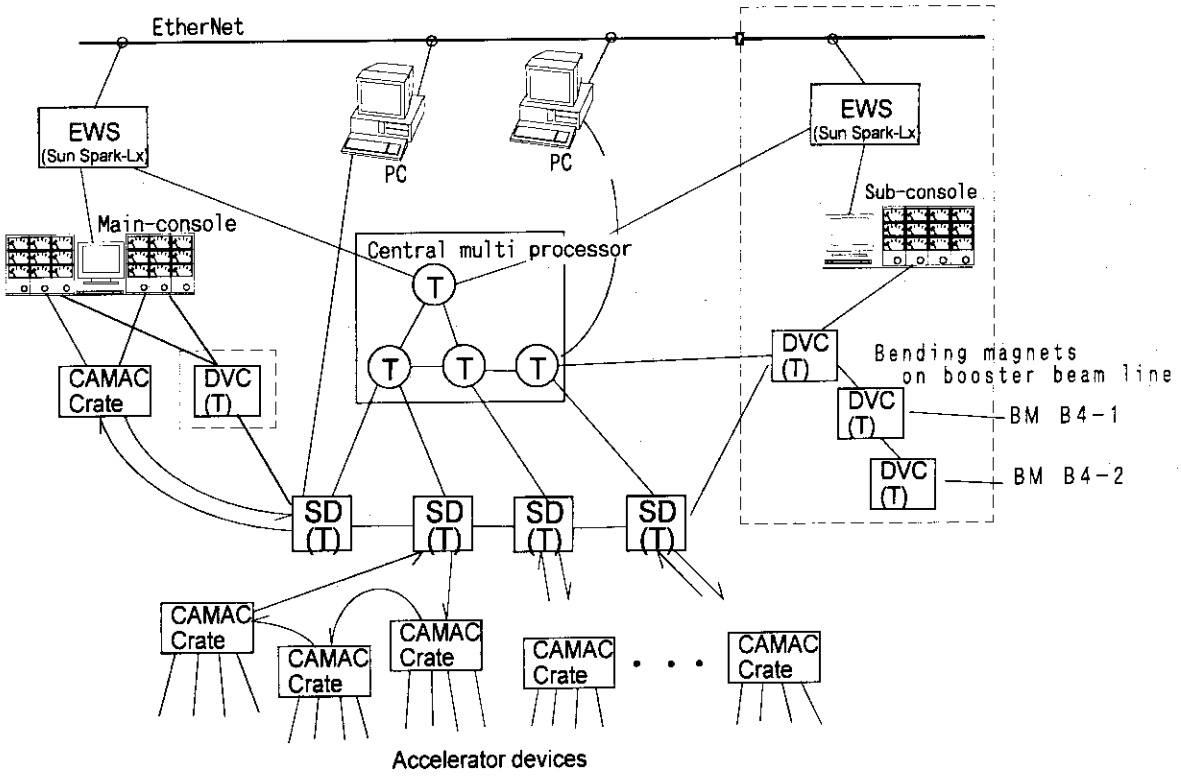

Figure 1. Configuration of control system for JAERI tandem accelerator :
T: transputer, SD:Serial highway driver,
DVC : Device controller. Dashed lines denote present expansion.

JAERI tandem accelerator has a post superconducting booster. The RF systems of the booster are controlled by dedicated control equipments which are independent of the control system of the tandem. It is the best choice to build a unified control system for both accelerators, for smooth operation of the two accelerators in the connected mode. But in our case, it was difficult because the control systems of the booster have been made independently from the control system of the tandem. As the second choice, we made a sub console of the tandem control in the RF control room of the booster. The console has a window display, eight assignable meter units and four assignable shaft encoders(valuators). We can control the tandem from the console in the same way as from the main console. The window display is controlled by an engineering workstation. The other part of the console is controlled by a transputer. Both processors are linked to the central processor of the control system through optical fibers. Adding to the fiber link, the workstation has connection to an Ethernet of the control system.

The serial highway drivers[3] are located at the front ends of the control processors to CAMAC serial highway system. We have developed a new type of driver to improve reliability and performance. The new drivers are separated into two parts, a control processor and one or more

serial highway interfaces. The interfaces perform much of the functions which have been done by the software in the old driver. These functions are generation and analysis of message packets and displaying highway error status on the front panels. The control processor controls the interfaces through a simple field bus. We can install several interfaces on the bus. The driver can control byte serial transfer, which our old drivers could not control. The major parts of the logic circuits are implemented in an FPGA(field programmable gate array).

The valuators on the control console are modified to accept a change in values crossing zero. A setting value of the valuator follows linearly to the rotation of the dial in the new specification. This modification enables natural control of beam steerers on a beam line of the accelerator. The old ones had an exponential control and could not allow crossing zero.

The central multi processor is the main engine of real time processing of the control system. Four transputer modules are connected together to construct the multi processor. New modules were made using almost same transputers(T805) as the previous modules, but their reliability on signal connections was greatly improved.

Controls of two bending magnets on the booster beam line have been included in the control system. They are controlled through device controllers using transputers. We intend to introduce local feed back control of magnetic fields using the controllers.

According to the change of the hardware configuration of the system, software of the system was modified at several points. They are an address scheme of data points of devices around the accelerator, protocols between the central system and the front end processors, programs of serial highway drivers etc. The programs were expanded to accept two control consoles and data points directly controlled by transputers.

References

1)S.Hanashima, JAERI TANDEM & V.D.G. Annual Report 1993 pp7-8.
2)S.Hanashima et al., Transputer/Occam Japan 5 IOS Press, 1993 pp69-81.
3)S.Hanashima, JAERI TANDEM & V.D.G. Annual Report 1995 pp7.

2. Nuclear Structure

2. 1 ISOTOPE SHIFTS OF OPTICAL TRANSITIONS IN SINGLY-IONIZED CERIUM

Y. ISHIDA[1], H. IIMURA, S. ICHIKAWA and T. HORIGUCHI[1]

Precise and systematic studies of hyperfine structure (HFS) and isotope shift (IS) of optical transitions provide the information of nuclear moments and changes of mean-square charge radii. The IS has been investigated in isotopic chains of various elements [1]. These investigations are of particular interest in the region of light rare earth elements because they give the opportunity to study the effect of neutron shell closure at N=82. Also, other nuclear structural changes are expected for the neutron-rich isotopes in this region. The chain of Ce isotopes seems to be favorable for these studies.

In this work, we newly measured the IS's of seven optical transitions in singly-ionized Ce for all stable isotopes by collinear laser-ion-beam spectroscopy. The changes of mean-square charge radii were determined from the IS's obtained in this work.

Figure 1 shows a schematic view of the apparatus. A single-mode tunable dye laser with a wavemeter (Coherent 699-29) and rhodamine 6G dye was pumped by an Ar-ion laser (Coherent INNOVA-100-20). A part of the laser beam was used for the polarization spectroscopy of $^{127}I_2$ which provided an absolute frequency reference with simple optical arrangement. Since a spectrum of only one Ce isotope can be taken at a time, it is necessary that the $^{127}I_2$ HFS spectra act as a reference for data on different isotopes. A temperature-stabilized confocal Fabry-Pérot interferometer (FPI) was used to calibrate the relative frequency of spectral lines. A Ce^+ ion beam was produced by using a surface ionization ion source. Samples with natural abundance (^{136}Ce: 0.19%, ^{138}Ce: 0.25%, ^{140}Ce: 88.5%, ^{142}Ce: 11.1%) were used in the form of oxides CeO_2. The ions were accelerated to 40 keV and mass-separated by an analyzing magnet. The counter-propagating laser beam excited the Ce ions to the upper levels. The laser-induced fluorescence (LIF) was collected by an ellipsoidal mirror and detected by a cooled PMT (Hamamatsu R2256). Color glass filters (Hoya B-390) suppressed stray light from the laser beam. The interaction region was defined with a cage kept at a constant potential of -3 kV, and accelerated ions were Doppler-tuned to resonance with the

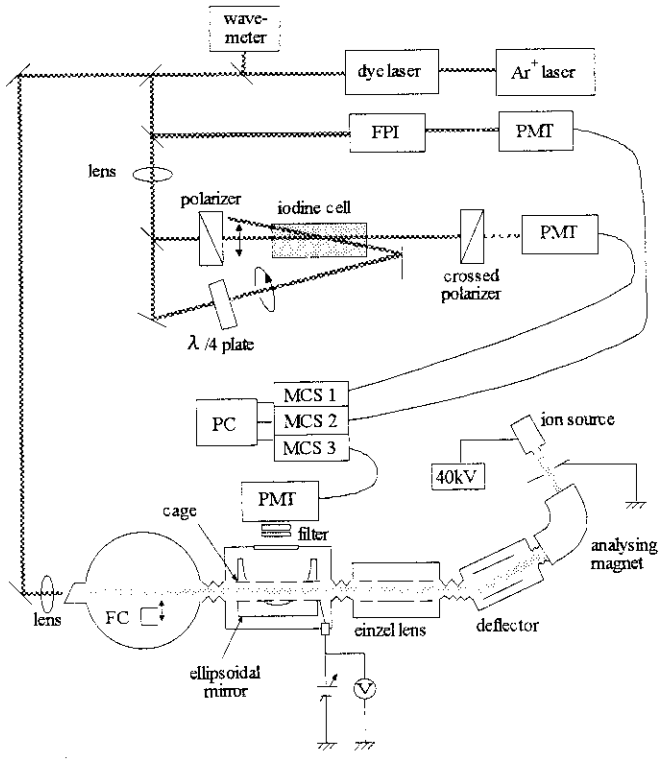

Fig. 1. Setup of the experimental apparatus.

[1]Department of Physics, Hiroshima University

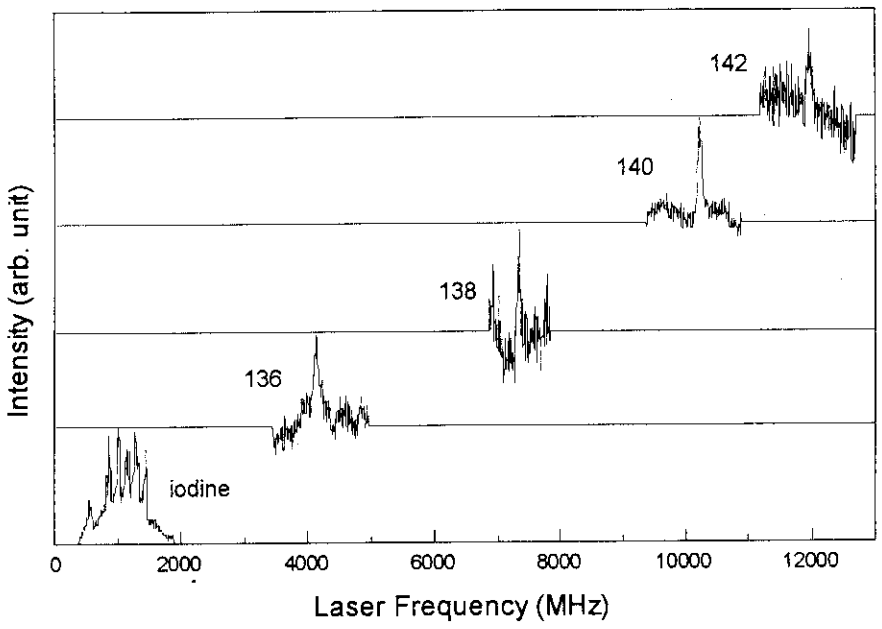

Fig. 2. Typical resonance peaks for the 570.0-nm transition. Four upper spectra with the mass number correspond to those of Ce. The lowest spectrum is the iodine HFS simultaneously measured with each Ce spectrum. The horizontal positions of the Ce spectra are determined by referring to one of the iodine HFS peaks.

laser frequency only inside the cage. Signals from the PMT's were simultaneously counted during the laser frequency scanning, and recorded by multichannel scalers controlled by a personal computer.

Seven optical transitions were measured in this work. The levels of Ce^+ are tabulated in Ref. [2]. The lower long-lived states are thermally populated. The upper levels mostly decay to the levels near the ground state emitting the photons of wavelength about 400 nm. Typical resonance peaks for the 570.0-nm transition are shown in Fig. 2. The spectra of stable isotopes of Ce have no HFS because their nuclear spins are zero. The observed linewidths of the Ce and $^{127}I_2$ peaks were about 100 MHz and 10 MHz full-width at half maximum, respectively. Relative frequency between each Ce peak and one of the $^{127}I_2$ HFS peaks was determined by comparison with the FPI spectrum. For each isotope, data were acquired from several scans, typically 15 GHz in width and lasting 450 seconds each. The observed shifts in the peaks of the Ce spectra were due to a combination of their IS's and different Doppler shifts. To obtain the IS, the contribution of Doppler shifts is subtracted from the observed shifts.

The IS is composed of the mass shift (MS) and the field shift (FS). The FS is induced by the finite nuclear charge distribution. The MS and the FS can be separated from the IS through the King-plot analysis. The changes of mean-square charge radii between stable isotopes were determined from the FS, and are listed in Table 1. The previous values are also listed in Table 1 for comparison. The values obtained in this work and those of other works including non-optical experiment [5] are in good agreement within the errors.

All the information obtained in this work may be useful for spectroscopic studies, such as the IS and HFS measurements of Ce radioactive isotopes. Work in this direction is in progress in our laboratory.

Table 1. Changes of mean-square charge radii $\delta \langle r^2 \rangle$ for the Ce stable isotopes.

$\delta \langle r^2 \rangle$ (fm^2)				
136-140	138-140	142-140	Method	Reference
-0.031(9)	-0.028(5)	0.282(11)	optical IS	this work
-0.026(4)	-0.032(3)	0.281(10)	optical IS	[3]
-0.015(6)	-0.021(4)	0.276(12)	review paper	[4]
——	——	0.274(10)	K X-ray IS	[5]

References

1) J. Billowes and P. Campbell, J. Phys. G **21** (1995) 707.
2) W. C. Martin, R. Zalubas and L. Hagan, Atomic Energy Levels — The Rare Earth Elements (US Government Printing Office, Washington DC, 1978).
3) Yu. P. Grangrsky, S. G. Zemlyanoi, N. N. Kolesnikov, B. K. Kul'djanov, K. P. Marinova, B. N. Markov, V. S. Rostovskii, Yu. G. Teterev, H. T. K. Hue and C. K. Tam, Sov. J. Nucl. Phys. **50** (1989) 757.
4) P. Aufmuth, K. Heilig and A. Steudel, Atom. Data and Nucl. Data Tables **37** (1987) 455.
5) C. W. E. van Eijk and M. J. C. Visscher, Phys. Lett. **33B** (1970) 349.

2. 2 LEVEL SCHEME OF ^{127}La FED BY THE ^{127}Ce ß-DECAY

H. IIMURA, S. ICHIKAWA, M. OSHIMA, J. KATAKURA, N. SHINOHARA,
M. MAGARA, A. OSA, M. ASAI[1] and H. YAMAMOTO[1]

Neutron-deficient nuclei in the A=120-130 mass region exhibit a transition from triaxial to prolate shapes, and thus they provide a good chance of testing various nuclear models. For the ^{127}La nucleus, in-beam γ-ray spectroscopic studies[1-4] were made to establish high-spin level structure, and several rotational bands were proposed. However, the level scheme of ^{127}La remains incomplete because the structure of low-spin levels has not been established. In the present work, we studied the level scheme of ^{127}La through the β-decay of ^{127}Ce ($T_{1/2}$=31 s) to clarify mainly the structure of low-spin levels. Recently a study of the ^{127}Ce β-decay by Genevey *et al.*[5] has also been made.

The experiments were performed by using the on-line mass separator at the tandem accelerator facility. The ^{127}Ce nucleus was produced by the reaction ^{nat}Mo(^{35}Cl,pxn)^{127}Ce with 185-MeV ^{35}Cl beam. Reaction products were ionized in a surface-ionization ion source, and mass-separated electromagnetically. In order to obtain ^{127}Ce activity free from the Cs and Ba isobars, the monoxide ions $^{127}Ce^{16}O^{+}$ were separated by setting the magnetic field at the mass number of 143. Gamma-ray singles and gamma-gamma coincidence measurements were made with HPGe detectors. To measure level half-lives, β-γ delayed coincidences were observed with a plastic scintillator and the HPGe detector. A simultaneous measurement of electrons and γ-rays was also made with Si(Li) and HPGe detectors to obtain internal conversion coefficients.

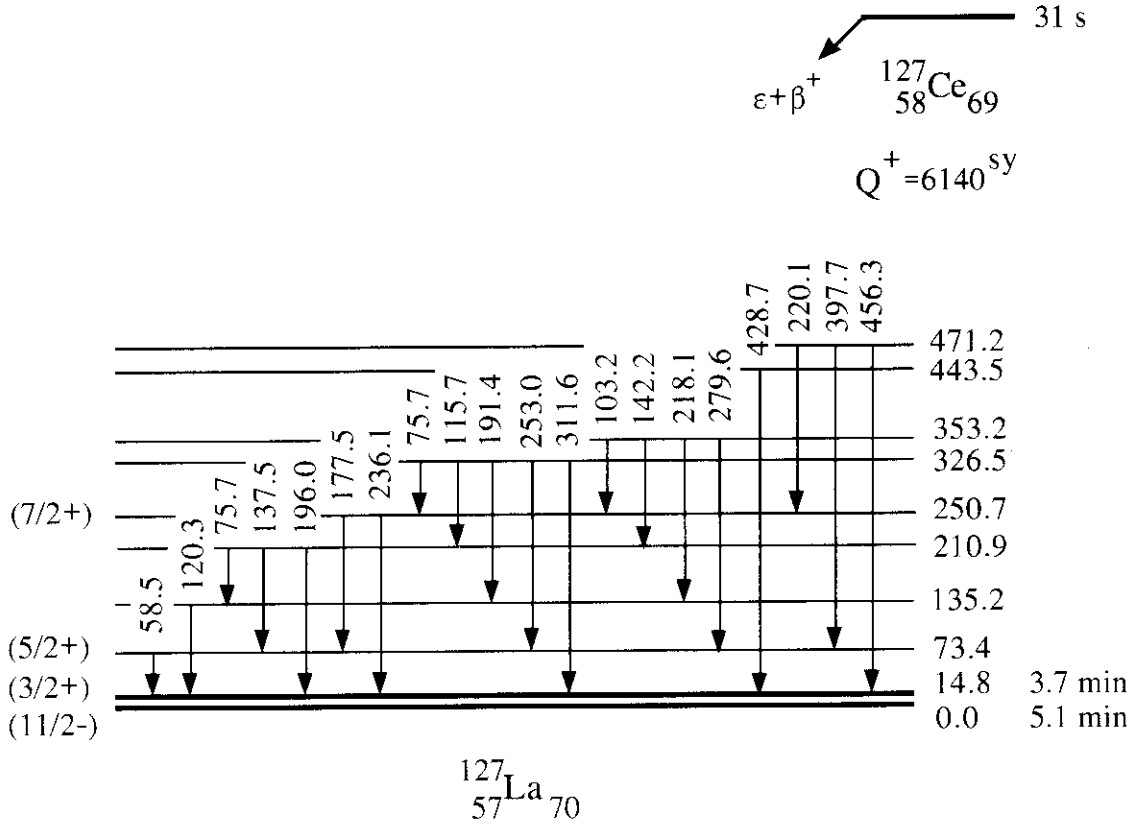

Fig. 1. Preliminary low-lying levels of ^{127}La populated in the decay of ^{127}Ce

[1]Department of Nuclear Engineering, Nagoya University

From the present measurements, a preliminary level scheme of ^{127}La has been obtained. The low-lying levels are shown in Fig. 1. The excited states were placed on the basis of the energies and coincidence relations of the γ-rays assigned to the decay of ^{127}Ce. The spins and parities are those of Nuclear Data Sheets[6]. From an in-beam γ-ray spectroscopic study, Ward *et al.*[3] proposed a 3/2+ band with 3/2+, 5/2+ and 7/2+ members at 14-, 73- and 249-keV, respectively. We confirmed this band as shown in Fig.1. Here, the band-head energy is from ref. 6. Other levels were not observed in in-beam studies and have been assigned in the level scheme both in this work and in the independent work of Genevey *et al.*[5]. The results from two β-γ spectroscopic studies are in good agreement except several differences. Further analysis is now in progress.

References

1) D.Ward *et al.*, Phys. Lett. **56B** (1975) 139.
2) P.J.Smith *et al.*, J. Phys. G**11** (1985) 1271.
3) D.Ward *et al.*, *Proc. Int. Conf. Nucl. Phys. In Our Times* (World Scientific, Singapore, 1993) p.218
4) K.Starosta *et al.*, Phys. Rev. C**53** (1996) 137.
5) J.Genevey *et al.*, Z. Phys., A**356** (1996) 7.
6) K. Kitao and M. Oshima, Nucl Data Sheets **77** (1996) 1.

2.3 COULOMB EXCITATION OF ^{155}Gd

M. OSHIMA, M. KIDERA,[1] Y. HATSUKAWA, K. FURUTAKA, T. HAYAKAWA, M. MATSUDA, H. IIMURA, H. KUSAKARI,[2] Y. IGARI,[2] M. SUGAWARA[3] and T. SHIZUMA[4]

In heavy-ion collisions it is well known that, when the surface-to-surface distance between two nuclei is larger than 3.5 fm, the interaction between the nuclei can be well described by the Coulomb force, and the nuclear force need not be taken into account. In this Coulomb excitation (COULEX) process, the excitation cross-section of a state can be calculated unambiguously from the $E\lambda$ matrix elements concerned. Due to the weak dipole correlation in atomic nuclei, *E2* excitation is the dominant excitation process. Thus, in a deformed nucleus, the ground band, whose members are connected by strong *E2* transitions with the ground state, is most strongly excited. So far there is no exception to this rule. Here, we show a new phenomenon of exceptionally strong population of the side band of ^{155}Gd, which has been observed in a Coulomb excitation experiment with a heavy-ion beam.

A ^{155}Gd target was bombarded with beams of 140-MeV ^{32}S, 240-MeV ^{58}Ni and 390-MeV ^{90}Zr from the tandem and booster accelerator. The target was a self-supporting metallic foil of 2.8 mg/cm^2, 91.8% enriched. The Coulomb-scattered projectiles were detected with two position sensitive silicon detectors. Gamma-rays in coincidence with the scattered projectiles were measured with a γ-ray detector array [1], which comprises 11 germanium detectors with BGO Compton suppressors. Figure 1 shows a level scheme of ^{155}Gd obtained in this experiment. The ground-state rotational band of ^{155}Gd is based on a Nilsson state of ν3/2-[521]. The positive-parity side band is composed predominantly of ν3/2+[651].
We observed members of the ground band up to $(31/2)^-$, where the 3 levels at 2137.7 keV, 2333.3 keV, and 2706 keV are newly assigned as $27/2^-$, $29/2^-$, and $(31/2)^-$ states, respectively. An interesting result is that the members of the positive-parity band were Coulomb excited up to $33/2^+$. Since the levels of this band are yrast, high-spin favored members of signature partners have already been established up to $(53/2^+)$ [2,3]. However, we could newly assign the unfavored members of $(27/2)^+$ and $(31/2)^+$ states at 1743.9 and 2335.0 keV, respectively.

The population of the side-band members transpired to be as large as the members of the ν3/2-[521] band. Since there is no strong feeding from the ground-band to the side-band members, the side-band members are considered to be populated via a direct COULEX process. Since the parities of the two bands are different, the side band members can be excited via *E1* or *E3* interband transitions. In order to evaluate the above excitation scheme we calculated the COULEX cross-section by taking into account *E2* strength for intraband transitions and *E1* and/or *E3* strengths for interband transitions. The former is derived from the previous work [4]. We adopted mostly the recommended upper limit [5] derived in a

[1]on leave from Kyushu University.
[2]Faculty of Education, Chiba University.
[3]Chiba Institute of Technology.
[4]Tandem Accelerator Center, Tsukuba University.

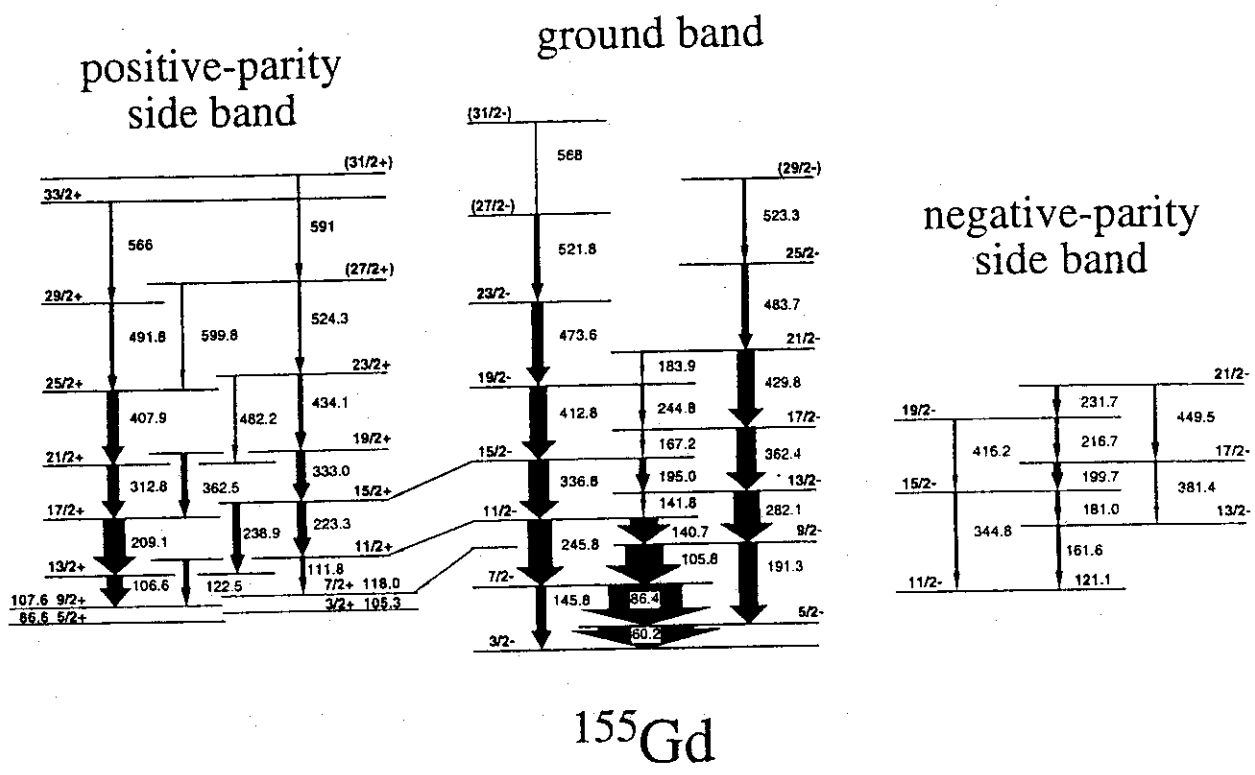

Fig. 1. A partial level scheme of ^{155}Gd.

compilation of the whole mass region for the latter, where the experimental values are not available. We used a computer code, *COULEX* [6], for this calculation. As a result, the excitation cross sections of the members of the side band were larger than those expected from the calculations, which took into account the recommended upper limits of *E1* or *E3* strengths. Such a large enhancement of the side band has not been reported so far. Further experiments will be performed to clarify the origin of this new phenomenon.

References

1) M. Oshima et al., Nucl. Instrum. and Meth. to be published.
2) G. Lovhoiden et al., Nucl. Phys. A148 (1970) 657.
3) M.A. Riley et al., Z. Phys. A 345 (1993) 121.
4) H. Kusakari et al., Phys. Rev. C 46 (1992) 1257.
5) W. Andrejtscheff et al., Atom. Data Nucl. Data Tables 16 (1975) 515; P.M. Endt, *ibid* 26 (1981) 47.
6) A. Winther and J. de Boer, in *Coulomb Excitation*, ed. K. Alder and A. Winther (Academic, New York, 1966) p.303.

2. 4 HIGH SPIN STATES OF ^{132}Cs

T. HAYAKAWA, J. LU[1], K. FURUNO[1], K. FURUTAKA, T. KOMATSUBARA[1], T. SHIZUMA[1], N. HASIMOTO[1], T. SAITOH[1], M. MATSUDA, Y. HATSUKAWA, M. OSHIMA

Nuclei in the mass A ~130 region are known to be γ soft and their shapes are influenced by quasi-particles in high-j orbitals. The nuclear shapes are affected by different shape-driving forces of low-Ω $h_{11/2}$ proton and high-Ω $h_{11/2}$ neutron. The high-spin states of odd-odd Cs nuclei has been studied both experimentally[1] and theoretically[2]. To extend the systematics of Cs isotopes, high spin states of ^{132}Cs have been investigated through in-beam spectroscopy. The nucleus ^{132}Cs was produced with the reaction ^{124}Sn (^{11}B, 3n) ^{132}Cs at a bombarding energy of 42 MeV with the Tandem accelerator at Japan Atomic Energy Research Institute (JAERI). The target consisted of a 1 mg/cm^2 layer of enriched ^{124}Sn on a thick Pb backing which served to stop the recoil nuclei. Gamma rays were detected with an array of 10 HPGe detectors with BGO Comptonsuppressors and a LEPS. A total of 2 $\times$ 10^8 γ - γ coincidence events were collected. The gated spectra were constructed from 4k $\times$ 4k matrix. The spin assignment was derived from DCO ratios. While J. -S. Tasi et al. [3,4] reported 17 low-spin excited states via ^{133}Cs(γ, n)^{132}Cs reaction, there was no information on high-spin states nor on γ transitions. Fig. 1 shows the level scheme of ^{132}Cs constructed from γ-γ coincidence relationships and intensity ratios. In this work, three new rotational bands with signature partner (1,2,3) and a stretched dipole band (4) were observed. The two rotational bands have negative parity and the other positive parity.The dipole transition band has been a topic of high-spin states in this region. Some dipole transition bands were found in odd-A Cs isotopes [4]. This is the first observation for doubly odd Cs nuclei.

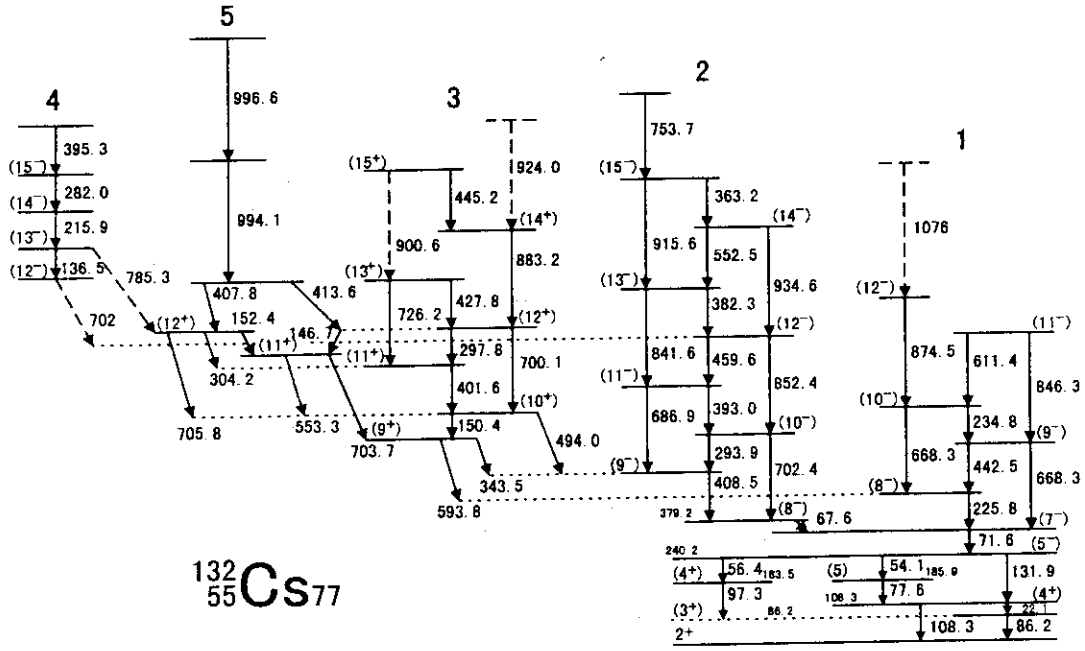

Fig.1 Level scheme of ^{132}Cs.

References

[1] T.Komatsubara, K.Furuno, T.Hosoda, J.Mukai, T.Hayakawa, T.Morikawa, Y.Iwata, N.Kato, J.Espino, J.Gascon, N.Gjørup, G.B.Hagemann, H.J.Jensen, D.Jerrestam, J.Nyberg, G.Sletten, B.Cederwall, and P.O.Tjøm: Nucl. Phys. **A557** (1993) 419c

[2] N.Tajima: Nucl. Phys. **572** (1994) 365

[3] J.-S.Tasi, W.V.Prestwich, and T.J.Lennett: Zeit. Phys. **322** (1985) 597

[4] R.B.Firestone, V.S.Shirley:Table of Isotopes 8th, Lawrence Berkeley National Laboratory, University of California(1996)

[1] Institute of Physics and Tandem Accelerator Center, University of Tsukuba, Ibaraki 305, Japan

2.5 YRAST SEQUENCES OF ^{62,64}Zn NUCLEI

K. FURUTAKA, H. NAKADA,[1] M. KIDERA,[2] M. MATSUDA, T. HAYAKAWA, Y. HATSUKAWA, T. ISHII, M. OSHIMA, S. MITARAI,[3] T. SHIZUMA,[3,4] M. SHIBATA,[3] H. WATANABE,[3] T. MORIKAWA,[3] T. KOMATSUBARA,[5] T. SAITOH,[5] N. HASHIMOTO,[5] H. KUSAKARI,[2] and M. SUGAWARA[6]

Since the numbers of neutrons N and protons Z are almost equal for nuclei in $A \sim 60$ region, several interesting phenomena are expected to occur, such as octupole correlation in ground states [1] and superdeformations [2–4]. However, the data have been rather scarce, because of difficulties in producing nuclei with $N \cong Z$ and in populating their high spin states. In order to study high spin states of these nuclei we have carried out an experiment using heavy ion beam and an array of Ge γ-ray detectors with a light charged particle detector array.

Experiment was performed at JAERI Tandem Accelerator facility. High spin states of ^{62,64}Zn nuclei were populated via the ^{28}Si+^{nat}Ca reaction at an incident energy of 120 MeV. ^{nat}Ca of 3 mg/cm^2 in thickness was used as a target, which was sandwiched between Au layers of 3 mg/cm^2 and 13mg/cm^2 to prevent oxidation and to stop the recoils. γ rays emitted in the reaction were detected with an array [5] of ten Ge detectors with BGO Compton suppressors, in coincidence with light charged particles (LCP) detected using a charged particle detector array with a large solid angle, Si-ball [6]. The data were sorted by LCP emission channels and for each channel a γ-γ correlation matrix was constructed.

The level structure of ^{62}Zn (^{64}Zn) was determined from the analysis of the γ-γ matrix for $2p1\alpha$ ($4p$) evaporation channel, considering γ-γ coincidence relationships and γ-ray intensities. Spins were determined from the analysis of DCO ratios of the γ rays in cascade. The proposed level schemes of these nuclei are shown in Fig. 1.

To understand structure of yrast sequences of these nuclei, the levels observed in the present study were compared with results of a shell-model calculation, which was done using the code VECSSE [7] in the $k \leq 3$ model space with $(0f_{5/2}\,1p_{3/2}\,1p_{1/2})^{A-56-k}(0g_{9/2})^k$. In Fig. 2 the shell model results as well as the observed yrast levels were shown. In the figure the solid points indicate the observed yrast levels, while the lines show calculated levels dominated by each of the $(0g_{9/2})^k$ $(k = 0, 1, 2, 3)$ configurations. According to the calculation, the coupling among the different k configurations is weak . The calculation reproduces the yrast levels quite well, including the negative-parity levels. From the figure, it can be clearly seen that these states are in shell-model nature, and the yrast states are characterized by the number of nucleons occupying the $g_{9/2}$ orbit.

[1]Chiba University
[2]Present address : RIKEN
[3]Kyushu University
[4]Present address : Tsukuba University
[5]Tsukuba University
[6]Chiba Institute of Technology

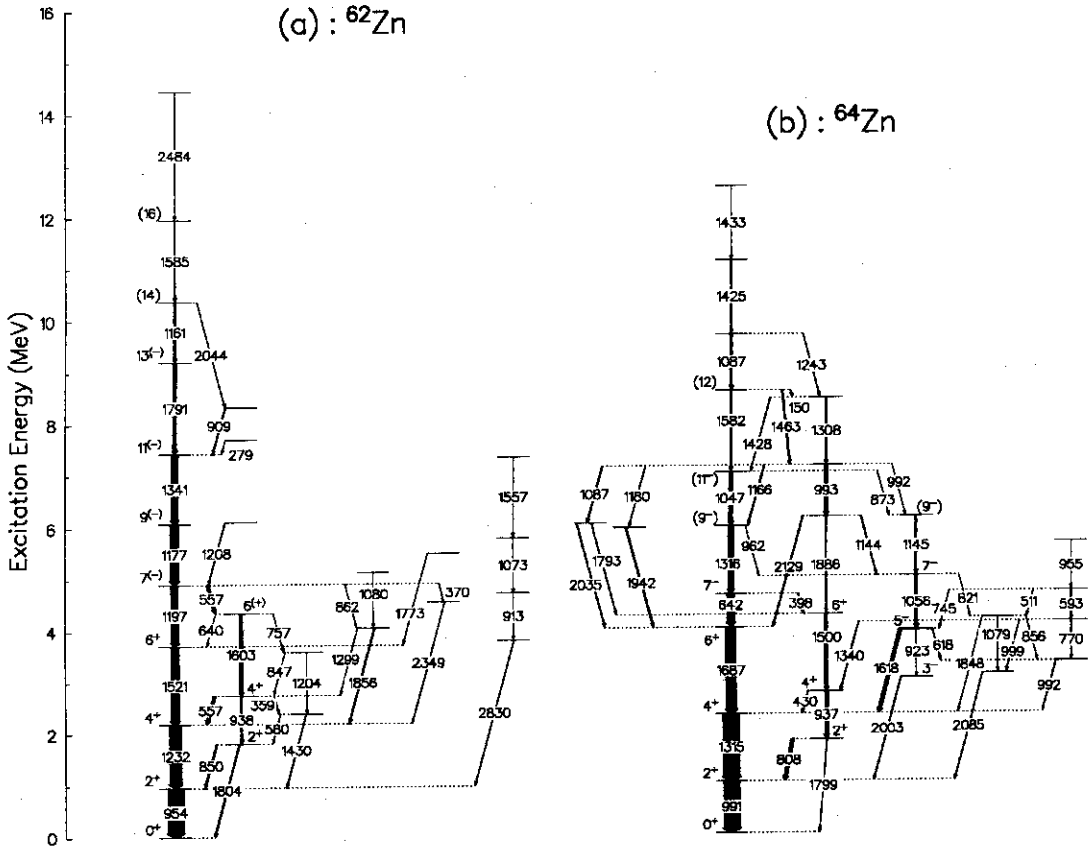

Figure 1: The proposed level schemes for (a)^{62}Zn and (b)^{64}Zn.

References

1) P. J. Ennis *et al.*, Nucl. Phys. **A535**, (1991) 392
2) T. Bengtsson *et al.*, Phys. Scr., **24**, (1981) 200-214
3) I. Ragnarsson *et al.*, Phys. Rep., **45**, (1987) 1-87
4) I. Ragnarsson, L.A.N.L. Report **LA-11964**, Oct. 1990
5) Oshima, M., *et al.*, to be published in Nucl. Instrum. Method Phys. Res. (1997)
6) T. Kuroyanagi *et al.*, Nucl. Instrum. Method **A316**, (1992) 289
7) Sebe, T., *et al.*: VECSSE, Program library of Computer Centre, University of Tokyo (1994).

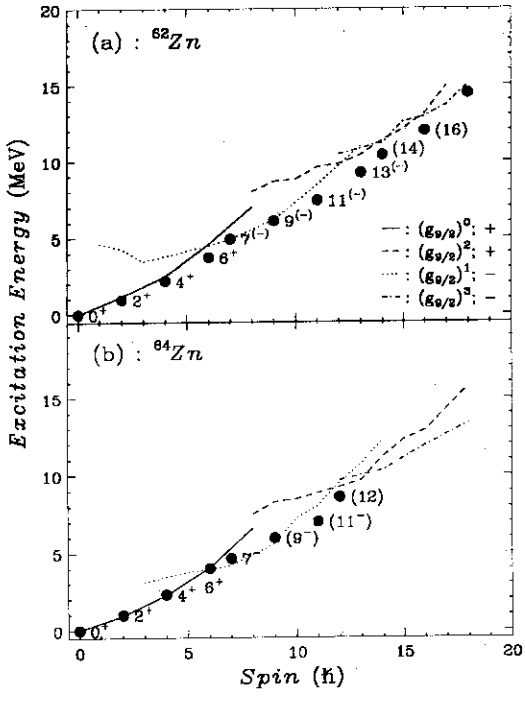

Figure 2: Comparison of the results of shell model calculation with experimenta data for (a)^{62}Zn and (b)^{64}Zn.

2.6 IN-BEAM SPECTROSCOPY OF ^{69}As

S. MITARAI[1], T. MORIKAWA[1], A. ODAHARA[1], H. TSUCHIDA[1], T. SIZUMA[2], T. SHIBATA[1], M. KIDERA[1], H. WATANABE[1], Y. GONO[1], J. MUKAI[2], M. OSHIMA, T. ISHII, Y. HATSUKAWA, K. FURUTAKA, T. HAYAKAWA, M. MATSUDA, T. KOMATSUBARA[3], E. IDEGUCHI[4],

The transitional nuclei around A=70 has revealed the interesting features, i.e. prolate deformation, oblate deformation and shape coexistence. Low lying states of ^{68,69}As were reported[1,2] because of the projectiles of light heavy ions(^{12}C,^{14}N,^{16}O,^{18}O) with low beam energies. In this experiment, high spin states of ^{68,69}As were polulated by the bombardment of ^{32,33}S-projectiles with 140 MeV beam energy on the ^{nat}Ca targets of thickness around 3mg/cm^2 with Au-backing(13 mg/cm^2). In-beam γ-γ coincidence measurement was carried out using JAERI mini crystal ball with 11 Anti-Compton Ge spectrometers in conjenction with the multiplicity filter for charged particles(Silicon ball) with 21 detector elements[3]. Lots of matrics with different combination of the detected charged particles are useful for removal of high multiplicity components from the specific matrix.

For example, a clean matrix for As isotopes(3p,3pn exit channels) was obtained as following:
[Clean As matrix] = (2p) + (3p) - 4.47(4p) + 5.0(5p) - 1.4(a2p) - 1.66(a3p) + (2ap) + (2a) + 10(a4p)
A symbol of (npma) corresponds to γ-γ matrix which is coincident with (n proton and m alpha) detection in Silicon ball.

Figure 1 shows a level sheme of ^{69}As which was constructed from the spectra gated on the clean matrix for As. In this experiment, a level scheme in ^{69}As includes 21 levels and 27 gamma rays. A strong cascade relation of 808, 1068, 1307 and 1471 keV γ rays is found, including a doublet of 1307 keV γ ray but is difficult to get the order of 1068, 1307 and 1471 keV gamma rays in the level scheme because of no braching gamma ray. Threfore, we put temporarily the order of the gamma rays in the scheme. Two rotational-like level sequnces have been found in ^{69}As isotope and one of them shows a backbending. A level scheme of ^{68}As obtained from this experiment is consistent with the most of the scheme in the recent paper[1] and added two gamma rays above the highest level.

References

1) A. Petrovici et al., Phys.Rev.C.53(1996) 2134
2) H.P.Hellmeister et al., Phys.Rev.C.17(1978) 2113
3) M. Oshima et al., submitted in Nucl.Instr.Meth.

1. Department of Physics, Kyushu University
2. Touwa University
3. Institute of Physics, University of Tsukuba
4. Institute of Physical and Chemical Research

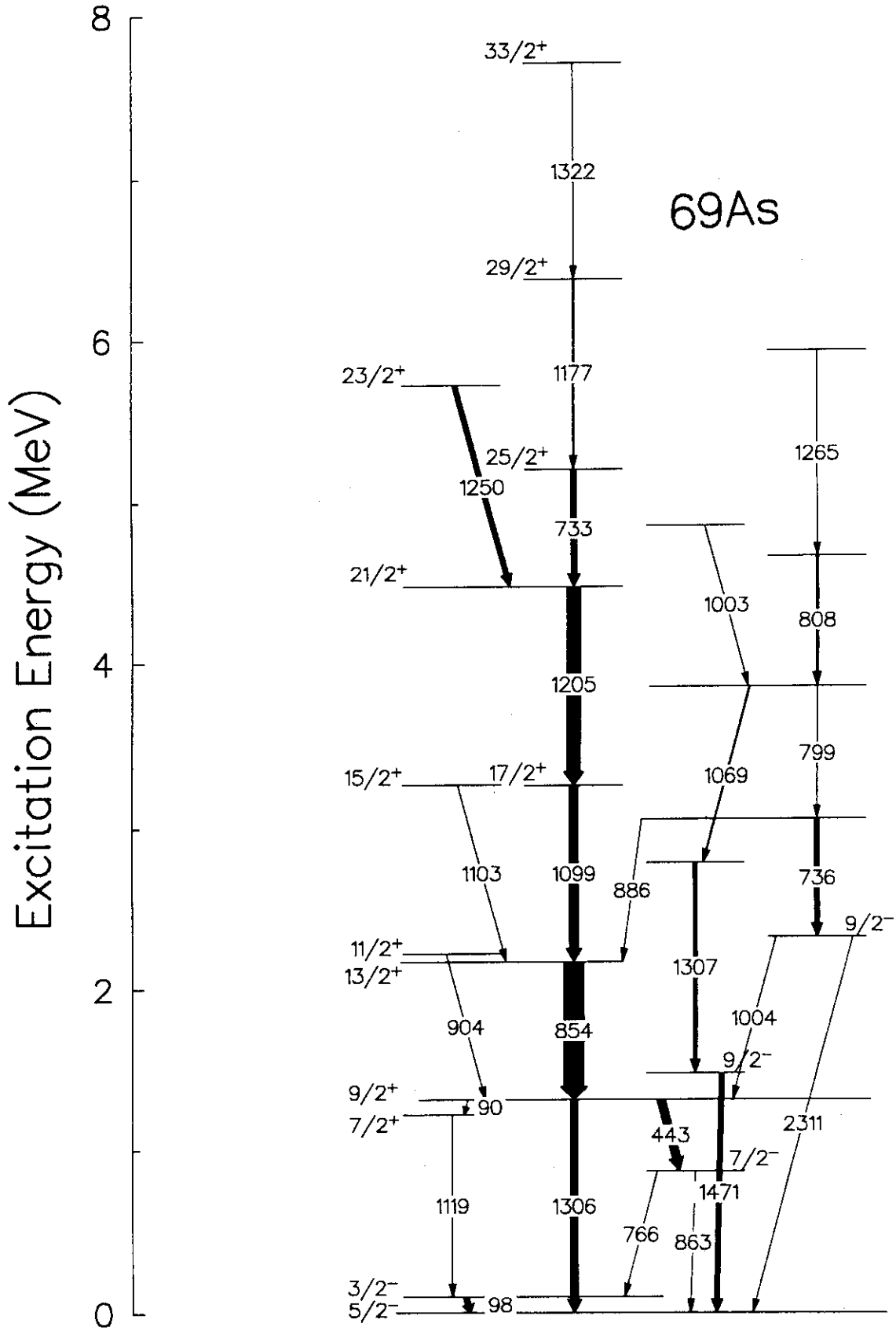

Fig. 1 The level schemes for ^{69}As obtained from the present work.

2. 7 HIGH SPIN STATES IN ^{61,63}Cu

Y. HATSUKAWA, T. HAYAKAWA, K. FURUTAKA, H. NAKADA[1], M. KIDERA[2], T. ISHII,M. OSHIMA, S. MITARAI[2], H. KUSAKARI[3], T. KOMATSUBARA[4], M. MATSUDA, M. SUGAWARA[5] and K. FURUNO[4]

The ^{61,63}Cu nuclei are close to the double magic nucleus ^{56}Ni, and their low-lying structures are known to be characterized by excitation of a few nucleons coupled with a double-magic core[1-4]. In our previous investigation[5], it was shown that the yrast sequences of ^{62,64}Zn can be characterized by the number of nucleons occupying the $g_{9/2}$ orbital. The aim of the present investigation is to extend the knowledge to the higher-spin state and analyze the yrast structures on the basis of large-scale shell-model calculations including the $g_{9/2}$ orbital.

To identify the g transitions in ^{61,63}Cu, experiments were carried out using a gold-backed Ca target with thickness of 300 μg/cm^2 in the tandem accelerator at the Japan Atomic Energy Research Institute. The target was bombarded with a 120 MeV ^{28}Si beam to populate states in the copper nuclei via the 3p1α(^{61}Cu) and 5p(^{63}Cu) evaporation channels. In-beam γ-rays were measured using an array[6] of 10 germanium detectors with BGO Compton suppressors in coincidence with the evaporated charged particles which were detected with a Si ball[7]. The Si ball selects the evaporation channels of the charged particles. The particle-g-g coincidence events were written event by event using magnetic tapes for an off-line analysis. The γ–γ coincidence relationships were derived from a coincidence matrix gated on the 3p1α(^{61}Cu) or 5p(^{63}Cu) evaporation channels.

Transition multipolarities was derived from DCO ratios, which were obtained from a γ–γ coincidence matrixes between the detectors at 90° and those at 31.5°. Level schemes of ^{61}Cu and ^{63}Cu, derived from this study, are shown in Fig. 1 and Fig. 2. The spin-parity and energy values in italics show the states and transitions newly assigned in this study. In the yrast sequence for ^{61}Cu, only the 1310 and 1409 keV γ transitions were known to be E2 and E1, respectively, from the previous investigations[1,2]. The 1361, 1038 and 1471 keV γ transitions were derived to be quadrupole(E2) transitions, while the 1112 keV γ transition to a dipole transition(M1 or E1). Since 1704 keV γ-ray is a doublet, the multipolarity of the high-lying 1704 keV γ-ray was determined in an analysis of the 529-1704 keV sequence. The 1869, 529 and 1704 keV transitions were assigned to be E2. The spins given are consistent with all available DCO results. We made a shell-model calculation in the $k \leq 3$ with the $(0f_{5/2}1p_{3/2}1p_{1/2})^{A-56-k}$ $(0g_{9/2})^k$ model space. The code VECSSE[8] was utilized.

In Fig. 3, the shell model results were compared with the experimental data for the yrast and near-yrast levels. The solid points indicate the observed levels, while the lines show the calculated levels dominated by each of the $(0g_{9/2})^k$(k=0,1,2,3) configurations. Note that the coupling is weak among the different k configurations. The calculation reproduces the yrast states quite well in the whole energy region under investigation. The crossing of the different k configurations accounts for the parity changes in the yrast levels, for example, $11/2^- \longrightarrow 13/2^+$.

1)Department of Physics, Chiba University, Chiba-shi, Chiba 260, Japan
2)Department of Physics, Kyushu University, Hakozaki, Fukuoka 812, Japan
3)Faculty of Education, Chiba University, Chiba-shi, Chiba 260, Japan
4)Department of Physics and Tandem Accelerator Center, University of Tsukuba, Ibaraki 305, Japan
5) Chiba Institute of Technology, Chiba 275, Japan

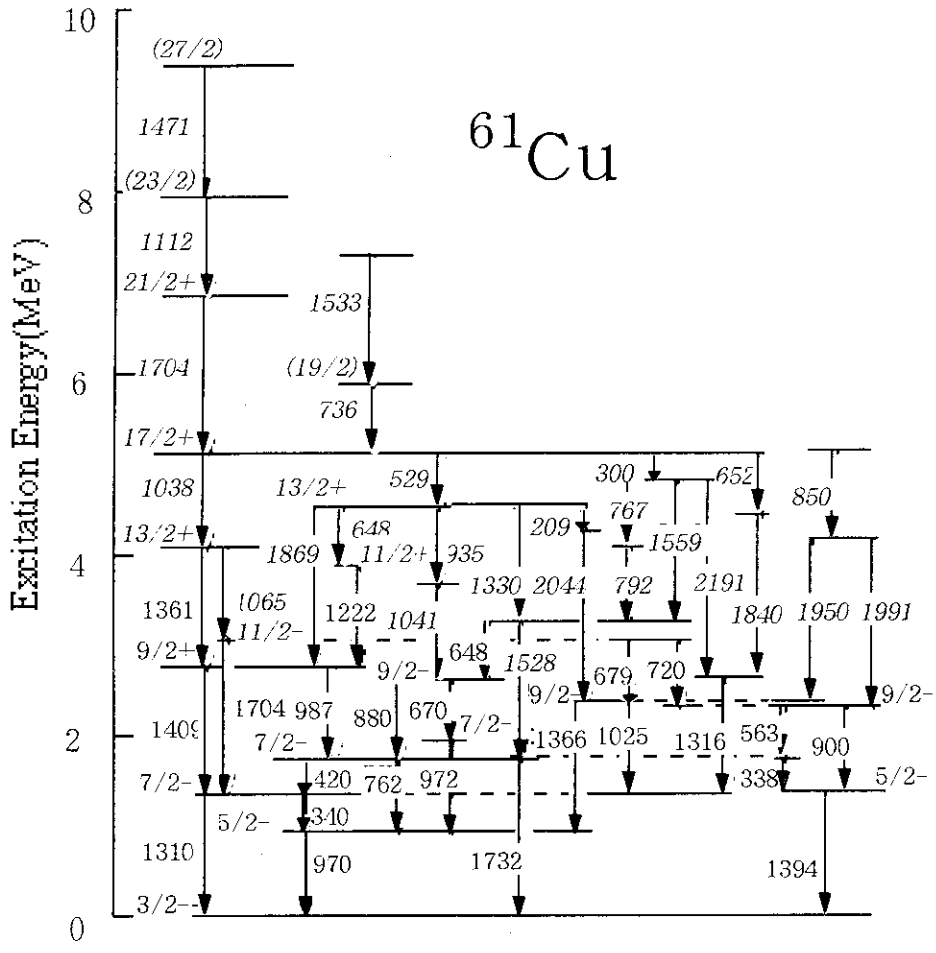

Fig.1 Partial level scheme of ^{61}Cu

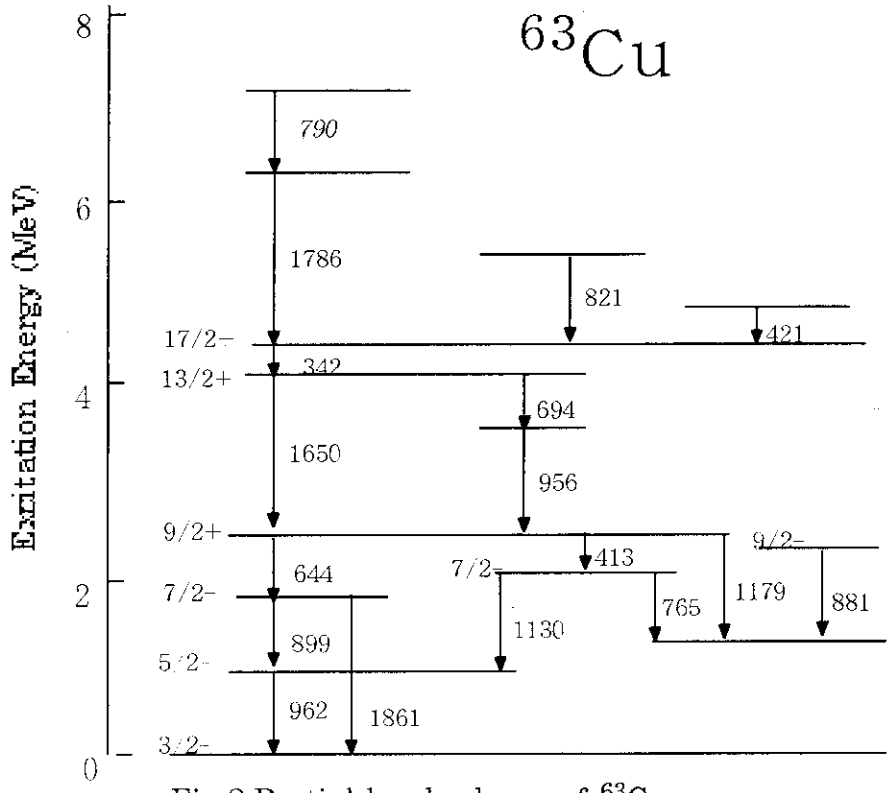

Fig.2 Partial level scheme of ^{63}Cu

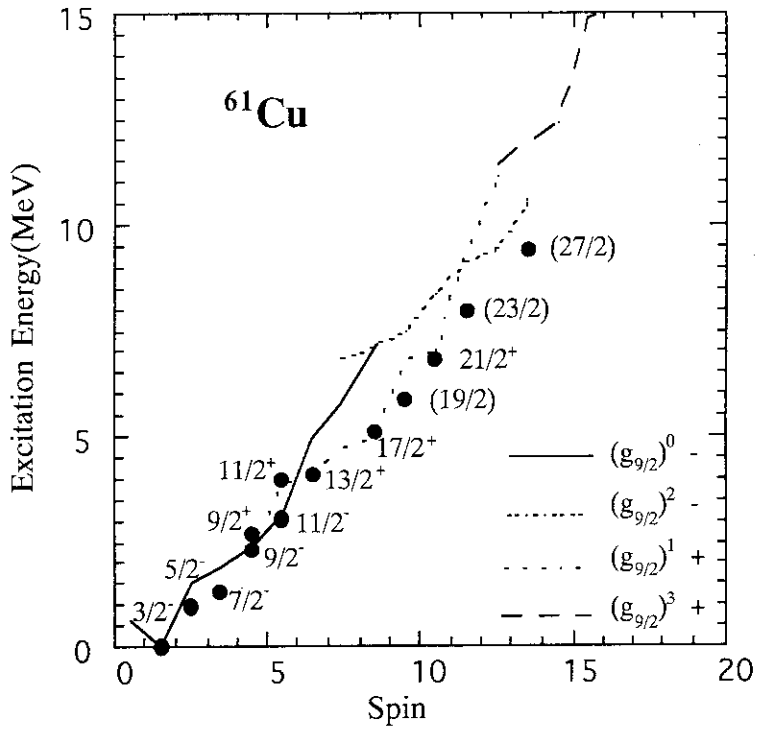

Fig.3 Comparison of the results of the shell model calculation with the experimental data for ^{61}Cu

It was suggested that the observed parity of the (27/2) level is negative. The ^{61}Cu nucleus has the more features in the yrast structure. It can be seen that strengths of γ-ray sequence concentrate at the yrast $17/2^+$ level. This fact seems to be related to the slope change within the k = 1 configuration in Fig. 3. According to the calculation, the $(f_{5/2}p_{3/2}g_{9/2})$ three-quasiparticle configuration is dominant at the $17/2^+$ level. The slope change at the $17/2^+$ originates in the structure change from the three-quasiparticle to the five-quasiparticle configuration. This structure change makes the $17/2^+$ state relatively low, in comparison with neighboring yrast states, as well as with the other 17/2 states. Thus, the yrast $17/2^+$ level is more predominate from the higher lying levels.

References

1) B. Heusch, et al., Nucl. Phys **A169**(1971) 145.
2) E. J. Hoffman, et al., Nucl. Phys. **A173**(1971) 146.
3) D. G. Sarantites, et al., Phys. Rev. **C8**(1973) 629.
4) L. P. Eckstrom and J. Lyttkens, Nucl. Data Sheets **38**(1983) 463;
Zhou Chunmei, Nucl. Data Sheets **67**(1992) 271.
5) K. Furutaka et al., Z. Phys in press. (1997)
6) M. Oshima, et al., to be published in Nucl. Instr. and Meth. Phys. Res. (1997).
7) T. Kuroyanagi, et al., Nucl. Instr. and Meth. **A316**, (1992) 289.
8) T. Sebe et al., VECSSE, Program library of Computer Centre, University of Tokyo (1994).

2. 8 DIPOLE BANDS IN ^{142}Gd

M.SUGAWARA[1], H.KUSAKARI[2], Y.IGARI[2], K.TERUI[2], K.MYOJIN[2], D.NISHIMIYA[2],S.MITARAI[3], M.OSHIMA, T.HAYAKAWA, M.KIDERA, K.FURUTAKA and Y.HATSUKAWA

Recently the interesting sequences of ΔI=1 dipole transitions(M1 bands) were found in the light Pb region and discussed extensively on the basis of a tilted-axis cranking approach[1]. S. Frauendorf suggested that the M1 bands would appear in case that high-spin proton particle states were combined with high-spin neutron hole states[2]. Similar M1 bands had been reported[3] in A≈130 region a few years before the discovery in the light Pb region. In particular those bands were found in every N=78 isotones from ^{135}La to ^{141}Eu[3,4,5]. In ^{142}Gd four ΔI=2 sequences were found, but no M1 bands have been reported so far[6]. The search for such M1 bands is the major purpose of the present study.

We made an in-beam spectroscopic study on high spin states of ^{142}Gd by the reaction of ^{111}Cd(^{35}Cl,1p3n)^{142}Gd. A 7-mg/cm^2 thick Cd foil, enriched in ^{111}Cd to 96.30% was bombarded with a 170-MeV ^{35}Cl beam. Gamma-rays from excited states populated after the reaction were measured by a γ-ray detector array[7] consisting of 11 BGO anti Compton spectrometers in coincidence with charged particles detected by a silicon ball[8] made up of 21 detector segments. Approximately 3.1×10^8 two- or higher fold γγ events were collected and sorted into an individual E_γ-E_γ matrix tagged with the number of protons and α particles detected in the Si ball. A relatively clean matrix for the 1pxn-channel was obtained by subtracting 2p and 1pα contributions from the 1p matrix. We constructed the level scheme of ^{142}Gd as shown in Fig.1 using this clean matrix. The spins and parities were deduced from the DCO ratios evaluated using the spectra gated by the appropriate stretched E2 transitions at lower excitation energy.

Before this experiment, four ΔI=2 sequences (denoted "gsb", "npb","($nh_{11/2}^{-2}$)" and "($ph_{11/2}^{2}$)" in Fig.1) were known up to (16^+), 13^-, 18^+ and 18^+ states respectively[6]. We could extend the E2 sequences labeled "($ph_{11/2}^{2}$)" and "($nh_{11/2}^{-2}$)" up to 24^+ and (22^+) states respectively. Moreover, three dipole cascades(denoted "(A)", "(B)" and "(C)" in Fig.1) were newly found. The excitation energies of "(A)" and "(B)" were centered around at 6MeV which equals to the sum of the excitation energies of ($\pi h_{11/2}^{2}$)10^+ and ($\nu h_{11/2}^{-2}$)10^+ states. The cascade "(C)" was of the highest excitation energy observed in this experiment, which was identified as decaying to both "(B)" and "($nh_{11/2}^{-2}$)" clearly from the coincidence relations, but we could not observe the linking transitions. It is worth while mentioning that cross over E2 transitions were observed only at the higher part of the cascade " (A) " (670 and 993keV). The deduced

[1]Chiba Institute of Technology

[2]Faculty of Education, Chiba University

[3]Faculty of Science, Kyushu University

B(M1)/B(E2) ratios for the I=19 and 21 states were 11.6(9) and 9.7(12) $(\mu_N/eb)^2$, respectively, which were very similar to the values for the M1 bands in A≈130 and the light Pb region. This may indicate that B(M1) value decreases as the spin gets higher. This feature will nicely fit to the character of "Shears Band". Therefore the lifetime measurement is highly desired to determine the B(M1) values within this dipole band.

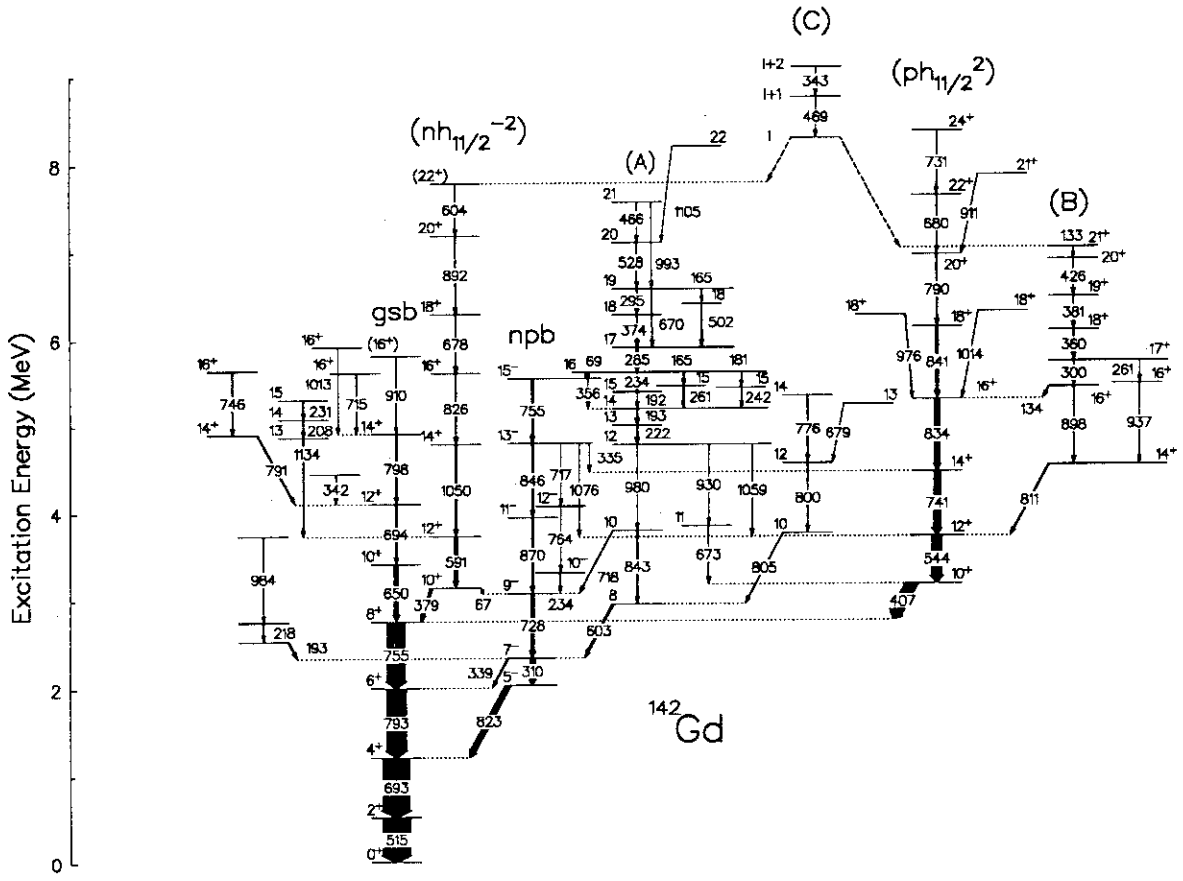

Fig.1 The level scheme of ^{142}Gd.

References

1) M.A.Deleplanque, Nucl. Phys. A557(1993)39c.
2) S.Frauendorf, Nucl. Phys. A557(1993)259c.
3) D.B.Fossan et al., Nucl. Phys. A520(1990)241c.
4) G.de Angelis et al., Phys. Rev. C49(1994)2990.
5) S.Lunardi et al., Phys. Rev. C42(1990)174.
6) W.Starzecki et al., Phys. Lett. B200(1988)419.
7) M.Oshima et al., Nucl. Instr. and Meth. (1997) to be published.
8) T.Kuroyanagi et al., Nucl. Instr. and Meth. A316(1992)289.

2. 9 HIGH-SPIN STATES IN ^{131}Cs

K. FURUNO[1], J. LU[1], T. SAITOH[1], N. HASHIMOTO[1],
K. UCHIYAMA[1], T. SHIZUMA[1], T. KOMATSUBARA[1],
M. OSHIMA, Y. HATSUKAWA, T. HAYAKAWA, K. FURUTAKA,
M. MATSUDA, T. ISHII and M. KIDERA[2]

Recently, bands connected with $\Delta I = 1$ transitions are observed in nuclei with the mass number around $A = 130$. In even-even nuclei of $Z \sim 56$, E2 cross-over transitions are usually weak and it is difficult to extract B(M1)/B(E2) ratios. This might be partly due to the alignment of protons in the $h_{11/2}$ orbital. Such cross-over E2 transitions would be observed in odd-A nuclei. In the nucleus ^{131}Cs, for example, the first band crossing caused by the alignment of $(\pi h_{11/2})^2$ will be blocked, so that the band with the $(\nu h_{11/2})^2 \pi h_{11/2}$ configuration would become the yrast band. The earlier experimental data, however, were very limited[1]. Only three bands were reported up to the spin of $(25/2^+)$. The present experiment is aimed at the establishment of more detailed band structures, the search for $\Delta I = 1$ bands involving both of M1 cascade and E2 cross-over transitions and the test of several theoretical models for the structure of $\Delta I = 1$ bands.

The experiment was carried out at the tandem accelerator facility in Japan Atomic Energy Research Institute. The excited states in ^{131}Cs were populated through the ^{124}Sn(^{11}B,4n)^{131}Cs reaction at a bombarding energy of 42 MeV. The target used was an enriched ^{124}Sn 1 mg/cm^2 thick with a lead backing of 4 mg/cm^2 thickness. A γ-γ coincidence measurement was performed with an array of 10 Compton suppressed Ge detectors. A total of 1×10^8 two-fold coincidence events were accumulated. A typical coincidence spectrum is shown in Fig. 1.

The level scheme established in the present experiment is shown in Fig. 2. This is constructed from the intensity balance and coincidence relations of γ rays. The spin assignment are mainly based on the measured DCO ratios. The bands 3, 4, 9 and 10 are in good agreement with those reported by Garg et al[1]. The band 4 is built on the $5/2^+$ ground state. According to previous data, the static magnetic moment of the ground state is reported to be $\mu = +3.543\mu_N$. The static quadrupole moment is also measured to be $Q = -0.575(6)$. From these experimental data, the configuration of the ground state is assigned to be $\pi g_{7/2}$. The configuration of $\pi d_{5/2}$ for the band 3 seems to be reasonable from the shell filling of the deformed shell model. The band 9 could be assigned to the $\pi h_{11/2}$ decoupled band from the systematic trend in this mass region. The band 10 is extended to the spin of $25/2^-$. Only the band head was reported for this band in the previous work[1].

Remarkable findings in the present experiment are the band 1 and 11. In the band 1, E2 cross-over transitions are definitely observed as well as $\Delta I = 1$ transitions. The parity was assigned to be positive because the DCO ratio of 1.03 for the 906 keV transition implies an E2 transition. The ratio of B(M1)/B(E2) is the order of 10 $(\mu_N/eb)^2$, which is very similar value of $\Delta I = 1$ bands in neighboring nuclei. From the spin alignment of this band, the band 1 would have the $(\nu d_{3/2}, s_{1/2})(\nu h_{11/2})^2 \otimes \pi g_{7/2}$. In contrast to the band 1, the band 11 has negative parity. This is determined from the DCO ratio of the 804 keV transition.

1 Institute of Physics and Tandem Accelerator Center, University of Tsukuba 305 Ibaraki, JAPAN

2 On leave from Kyushu University, Hakozaki, Fukuoka, Japan

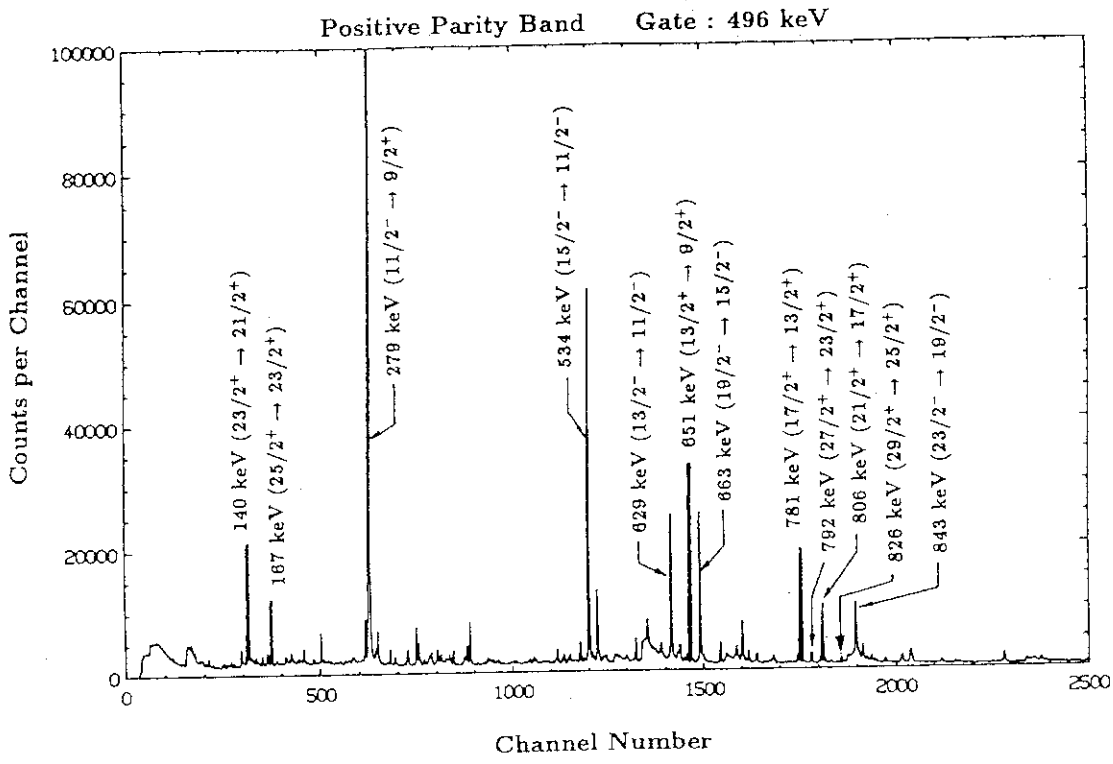

Fig. 1. A coincidence spectrum obtained by placing a gate on the 496 keV γ ray in the band 3 in ^{131}Cs.

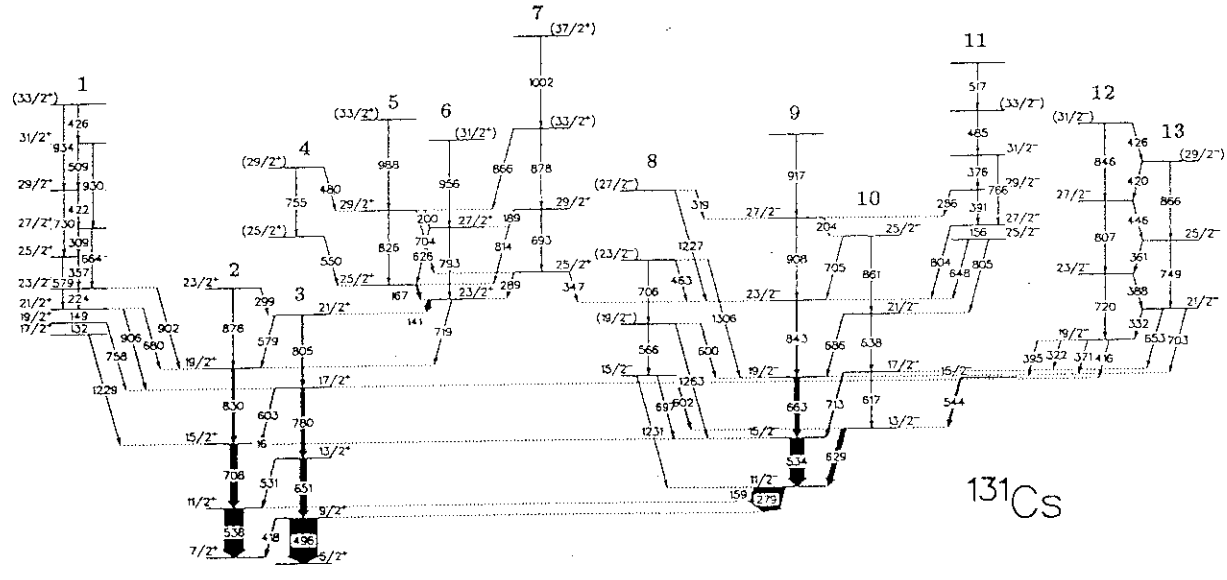

Fig. 2. The level scheme of ^{131}Cs

The band 1 is a good candidate of the multi quasi-particle magnetic dipole band which can be analyzed in terms of the tilted-axis cranking model. Unlike the band 1, the cross-over E2 transitions are very weak in the band 11. The band 12 and 13 would be a strongly coupled band consisting of high-K neutrons. More detailed analysis are in progress.

References

1) U. Grag *et al*, Phys. Rev. C **19**(1979)207.

2) Table of isotopes, 8th edition ed. R.B. Firestone and V.S. Shirley(1996).

2.10 NUCLEAR g-FACTORS OF THE YRAST BAND IN ^{134}Ce

N. HASHIMOTO[1], T. SAITOH[1], J. LU[1], T. KOMATSUBARA[1], K. FURUNO[1]
M. OSHIMA, Y. HATSUKAWA, T. HAYAKAWA, K. FURUTAKA,
M. MATSUDA, T. ISHII and M. KIDERA[2]

A remarkable feature of the high-spin band structure in even-even nuclei around the mass number $A = 130$ is that two s-bands having the configuration of $(\pi h_{11/2})^2$ or $(\nu h_{11/2})^{-2}$ appear at almost same excitation energy[1]. In the nucleus ^{134}Ce, two s-bands are reported[2]. One is a band built on the 10^+ state at an excitation energy of 3209 keV, and the other is also built on the 10^+ state at 3719 keV. The former band is, hereafter, named as "band A", while the latter as "band B". Bertschat *et al.* have measured the g factor of the $I^\pi = 10^+$ state in "band A" at an excitation energy of 3209 keV[3]. The experimental value of $g = -0.187(2)$ is consistent with the neutron configuration of $(\nu h_{11/2})^{-2}$, and also fits to the systematic trend observed in other isotones. On the other hand, Zemel *et al.* have measured the g factor of the $I^\pi = 10^+$ state in "band B" at 3719 keV[4]. The result of $g = -0.30(25)$ suggests that the configuration would be neutron dominant. However, the proton configuration of $(\pi h_{11/2})^2$ seems to be more preferable than the neutron configuration from the systematic trend in this mass region. In order to remove this discrepancy, we have measured g factors of levels around the 10^+ states at 3719 keV using transient magnetic field.

The experiment was performed at the Japan Atomic Energy Research Institute(JAERI) using the accelerator complex consisting of the 20UR tandem accelerator and the superconducting linear accelerator. The excited states of ^{134}Ce were populated through the ^{11}B(^{127}I,$4n$)^{134}Ce reaction with ^{127}I beam at a bombarding energy of 583 MeV. A natural boron target 582 μg/cm^2 thick was prepared on a foil of iron by vacuum evaporation using electron bombardment. The thickness of the iron foil was 79 mg/cm^2. Nuclei of ^{134}Ce recoiled through the boron target penetrate into the iron foil. The thickness of the target was adjusted in such a way that the perturbation starts at a time of the population of the 12^+ and 14^+ states. The velocity of ^{134}Ce nuclei is as fast as 9 % of light velocity at the entrance of the iron layer. The transient magnetic field at this velocity can be estimated to be about 4000 T[5]. Nuclei of ^{134}Ce, therefore, are perturbed for a few ps by the transient field, and later by the internal magnetic field in iron after their stop. The magnitude of the internal magnetic field is known to be -35 T, so that the transient field is about 100 times stronger than the internal field. Thus the 10^+ and 14^+ states levels which decay within a few ps after the population would mainly be perturbed by the transient magnetic field.
In order to magnetize the iron foil, the target was placed in an external magnetic field(0.15 T) generated by rare-earth permanent magnets. The assembly of the target and permanent magnets was positioned at the center of an array of 9 Compton-suppressed Ge detectors which was constructed in the Tsukuba-JAERI tandem collaboration. Gamma rays were observed at 9 angles of $\theta = \pm 31.7°$, $\theta = \pm 58.2°$, $\theta = 180° \pm 31.7°$, $\theta = 180° \pm 58.2°$ and $\theta = \pm 90°$ with respect to the beam direction. The yields of γ rays were measured by changing the direction of the external magnetic field every 30 min. Mean Larmor precession angles were extracted from the ratios of γ-ray intensities at angles of 31.7° and 58.3° with respect

1 Institute of Physics and Tandem Accelerator Center, University of Tsukuba, Tsukuba, Ibaraki 305 JAPAN
2 Kyushu University, Hakozaki, Fukuoka 812, Japan.

to the beam direction for external magnetic fields up and down. In order to minimize spurious ratios, which were mainly ascribed to different efficiencies of the γ-ray detectors, the so-called double ratio method was employed according to the prescription described in ref [5].

The experimental double ratios are presented in Fig. 1. In the detector arrangement in the present experiment, the double ratios R should be smaller than unity for E2 transitions if g factors have positive sign. As seen from Fig. 1, the double ratios for E2 transitions originated from the band B in ^{134}Ce are smaller than unity. This implies that the g factors of levels near the band head of the band B are positive and consistent with the configuration of $(\pi h_{h11/2})^2$. We have obtained the double ratio of 0.95 for the 1126 keV γ ray which depopulates the $I^\pi = (5^-)$ levels at 2175 keV. The multipolarity of this transition is known to be E1 from in-beam spectroscopy. The double ratio should be $R > 1$ for E1 transitions, if the g factor is positive. The experimental result of $R < 1$ suggests that the g factor is negative for the $I^\pi = (5^-)$ state. The band built on this state has considered to have a configuration of $(\nu h_{11/2})^{-1} \otimes (\nu s_{1/2})^{-1}$. Moreover, the $I^\pi = (5^-)$ state is mainly fed from the $I^\pi = (7^-)$ state at 2707 keV, which has a configuration of $\nu h_{11/2} \otimes \nu d_{3/2}$. We have made the assignment of these configurations on the basis of the experimental systematics for the spin alignments, band crossing frequencies, and/or experimental routhians for neighboring nuclei. It is clearly expected that neutron quasiparticles play a crucial role in these configurations. The negative g factor suggested from the present experiment strongly support this feature. The double ratio for the $I^\pi = 10^+$ isomeric state at 3209 keV with the halflife of 308 ns is unity. This result is very reasonable because the angular distribution of γ rays emitted from this state becomes isotropic due to the strong perturbation for a long lifetime.

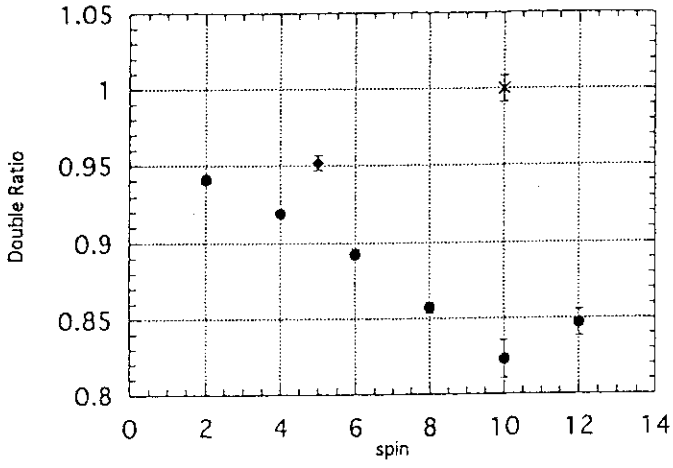

Fig. 1. Experimental results of double ratios. The ratios for the E2 transitions in the ground state band are marked by full circles. A diamond mark indicates for the double ratio of the 1126 keV transition(see text). The ratio for the transition from a long-lived isomeric state at 3209 keV is plotted in a cross.

References

1) R.Wyss, A.Granderath, R.Bengtsson, P.von Brentano, A.Dewald, A.Gelberg, A.Gison, J.Gison, S.Harissopulos, A.Johnson, W.Liberz, W.Nazarewicz, J.Nyberg and K.Schiffer, Nucl. Phys. **A505** (1989) 337.
2) M.Müller-Veggian, H.Beuscher, D.R.Haenni, R.M.Lieder and A.Neskakis, Nucl. Phys. **A 417** (1984) 189.
3) H.H.Bertschat, H.E.Mahnke, E.Dafni, F.D.Davidovsky and M.Hass, Phys. Lett. **101A**, 507 (1984).
4) A.Zemel, C.Broude, E.Dafni, A.Gelberg, M.B.Goldberg, J.Gerber, G.J.Kumbarztzki, and K.H.Speidel, Nucl. Phys. **A 383** 165 (1982).
5) D.Ward, O.Häuser, H.R.Andrews, P.Taras, P.Skensved, N.Rud and C.Broude, Nucl. Phys. **A330** 225 (1979).

2.11 ISOMER-SCOPE

T. ISHII, M. ITOH[1], M. ISHII, A. MAKISHIMA[2], M. OGAWA[1], I. HOSSAIN[1], T. HAYAKAWA and T. KOHNO[1]

A new instrument, isomer-scope, has been constructed to observe the ns-μs isomers produced by deep inelastic collisions. As shown in Fig. 1, it consists of a Si detector, a γ-absorber and Ge detectors. The Si detector catches projectile-like fragments(PLF) and gives the energy and timing signals. The γ-absorber shields the Ge detectors from strong γ-radiation generated in the target. Thus, the isomer-scope greatly intensifies the γ-rays from the isomers of PLF in the PLF-γ(-γ) coincidences. The experiment was carried out using the reaction 635 MeV ^{76}Ge +^{198}Pt. The energy spectrum measured with the Si detector is shown in Fig. 2(a) and the γ-ray spectrum in coincidence with a differnt energy of PLF is shown in Fig. 2(b). The γ-rays from the isomers of PLF were clearly observed in the spectrum gated on **B**, or the region of the energy-dumped PLF. We observed transition cascades from 29 isomers. In them, a new isomer of ^{69}Cu was found to be excited at 2741 keV with $T_{1/2} = 0.36(3)$ μs

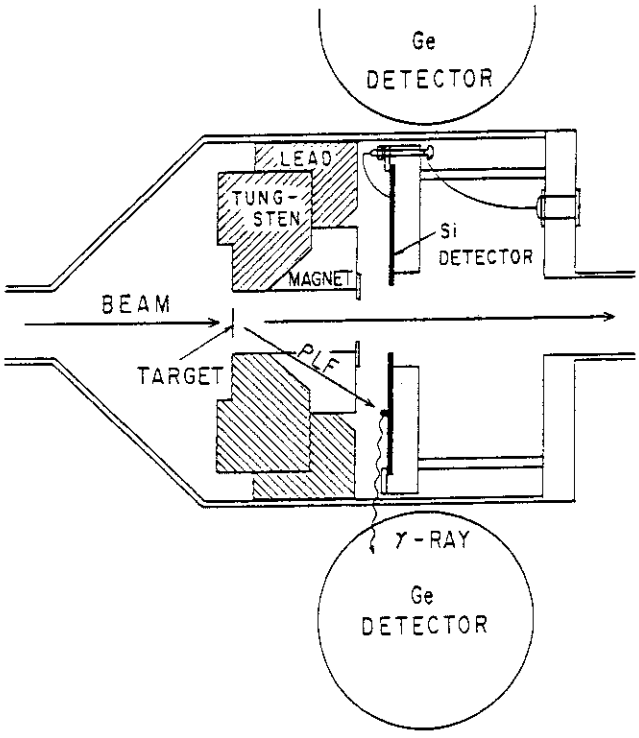

Fig. 1 Isomer-scope

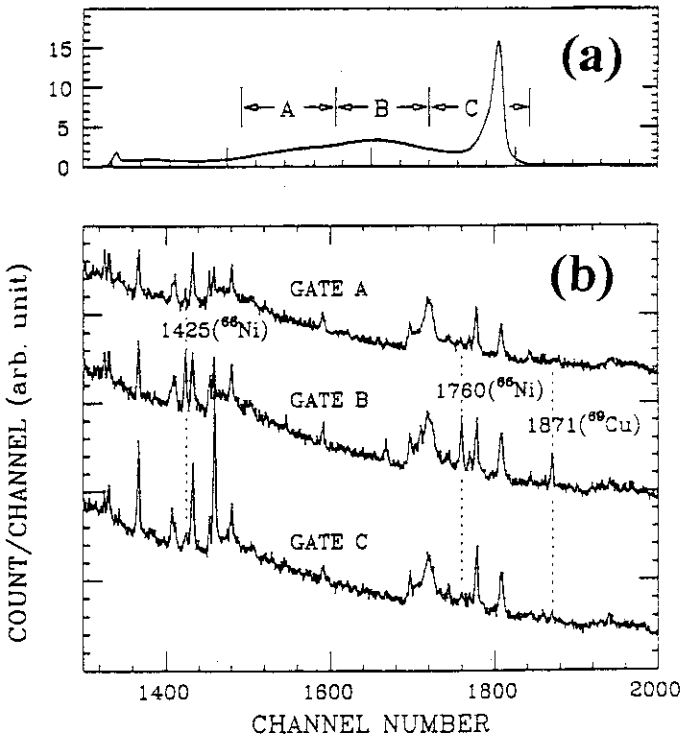

Fig. 2 (a) Energy spectrum of PLF measured with the Si detector. (b) Gamma-ray spectra in coincidence with PLF of different energies.

[1]Department of Energy Sciences, Tokyo Institute of Technology
[2]Department of Liberal Arts and Sciences,National Defense Medical College

2.12 ENERGY RESOLUTION IMPROVEMENT OF THE GAS COUNTER INSTALLED IN "ENMA" FOR LIGHT IONS

A.YAMAZAKI[1], T.YAMAYA[1], H.ISHIYAMA[1], M.KATO[1], J.TOJIMA[1], T.KUZUMAKI[1], H.YAHATA[1], T.SUEHIRO[2], S.KATO[3], Y.SUGIYAMA and S.HAMADA

The alpha cluster model plays an important role for the study of nuclear structure. The study of the p-shell nuclei was one of the earliest subjects for the alpha cluster model, and it developed to a sd-shell nuclei region. Recently, the alpha cluster structure has been shown to exist even in the region of fp-shell nuclei [1, 2] .

For investigation of the alpha cluster structure, alpha transfer reactions are powerful tools. Especially, the (^{6}Li,d) reaction has been used for a lot of studies of the alpha cluster structure. One of aims in the present work is to search for the alpha cluster structure with this reaction in heavy nuclei like around A=200 region nuclei.

The magnetic spectrograph ENMA has been designed for a heavy-ion reaction studies [3], so that the focal plane detector of this spectrograph has been made to be convenient for detection of heavy ions. We modified it for detection of light ions.

A large difference between light- and heavy-ions in detection by a gas counter is the magnitude of the energy loss when they pass through a gas. In order to obtain a good position resolution, various modifications were tried to the detector. At first, a single anode wire was replaced with multi-wires to enhance charge collection. Secondary, counter gases and gas pressures were searched, and we obtained a value of 950 mbar as an optimum gas pressure, in which Ar and CO_2 gases shared 900 mbar and 50 mbar, respectively. Consequentry, a new position sensitive counter consists of three resistive anodes which are joined each other at the both ends. Electric potential for anode wires was +1100 V.

[1]Department of Physics, Tohoku University.
[2]Tohoku Institute of Technology.
[3]Department of Physics, Yamagata University.

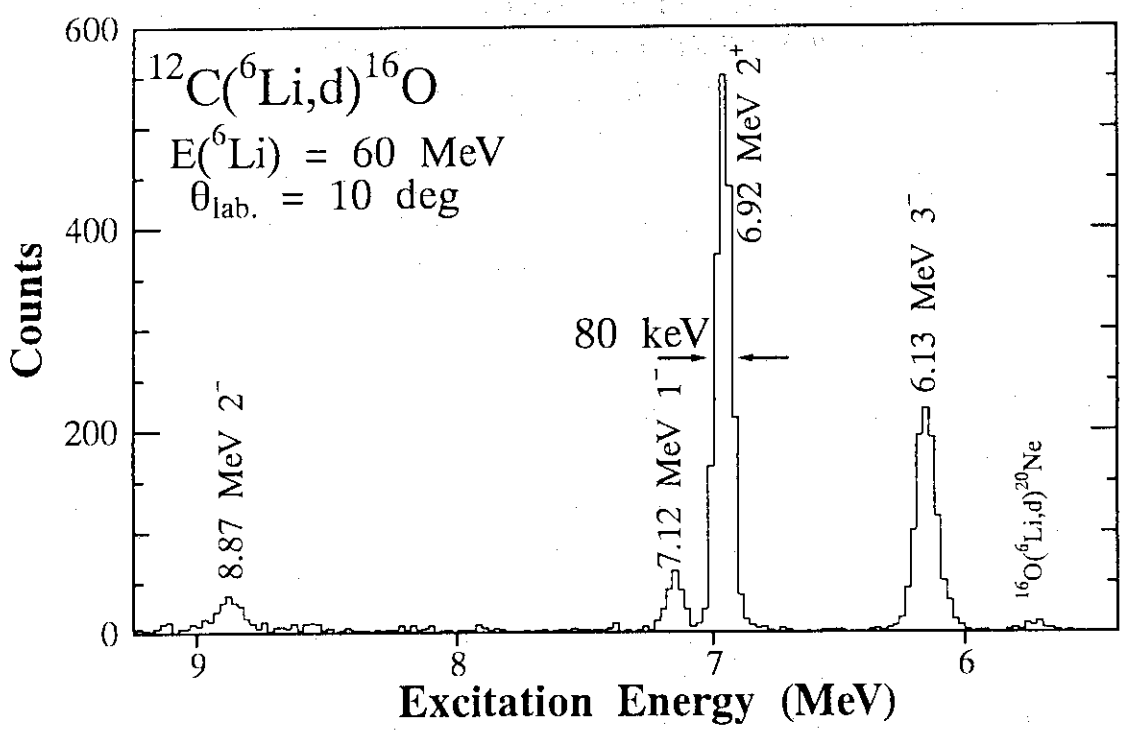

Fig. 1: An energy spectrum of deuteron from the reaction $^{12}C(^{6}Li,d)^{16}O$. Energy resolution for the most prominent peak (6.92 MeV, 2^+) is 80 keV at FWHM.

Figure.1 is a typical performance in deuteron energy spectrum of the $^{12}C(^{6}Li,d)^{16}O$ reaction. Energy resolution for a prominent peak was 80 keV at FWHM. As a result of these developments, light ions can be detected with a good energy resolution. this will make it possible to study the alpha cluster structure in heavy nuclei around A=200.

References

1) T.Yamaya, S.Oh-ami, M.Fujiwara, T.Itahashi, K.Katori, M.Tosaki, S.Kato, S.Hatori and S.Ohkubo, Phys. Rev. C42(1990)1935
2) T.Yamaya, M.Saitoh, M.Fujiwara, T.Itahashi, K.Katori, T.Suehiro, S.Kato, S.Hatori and S.Ohkubo, Nucl. Phys. A573(1994)154
3) Y.Sugiyama, H.Shikazono, H.Ikezoe and H.Ikegami, Nucl. Instr. and Meth. 187(1981)25

3. Nuclear Reactions

3. 1 SEARCH FOR NEW SEABORGIUM ISOTOPES

H. IKEZOE, T. IKUTA, S. MITSUOKA, S. HAMADA, Y. NAGAME,
I. NISHINAKA, K. TSUKADA and T. OHTSUKI[1]

Many new isotopes of trans-actinide nuclei have been synthesized by the hot fusion reactions[1], where targets of actinide nuclei have been bombarded by heavy-ion beams. This type of the fusion reactions has an advantage that an extra-push energy[2] is not needed to overcome the Coulomb barrier between a target and a projectile. On the other hand, since the excitation energy of the compound nucleus is large (40 ~ 60 MeV) in the hot fusion reaction, the survival probability of evaporation residues by emitting neutrons becomes extremely small. Therefore it is important to make the excitation energy as small as possible by selecting the bombarding energy close to the Coulomb barrier.

In the present experiment, neutron rich ^{30}Si beams were used to bombard a ^{238}U target to produce a new isotope of Seaborgium (Z = 106). It is noted that the Q-value of the present reaction system becomes smaller by the amount of 5.7 MeV compared to the reaction ^{238}U + ^{28}Si. The bombarding energy was chosen to be 163 MeV, which was about 3.5 MeV larger than a calculated fusion barrier (the Bass barrier). The main evaporation channel was estimated to be 5n channel. The JAERI recoil mass separator[3] was used to select in flight the evaporation residues and focus them to a silicon strip detector[4] placed at the end of the recoil mass separator. The detection method of decay events from the evaporation residues implanted in the detector is shown in Ref. [4]. The average beam current was 45 pnA and the total dose was 1.6×10^{17} particles for the accumulation time of 6.5 days. No decay event from ^{263}Sg was detected in the present experiment and the upper limit of the cross section σ_{5n} was estimated to be 180 pico barn. The overall detection efficiency, including the transport efficiency in addition to the angular spread and the charge state distribution of the evaporation residues, was about 3%. We are currently in process of increasing the efficiency up to 9% by changing a focus condition of the JAERI recoil mass separator.

References

1) Yu. Ts. Oganessian, Nucl. Phys. **A488** (1988) 65c.
2) W. J. Swiatecki, Nucl. Phys. **A376** (1982) 275.
3) H. Ikezoe, et al., Nucl. Instr. and Meth. **A376** (1996) 420.
4) H. Ikezoe, et al., Phys. Rev. **C54** (1996) 2043.

[1]Laboratory of Nuclear Science, Tohoku University, Taihaku-ku, Sendai 982, Japan

3. 2 NEW NEUTRON DEFICIENT ISOTOPE ^{212}Pa

S. MITSUOKA, H. IKEZOE, T. IKUTA, Y. NAGAME, K. TSUKADA,
I. NISHINAKA, and Y.L. ZHAO [1]

In resent years new radioisotopes close to the proton drip-line have been produced in the light actinide region and nuclear structure far from stability has been intensively studied. In the present work, the α-decay properties of the new neutron deficient odd-odd isotope ^{212}Pa were investigated [1] using the JAERI recoil mass separator (JAERI-RMS) [2].

A 182.5 MeV beam of $^{35}Cl^{11+}$ supplied from the JAERI-tandem accelerator was used to bombard a ^{182}W target (513 μg/cm^2 thickness). Fusion evaporation residues (ER's) were separated in-flight from the primary beam by the JAERI-RMS and implanted into a double-sided position sensitive silicon detector (PSSD). The energies and two-dimensional positions of the implanted ER and their subsequent α-decay particles were registered together with the times associated with the detection. The experimental details are shown in Refs. [1] and [3]. The observed short-lived activities were identified based on the fact that the α-decay chains occurred with time intervals related to their half-lives at the same position as that of the ER within the PSSD position resolution.

Figure 1 shows a two-dimensional matrix of the correlation between parent and daughter α decays of type ER-α_1-α_2. Two groups of correlated three events (A and B) were observed at higher parent energies than 8.0 MeV. The low energy group (A) is identified as the decay of parent nuclei ^{214,215}Pa. An unique assignment was impossible because of slight differences in the α-particle energies and half-lives in the ^{214}Pa–^{210}Ac–^{206}Fr and ^{215}Pa–^{211}Ac–^{207}Fr chains.

Three decay events (B in Fig. 1) are listed in Table I, together with the observed positions, energies and the time interval between the subsequent decays. The α-decay energy $E_{\alpha 2}$ = 7.550(30) MeV of the first event is consistent with the reported value of 7.572(15) MeV in the decay from the ground state of ^{208}Ac [4] and also 7.585(15) MeV of ^{209}Ac [5]. The granddaughter decay of $E_{\alpha 3}$ =7.050(30) MeV is consistent with 7.029(4) MeV of the ground state decay of ^{204}Fr [5], but inconsistent with 6.917(3) MeV of ^{205}Fr [5]. The observed time intervals in this chain are in agreement with the reported half-lives [4, 5]. Therefore this decay chain is assigned to the decay of the new isotope ^{212}Pa. The second and third decay chains listed in Table I are also assigned to ^{212}Pa–^{208}Ac–^{204}Fr–^{200}At chain. The α_4 in second chain and the α_3 in third chain probably did not deposit the full energy in the PSSD and not be detected by the surrounding detectors.

It has been reported that there are two α-decaying states in doubly odd nucleus ^{208}Ac [4]; the ground state decay with spin-parity of 3^+ and the isomeric state with 10^- [4]. ^{204}Fr has a decaying state of 7^+ isomer in addition to 3^+ and 10^- [6]. Although weak transitions with change in spin and parity in α decay of ^{204}Fr have been reported, there is in general a strong trend for a transition without spin and parity changes [6]. All α decays observed in the present experiment were ground state-to-ground state transitions in the ^{208}Ac–^{204}Fr–^{200}At

[1]Tokyo Metropolitan University

chain and no α decay to the isomeric states quoted above was observed. It is, therefore, highly probable that the observed α decay of the ^{212}Pa originates from its ground state.

The obtained α-decay properties of the new isotope ^{212}Pa are E_α = 8.270(30) MeV and $T_{1/2}$ = $5.1^{+6.1}_{-1.9}$ ms. The reduced width W_α was estimated to be 33^{+21}_{-19} keV assuming s-wave α transition in the same manner as Rasmussen [7]. The obtained W_α is consistent with the values of neighboring Pa isotopes (neutron number $\leq$ 126). The production cross-section for the five neutron evaporation residue ^{212}Pa was estimated to be about 0.5 nb when a 19 % calculated transmission efficiency of the JAERI-RMS is assumed.

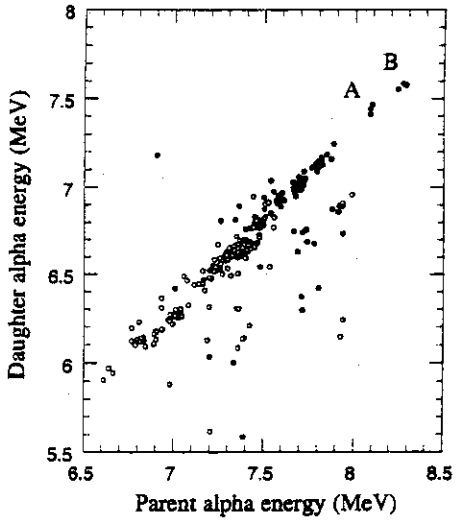

FIG. 1. Two-dimensional matrix showing the correlation between parent and daughter α decays of type ER-α_1-α_2 following the reaction of ^{35}Cl+^{182}W. Closed (open) symbols are with time gates of 500 ms (50 s) for ER-α_1 and 50 s (1000 s) for α_1-α_2. Escaped events which did not deposit the full energies in the PSSD are included. The correlated events labeled by *A* and *B* correspond to the α decays from ^{214,215}Pa and ^{212}Pa, respectively.

TABLE I. Strip numbers of the PSSD, two-dimensional positions, energies, and time intervals of the measured evaporation residues and the subsequent α-decay particles at parent α-decay energies larger than 8.2 MeV. The events indicated by the time interval of zero represent the ER implanted in the PSSD.

Event no.	Type	Strip no. Front	Strip no. Back	Position in strip (mm) Front	Position in strip (mm) Back	Energy (MeV)	Time interval
1	ER	9	4	2.30	5.59	14.163	0
	α_1	9	4	2.34	5.53	8.242	10 ms
	α_2	9	4	2.26	5.51	7.552	176 ms
	α_3	9	4	2.29	5.25	7.048	7.53 s
2	ER	13	3	0.78	3.65	16.113	0
	α_1	13	3	0.76	3.65	8.271	5 ms
	α_2	13	3	0.72	3.83	7.584	840 ms
	α_3	13	3	0.76	3.68	7.045	2.07 s
	α_4	13	3	0.75	3.55	3.022	184 s
3	ER	10	2	2.57	3.59	14.387	0
	α_1	10	2	2.55	3.33	8.286	7 ms
	α_2	10	2	2.61	3.57	7.576	21 ms
	α_3	10	2	2.55	3.38	6.482	3.61 s
	α_4	10	2	2.61	3.46	6.471	61.0 s

References

1) S. Mitsuoka, H. Ikezoe, T. Ikuta, Y. Nagame, K. Tsukada, I. Nishinaka, Y. Oura, and Y.L. Zhao, Phys. Rev. C **55**, 1555 (1997).
2) H. Ikezoe, Y. Nagame, T. Ikuta, S. Hamada, I. Nishinaka, and T. Ohtsuki, Nucl. Instr. and Meth. **A376**, 420 (1996).
3) H. Ikezoe, T. Ikuta, S. Hamada, Y. Nagame, I. Nishinaka, K. Tsukada, Y. Oura, and T. Ohtsuki, Phys. Rev. C **54**, 2043 (1996).
4) M. Leino, J. Uusitalo, T. Enqvist, K. Eskola, A. Jokinen, K. Loberg, W.H. Trzaska, and J. Äystö, Z Phys. A **348**, 151 (1994).
5) A. Rytz, Atomic Data and Nuclear Data Tables **47**, 205 (1991).
6) M. Huyse, P. Decrock, P. Dendooven, G. Reusen, P. Van Duppen, and J. Wauters, Phys. Rev. C **46**, 1209 (1992).
7) J.O. Rasmussen, Phys. Rev. **113**, 1593 (1959).

3. 3 IDENTIFICATION OF NEUTRON DEFICIENT AMERICIUM ISOTOPE ^{236}Am USING THE GAS-JET COUPLED JAERI-ISOL

K. TSUKADA, Y. OURA[1], S. ICHIKAWA, Y. NAGAME, I. NISHINAKA, K. HATA, Y. HATSUKAWA, N. SHINOHARA, K. SUEKI[1], T. OHYAMA[1], H. NAKAHARA[1], M. ASAI[2], T. HIROSE[2], Y. KOJIMA[2], H. YAMAMOTO[2], K. KAWADE[2]

There has been great progress in the frontiers of short-lived isotopes far from the β stability line by means of in-flight and on-line mass separations. In the region of neutron-deficient Am, Cm and Bk isotopes, many unknown isotopes are expected to decay mainly via orbital electron capture (EC), which enables us to detect them with a radiochemical method or an isotope separator on-line (ISOL). In fact, by improving a rapid chemical separation method, the new isotopes ^{238}Bk and ^{235}Am have been identified recently [1,2].

To study the nuclear properties of unknown neutron deficient americium isotopes produced in heavy ion fusion reactions, we have developed a composite system consisting of a gas-jet transport apparatus, including a multiple target system, and a thermal ion-source at an ISOL. The multiple target system is designed to increase the effective target thickness and collect efficiently the reaction products recoiling out from each target. The performance of the system has been tested using the ^{143m}Sm isotope produced in the ^{141}Pr(^{6}Li, 4n) reaction and ^{237}Am in the ^{235}U(^{6}Li, 4n) reaction. The separation efficiencies of the whole system have been evaluated to be 0.14% for ^{143m}Sm and ~0.1% for ^{237}Am.

With this system, search for the unknown isotope ^{236}Am produced in the ^{235}U(^{6}Li, 5n) reaction has been performed. A stack of seventeen ^{235}U targets was bombarded with a 50 MeV ^{6}Li beam of about 200 pnA intensity. Figure 1 shows the γ-ray spectrum obtained at the mass-236 fraction. Pu KX-rays associated with the EC decay of ^{236}Am were observed. Figure 2 shows the decay curve of the Pu KX-ray intensities. The half-life of ^{236}Am is evaluated to be 4.4 $\pm$ 0.8 min, and the production cross section is estimated to be about 30 μb. The half-life are in agreement with a predicted value of 8.87 min for ^{236}Am [3] within a factor of ~2.

References

1) S. A. Kreek *et al.*, Phys. Rev **C49** (1994) 1859.
2) J. Guo *et. al.*, Z. Phys. **A255** (1996) 111.
3) M. Hirsch *et. al.*, At. Data Nucl. Data Tables **53** (1993) 165.

[1]Tokyo Metropolitan University
[2]Nagoya University

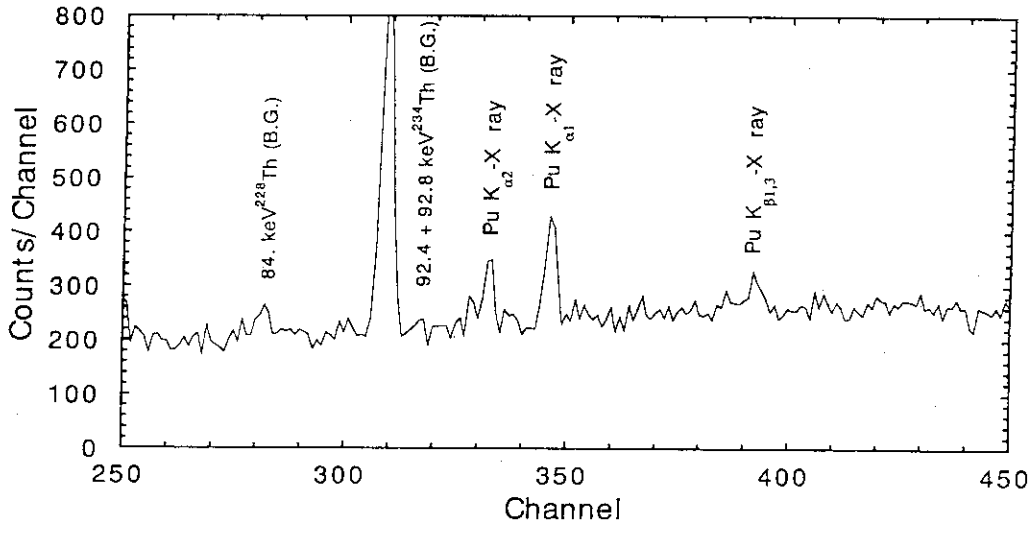

Figure 1: γ-ray spectrum obtained at the mass-236 fraction with a LEPS

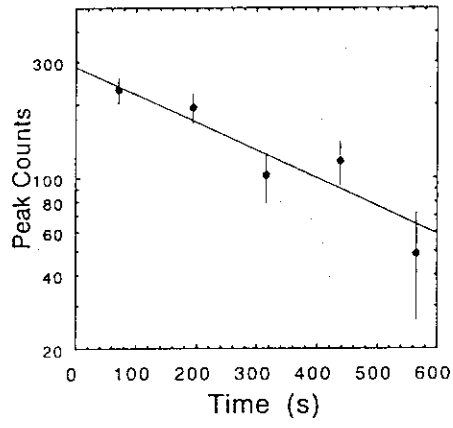

Figure 2: Decay curve for Pu KX-ray counts measured with LEPS.

3. 4 IDENTIFICATION OF NEW NEUTRON-RICH RARE-EARTH ISOTOPES PRODUCED IN PROTON-INDUCED FISSION OF ^{238}U

S. ICHIKAWA, K. TSUKADA, M. ASAI[1], A. OSA, Y. KOJIMA[1], T. HIROSE[1], Y. OURA[2], M. SHIBATA[1], I. NISHINAKA, Y. HATSUKAWA, H. IIMURA, K. HATA, Y. NAGAME and K. KAWADE[1]

In recent years, new neutron-rich rare-earth isotope ^{166}Tb produced via the proton-induced fission of ^{238}U have been identified using the JAERI-ISOL coupled to a gas-jet transport system [1]. The gas-jet transport system connected to the target chamber was designed to efficiently collect fission fragments recoiling from the target and quickly transport into a thermal ion source. The thermal ion source was used to ionize efficiently rare-earth elements having the ionization potential below 6 eV. The performance of the gas-jet coupled thermal ion source was tested using short-lived isotopes produced via the proton-induced fission of ^{238}U [2]. The separation efficiency of the whole system was measured to be a few percent for La, Pr, Pm and Eu, and the delay time between production of atoms and extraction of the ion was evaluated to be 2 $\sim$ 3 s. With this system, search for unknown neutron-rich rare-earth isotopes ^{161}Sm and ^{165}Gd produced in the proton-induced fission of ^{238}U were carried out. The atom of interest was ionized as its monoxide ion in the thermal ion source, and then mass-separated at the mass-A+16 fraction.

A stack of ^{238}U targets was bombarded with 20 MeV proton beam of about 1 mA intensity provided by the 20 MV tandem accelerator at JAERI. Each target was electrodeposited with a thickness of about 4 mg/cm^2 on an aluminum-foil backing, and located inside the target chamber. Fission products emitted isotropically from the target were thermalized in Ar gas loaded with KCl aerosols, and then transported into the ion source through a capillary. The transported atoms were ionized in the thermal ion source, and mass-separated electromagnetically. The mass-separated ions of interest were collected on an aluminum-coated Mylar tape in a tape transport system, and periodically transported to a measuring position. The measuring position was equipped with two plastic scintillators, a 50-mm dia. x 10-mm thick planar-type HPGe detector and a 28% coaxial n-type HPGe detector. With this detector system, β-γ, γ-γ coincidence and γ-ray singles were measured. The coincidence data were recorded event by event together with the time information used in a half-life analysis. Singles γ-ray spectra for all HPGe detectors were measured with a multispectrum scaling technique using 16 x 4096-channel pulse-hight analyzers.

In β-coincident X/γ-ray spectra observed at the mass 177 and 181 fractions, Eu and Tb KX-rays associated with the β-decay of ^{161}Sm and ^{165}Gd were clearly identified and contamination from other molecular beams was almost negligible. The haf-lives were determined to be 4.8 $\pm$ 0.8 s for ^{161}Sm and 10.3 $\pm$ 1.6 s for ^{165}Gd, respectively. In Table 1, the experimental half-lives are compared with theoretical predictions by Tachibana et al. [3] with the gross theory and by Staudt et al. [4] with the proton-neutron quasi-particle random-phase approximation (pn-QRPA) model. The calculated half-life values depend considerably on the input data of the Qb value. With the gross theory, the calculated half-life values are in agreement with experimental

[1]1 Nagoya University, Nagoya 464-01.
[2]2 Tokyo Metropolitan University, Hachioji, Tokyo 192-03.

ones within a factor of ~ 1.5 using the Q_β values of 4.80 MeV for 161Sm, 4.19 MeV for ^{165}Gd evaluated by Audi and Wapstra [9]. If we take the evaluated Q_β value of 4.98 MeV for ^{161}Sm [10], 4.35 MeV for ^{165}Gd [6], their calculated half-life values agree well with experimental ones.

Table 1: The measured half-life of ^{161}Sm and ^{165}Gd compared with the results of two theoretical predictions

Nuclide	Present experiment	Theoretical predictions			
		Gross theory[3]		pn-QRPA model[4]	
		half-life(s)	Q_β (MeV)	half-life(s)	Q_β(MeV)
^{161}Sm	4.8 ± 0.8 s	9.35[a]	4.572[5]	12.6 s	4.98[8]
		5.821[a]	4.90[6]		
		4.156[a]	5.15[7]		
^{165}Gd	10.3 ± 1.6 s	34.3[a]	3.76[5]	18.4 s	4.14[8]
		27.97[a]	3.83[7]		
		12.33[a]	4.35[6]		

[a] T. Tachibana: private communication (1997).

References

1) S. Ichikawa, M. Asai, K. Tsukada, A. Osa, T. Ikuta, N. Shinohara, H. Iimura, Y. Nagame, Y. Hatsukawa, I. Nishinaka, K. Kawade, H. Yamamoto, M. Shibata and Y. Kojima, Nucl. Instr. Meth. A **374**,330 (1996).
2) M. Asai, K. Tsukada, S. Ichikawa, A. Osa, Y. Kojima, H. Yamamoto, K. Kawade, Y. Nagame, N. Shinohara, H. Iimura, I. Nishinaka and Y. Hatsukawa, J. Phys. Soci. Japan, **65**, 1135 (1996).
3) T. Tachibana and M. Yamada ENAM 95 (Proc. of International Conf. on Exotic Nuclei and Atomic Masses), Editions Frontieres, Gif-sur-Yvette, p.763.
4) A. Staudt, E. Bender, K Muto and H. V. Klapdor-Kleingrothaus, At. Data and Nucl. Data Tables **44**, 79 (1990).
5) P. Möller, J. R. Nix, D. W. Myers and W. J. Swiatecki, At. Data and Nucl. Data Tables **59**, 185 (1995).
6) J. Jänecke and P. J. Masson, At. Data and Nucl. Data Tables **39**, 265 (1988).
7) Y. Aboussir, J. M. Pearson, A. K. Dutta and F. Tondeur, At. Data and Nucl. Data Tables **61**, 127 (1995).
8) P. Möller and J. R. Nix, At. Data and Nucl. Data Tables **26**, 165 (1981).
9) G. Audi and A. H. Wapstra, Nucl. Phys. A **595**, 409 (1995).
10) G. Audi and A. H. Wapstra, Nucl. Phys. A **565**, 1 (1993).

3. 5 PAIR TRANSFER REACTIONS IN THE NICKEL REGION AND A POSSIBLE EXISTENCE OF THE NUCLEAR JOSEPHSON EFFECT

Y.SUGIYAMA, S.HAMADA, T.IKUTA and A.YAMAZAKI[1]

It was pointed out that the nuclear Josephson effect could be observed in pair-transfer reactions between superfluid nuclei near the Coulomb barrier, since the probability of pair-transfer could be enhanced by the coherent nature of the nuclear states in both nuclei[1]. Recently Mermaz et al. observed the enhancement of the experimental cross section of pair transfer reactions with respect to the theoretical ones in the $^{32}S+^{34}S$ system and suggested an evidence of a nuclear Josephson effect[2].

We measured elastic scattering for $^{58}Ni+^{60}Ni$, $^{62}Ni+^{64}Ni$ and neutron pair-transfer reactions for $^{58}Ni+^{64}Ni$ by using the JAERI tandem accelerator and the heavy-ion magnetic spectrograph "ENMA"[3]. Angular distributions for $^{58}Ni+^{60}N$ at $E_{cm}=127.1$MeV, for $^{62}Ni+^{64}Ni$ at $E_{cm}=123.0$ MeV and for $^{58}Ni+^{64}Ni$ at $E_{cm}=118.8$MeV are shown in Fig.1. Bell shaped structures are observed at the backward angles in elastic scattering which are due to the two-neutron transfer process. The data were analyzed with the computer code Ptolemy. The elastic scattering amplitude was obtained by the coupled-channels calculation including the first 2^+ and 3^- states of target and projectile nuclei. The two-neutron transfer amplitude was calculated by using the macroscopic pair-transfer form factor of $F(r)=(\beta_p R/3A)(\delta U/\delta r)$, where β_p was the pair-deformation parameter which measured the collective strength of the pair modes[4]. R,A and U are the nuclear radius, mass number and the optical potential, respectively. For the case of superfluid systems, a large pair-transfer cross section is predicted by the BCS approximation in which the pair-deformation parameter β_p is expressed as $\beta_p=2\Delta/G$, where Δ and G are the gap parameter and the pairing strength[5].

The calculated results are shown by solid lines in Fig.1. The data of the $^{58}Ni+^{60}Ni$ system are reproduced well with a pair-deformation parameter of $\beta_p=7.0$, while for the $^{58}Ni+^{64}Ni$ and $^{62}Ni+^{64}Ni$ systems the parameter increases to $\beta_p=8.4$ and 9.0, respectively. The result indicates the pair-transfer cross section increases as the number of valence neutrons. In the BCS approximation mentioned above,the pair-deformation parameter for the Ni+Ni system is estimated as $\beta_p\sim9.5$ with the approximated values of $\Delta=12/A^{1/2}$ (MeV) and $G=20/A$ (MeV). Therefore the $^{62}Ni+^{64}Ni$ system is seen to have the large pair-transfer cross section comparable to the one predicted for the the g.s. BCS wave function nuclei.This result can suggest a possible existence of the nuclear Josephson effect in $^{62}Ni+^{64}Ni$ system.

References

1)V.I.Gol'danskii and A.I.Lapkin, Th. Eksp.Theor. Fiz.53(1967)1032.
2)M.C.Mermaz and M.Girod, Phys. Rev. C53(1996)1819.
3)Y.Sugiyama et al.,Phys. Rev. C55(1997)R5.
4)C.H.Dasso and G.Pollarolo, Phys. Lett. 155B(1985)223.
5)D.R.Bes, P.Lotti, E.Maglione and A.Vitturi, Phys. Lett. 169B(1986)5.

[1]Physics Department,Tohoku University

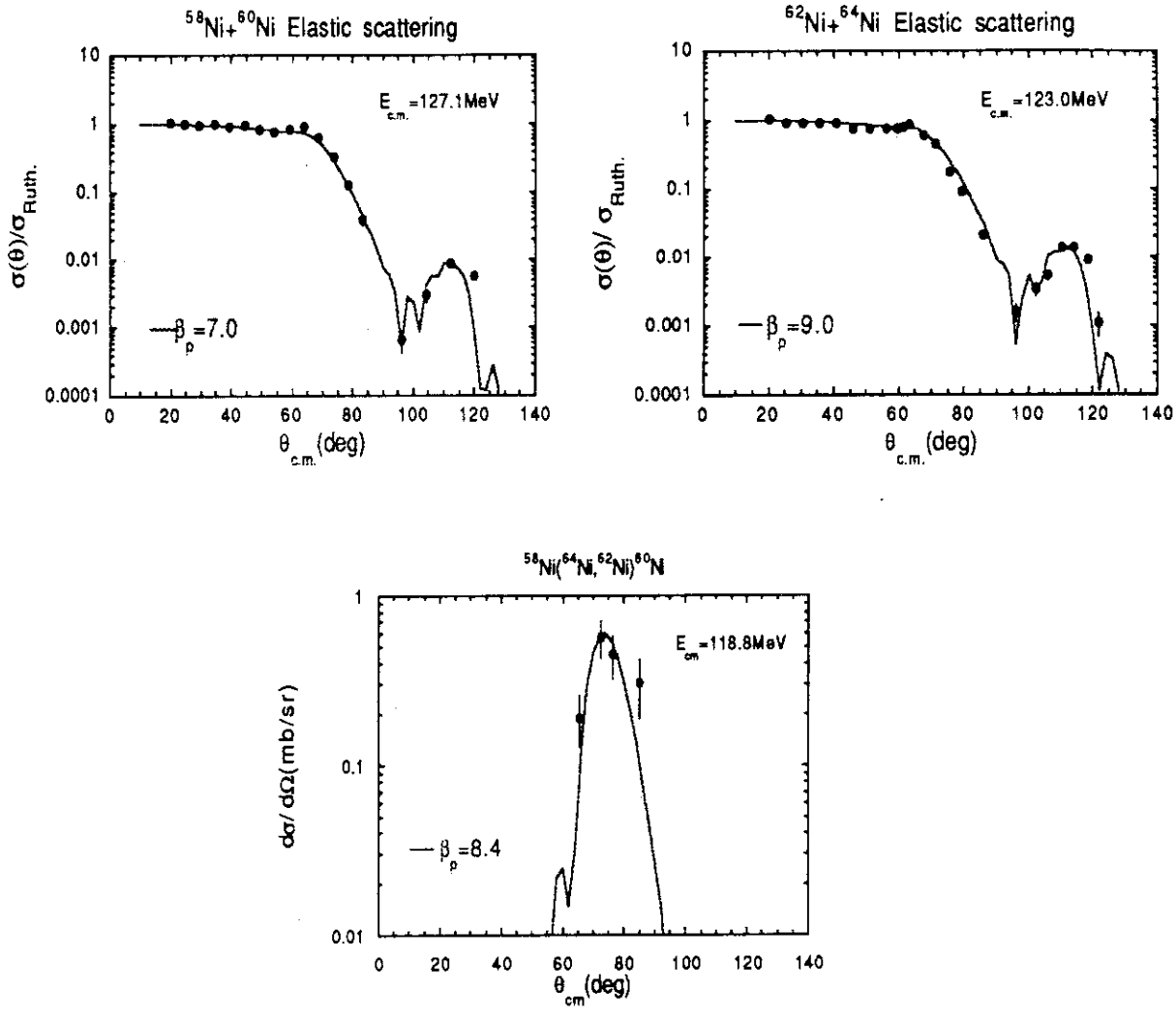

Fig.1 Angular distributions for elastic scattering of ^{58}Ni+ ^{60}Ni and ^{62}Ni+ ^{64}Ni and for the neutron pair transfer reaction of ^{58}Ni+ ^{64}Ni. Solid lines are the results of the theoretical calculations.

3. 6 STUDY OF PROTON RADIOACTIVITIES IN THE VICINITY OF ^{100}Sn

T. IKUTA, H. IKEZOE, S. MITSUOKA, Y. NAGAMA, K. TSUKADA AND I. NISHINAKA

The first identification of doubly-magic nucleus ^{100}Sn was achieved by using the projectile fragmentation technique[1,2]. The production rate was very low and its observation demonstrated only that it was unbound against proton decay. In this region of the nuclear chart, it is recognized that fusion evaporation reactions are very competitive with fragmentation reactions. The most favorable fusion evaporation reaction to produce ^{100}Sn is expected to be ^{58}Ni(^{50}Cr, α4n) reaction. The recent experiment performed at GANIL exhibits the production cross section of 40 nb which is three order of magnitude larger than the ones in fragmentation reactions[3].

We have performed ^{58}Ni(^{58}Ni, α3-4n) reaction to produce new Xe isotopes and studied their subsequent decays using the JAERI recoil mass separator. A 1.0 pnA beam of 280 MeV ^{58}Ni ion was used to bombard a 600 μg/cm^2 thick isotopically enriched ^{58}Ni target over a period of 56 hours. The present electronic system was ready for the analysis of successive events at least more than 300 μs interval. This limitation mainly originates from long conversion time of our ADC(80 μs). Actually this value is not sufficient to investigate parent-daughter decay correlation in this region. To identify parent decays with time interval shorter than 300 μs, an additional amplifier was used. Figure 1 shows a spectrum obtained with this amplifier. Proton decay of ^{109}I(E_p=0.81 MeV, $T_{1/2}$=100 μs) and subsequent α decay of daughter nucleus ^{108}Te was successfully observed.

Typical beam intensity of 1.0 pnA was not sufficient to produce ^{109}Xe and at least ten times higher beam intensity was required. After this experiment, we investigated new optical condition of the JAERI-RMS. According to the matrix ion-optical code GIOS[4], acceptance angle of the horizontal direction was three times larger where the M/Q dispersion to be zero than the one in normal condition(M/Q=-1.1 mm/%). We expect that the JAERI-RMS with this condition still shows sufficient separation ability in the new isotope search experiments. Now the experiments for measurements of the transport efficiency of the JAERI-RMS is under preparation.

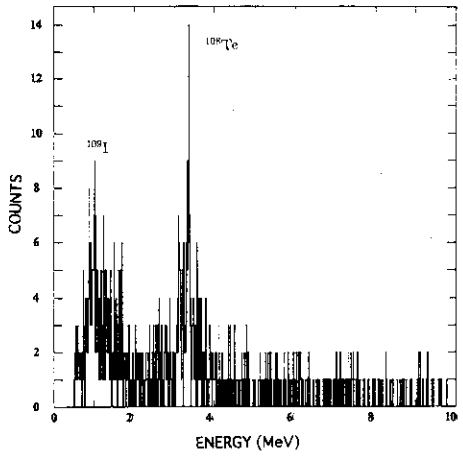

Fig. 1. Decay events measured within the time interval of 300 μs from the detection of residue event.

References

1) R. Schneider, J. Friese, J. Reinhold et al, Z. Phys. **A348**, 241(1994)
2) M. Lewitiwicz, R. Anne, G. Auger et al, Phys. Lett. **B332**, 20(1994)
3) W. Mittig, M. Chartier, J. C. Angélique et al, Nucl. Phys. **A616**, 329c(1997)
4) H. Wollniket al., GIOS a program for the design of general ion-optical systems.

3. 7 CORRELATION BETWEEN MASS DIVISION MODES AND NEUTRON MULTIPLICITY IN FISSION OF LIGHT ACTINIDES

I. NISHINAKA, Y. NAGAME, K. TSUKADA, S. ICHIKAWA, H. IKEZOE, Y.L. ZHAO [1], Y. OURA [1], K. SUEKI [1], H. NAKAHARA [1], M. TANIKAWA [2], K. TAKAMIYA [3], and K. NAKANISHI [3]

In order to understand how the deformability of fragments is related to the mass division modes, we have measured TKE and neutron multiplicty (ν) as a function of fragment mass number in the p + ^{232}Th, ^{238}U fission reactions using a double-TOF technique. The correlation between fragment mass, TKE and ν has been investigated.[1]

Proton beams at $E_p = 11 \sim 16$ MeV were supplied from the JAERI tandem accelerator to bombard the ^{232}Th and ^{238}U targets (70 μg/cm^2) evaporated on carbon backing foils (30 μg/cm^2). Two microchannel plate detectors (MCPDs) and an SSD were placed at Θ_{lab}=50° to measure the velocity and energy of a fission fragment. An MCPD and a two-dimensional position sensitive (10 cm x 10 cm) parallel plate avalanche counter were set at Θ_{lab}=129° at the opposite side of the beam direction to detect the complementaly fragment. The flight path and solid angle of the former detector were 55 cm and 0.17 msr, and those of the latter were 50 cm and 32 msr.

The number of neutrons emitted from the fragment is obtained from the defference between the primary fragment mass number and the secondary one. Figure shows the average ν (a), the average TKE (b) and the mass yields (c) as a function of primary fragment mass number. The closed and open symbols indicate the results for the 13.2 MeV p+^{232}Th and the 12.8 MeV p+^{238}U reactions, respectively. The shapes of the neutron multiplicity as a function of fragment mass number in both the reactions show the "saw-tooth" structure, in which the multiplicity increases with fragment mass as a whole but shows a large dip is observed in the region of the mass number A $\sim$ 130. In the p + ^{232}Th reaction, another dip is clearly observed around A $\sim$ 100. These dips are correlated to the peaks of the asymmetric mass distribution where the average TKE of fragments show maxima.

We are going to analyze the correlation between the mass division modes and the neutron multiplicity in view of the energy balance in the fission process.

References

[1] Y. Nagame *et al.*, Phys. Lett. **B387**, (1996) 26.

[1]Faculty of Science, Tokyo Metropolitan University
[2]School of Science, The University of Tokyo
[3]Faculty of Science, Osaka University

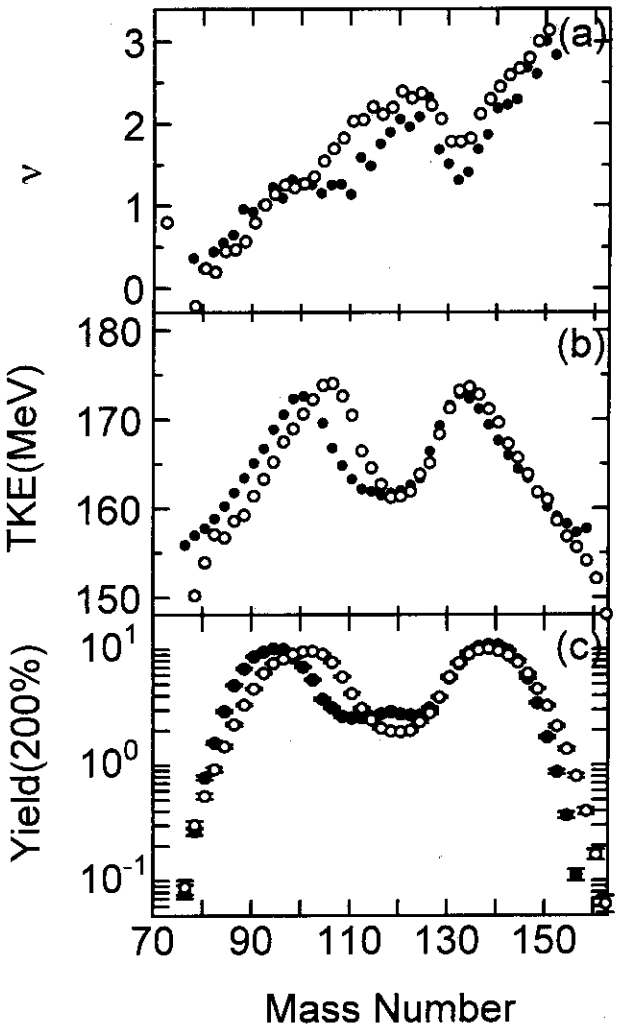

Figure:(a) Average number of neutrons emitted per fragments, (b) average total kinetic energies, and (c) mass distribution of primary fragments as functions of primary fragment mass in the 13.2 MeV p+^{232}Th (closed symbols) and the 12.8 MeV p+^{238}U (open symbols) reactions.

3. 8 THE PROPERTIES OF SCISSION SHAPES IN ^{244}Pu(p,f)

Y.L. ZHAO[1], Y. NAGAME, I. NISHINAKA, K. TSUKADA, S. ICHIKAWA, Y. HATSUKAWA, K. HATA, H. IKEZOE, Z. QIN[2], Y. OURA[1], K. SUEKI[1], H. NAKAHARA[1], M. TANIKAWA[3], T. OHTSUKI[4], and H. KUDO[5]

Recently it has been being conscious of the significance of precise and systematical study on scission properties in the exit of fission process in order to thoroughly understand the mechanism of nuclear fission. Theoretically, the multi- mode (include two modes) fission model [1] based on the calculations of scission shapes has achieved an outstanding success in reproducing some experimental observations. The quantitative calculations of the fragment properties depend on the scission shapes. But the scission shape of fissioning nucleus cannot be obtained from the model itself, therefore, the experimental investigation of the scission properties becomes quite necessary.

By using the JAERI tandem accelerator, we have studied the low energy proton- induced fission of light actinides and found that there were at least two deformation paths from saddle to scission [2]. In those experiments, the properties of two kinds of scission shapes have been investigated, too. In this report, the similar study is applied to the fission of heavier actinide, ^{244}Pu, induced by 15 MeV proton beam, to test the effects of nucleons of fissioning nucleus on scission properties. The experimental method is similar as described in ref. [3].

The total kinetic energy (TKE) and mass number for each fission fragment were obtained from the measurement of their velocities. The TKE distributions for fragment mass number between pure symmetric (A $A_f/2$) and pure asymmetric (A>138) ranges were deviated from a single Gaussian; it was hence decomposed by assuming two Gaussian distributions, the parameters were determined from the experimental data systematics. As the TKE is mostly arisen from the Coulomb force at the moment of rupture of the neck, two components of TKE distributions mean an existence of two kinds of the distances between the charge centers of complementary fragments. Namely two categories of the scission shapes which lead to the same mass split. The properties for these two kinds of scission shapes are shown in fig. 1, the low TKE component smoothly varies along the line passes through the triangles with charge distance around 18.5 fm, on the other hand, the high TKE component goes through the closed circles with its charge distance about 17 fm. The standard deviation for the former scission shape is about 1.5 fm and that for the latter is about 1.2 fm. For instance, when we consider the mass split of producing A=130 fragment, it results from two types of scission nucleus, as together illustrated in fig. 1. This behavior shows similar features with that in the fission processes of light actinides. But the different property between two kinds of scission shapes becomes smaller as compared to that in light actinides fission. The interesting question is, where is the upper limit at where the property difference between two kinds of scission shapes disappears? The further works are needed.

As a summary, a schematical picture is sketched in fig. 2 on basis of both the light actinides fission [2,3] and the present experimental results. When the compound nucleus deform near to the saddle, they are divided into two groups due to the emergence of role of nuclear shell. The elongated scission shape is the products of one group while the compact scission shape is resulted from the other.

[1]Department of Chemistry, Tokyo Metropolitan University
[2]Institute of Modern Physics, Lanzhou, China
[3]Department of Chemistry, University of Tokyo
[4]Laboratory of Nuclear Science, Tohoku University
[5]Department of Chemistry, Niigata University

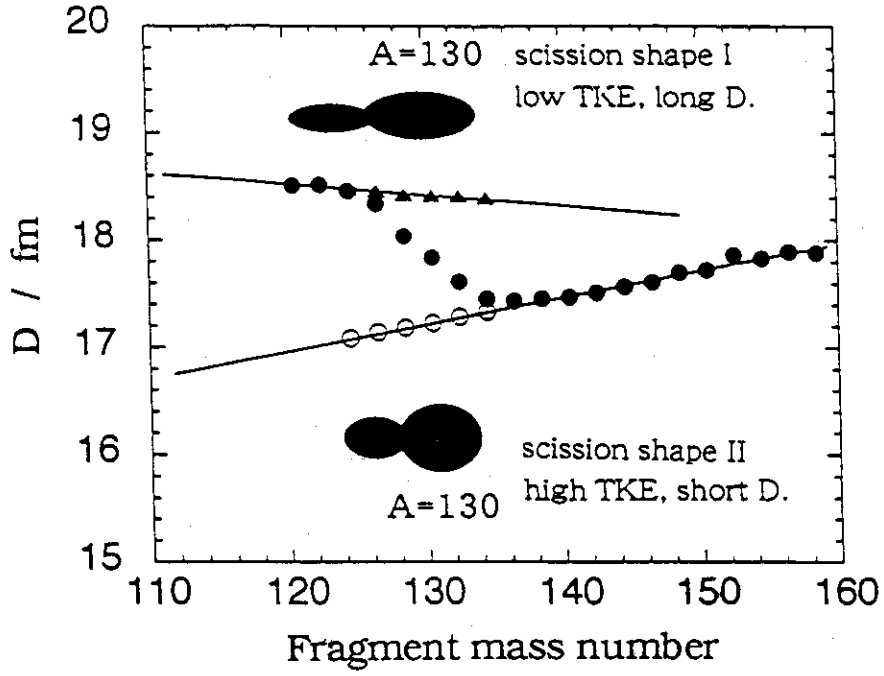

Fig. 1. The centre distance between a pair of fragments at the moment of rupture of the neck. Two lines are drawn to indicate the two groups of nucleus corresponding to the two types of scission shapes.

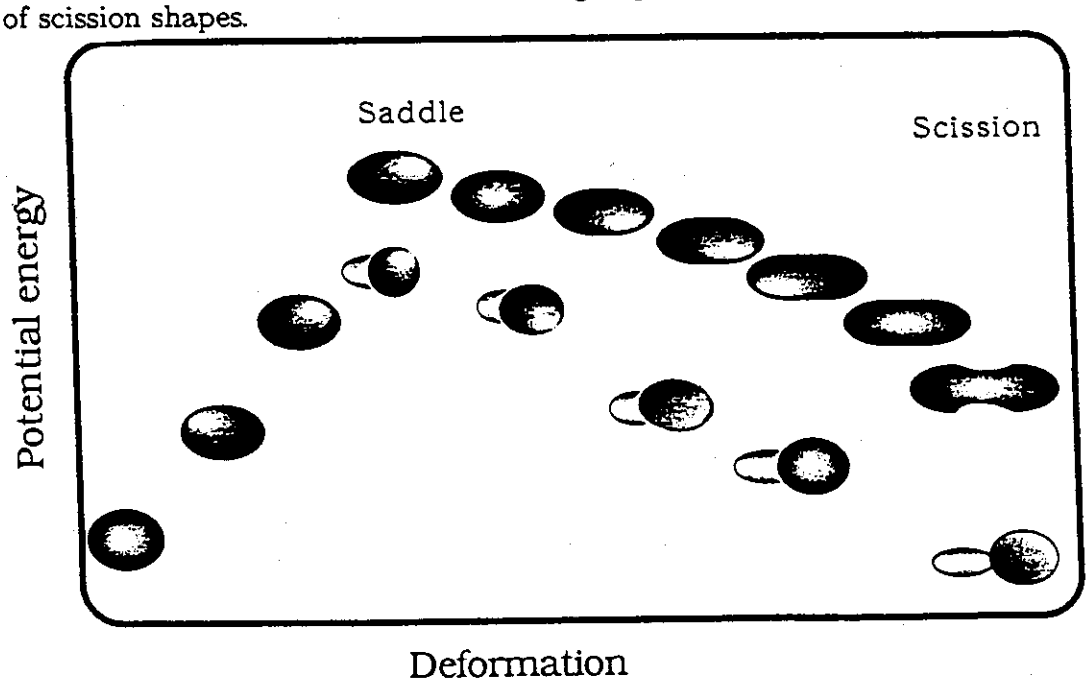

Fig. 2. A schematically picture is sketched to describe the two categories of scission shapes and their formation processes.

References
1) U. Brosa, S. Grossmann, A. Muller, and E. Becker, Nucl. Phys. **A502**, 423 (1989).
2) Y. Nagame, I. Nishinaka, K.Tsukada, Y. Oura, S. Ichikawa, H. Ikezoe, Y. L. Zhao, K. Sueki, H. Nakahara, M.Tanikawa, T. Ohtsuki, H.Kudo, Y. Hamajima, K. Takamiya, and Y. H. Chung, Phys. Lett. B **387** (1996) 26.
3) Y. Nagame, I. Nishinaka, K.Tsukada, Y. Oura, S. Ichikawa, H. Ikezoe, Y. L. Zhao, K. Sueki, H. Nakahara, M.Tanikawa, T. Ohtsuki, H.Kudo, Y. Hamajima, K. Takamiya, and Y. H. Chung, Radiochem. Acta, (1997), in press.

3. 9 DUALITY MECHANISM OF σ-/π- BINDING BANDS IN CRC PROCESS OF ^{9}Be-^{10}Be^{10}B-^{11}B NUCLEI

S.HAMADA, T.IKUTA, K.SUGIYAMA, A.YAMASAKI*

Cluster structure and the clustering aspect of nuclei in scoping the molecular similarity in atomic substances have been a good test for the study of light nuclei in a few recent decades.[1] The basic physical concepts of this α clustering aspects are formed by the description of the two perspective of the nuclear matter. The dispersion of single particle shell orbitals which behaves as the dilute nuclear matter gas and the concentration of the matter density preforming the α blobs into α-n rings and/or α-n linear chains, hence the phase transition between these different thermodyanamical states.

Starting from A=6,7 and 8 nuclei, where the ground and lower continium state of ^{6,7}Li is known as loosly bound alpha-cluster structure having large component of α+d and α+t form factors, respectively.[2] Ground state of ^{8}Be is unstable, that decays spontaneously into two alpha particles. This nature leads us to the folowing remarkable steps of primordial astrophysical Helium burning and also of α-nuclear synthesis, as is described in Ref.[3]

$$\alpha + \alpha \rightleftharpoons {}^{8}Be,$$
$$\alpha + {}^{8}Be \rightleftharpoons^{12} C^{*}(7.65MeV),$$

but, what the *thermal equilibrium "Salpeter-process"* requires in Gamov energy region, has been considered for long time to have quite enigmatic cluster structure of ^{12}C*(7.65MeV) [4], constituent α-n blobs chain as mentioned above.

As of it's difficulty in nature to reveal the 3α cluster linear chain explicitely, this direct Helium burning process is not well understood. In fact, cosmological nuclear abundance of mass A=6,7 and the mass-gap in A=8 is suggestive quite interestingly for several significant reaction passes, such as ^{6,7}Li+α and ^{7}Be+α, alternative to the thermal Helium barning, even if it is in astrophysical relevant energy region [5].

Such critical particle emission thresholds lie relatively high in the excitation energy of $^{9-11}$Be, $^{9-13}$B nuclei. For one example in ^{9}Be and ^{9}B nuclei, binding energy of deuteron + core nucleus system lie 16.70 MeV and 16.49 MeV, for ^{7}Li + d and ^{7}Be + d, respectively. Those for triton are 17.69 MeV of ^{6}Li + t and 20.91 MeV of ^{6}Be + t. Hence, of it's charge exchange combinations, we find ^{6}He + ^{3}He at 21.18 MeV and ^{6}Li + ^{3}He at 16.60 MeV.

Here we can attach a relevance of charge conjugate cluster combinations, t + ^{6}Li and ^{3}He + ^{6}Li, both having the same core ^{6}Li, in quite reasonable energy gap within 1 MeV. Also within this energy gap, more unstable components of t +^{6}Be and ^{3}He + ^{6}He lie near the analog halo-like structure in ^{9}Li. This characteristic feature of particle unbound states attracts very intensive theorethical interests[6] since the relevant multi-cluster configurations surviving in shell orbital description reinforce the treatment and developpement of LCAO description for molecular orbits of nuclear matter.

Here, we investigated the nuclear structure of ^{11}B nuclei via ^{9}Be(^{6}Li, α) ^{11}B reaction which reveled an importance of succeeding several reaction channels of intermediate excitation states, stepping from ^{9}Be through ^{10}Be and ^{10}B, upto final residual states of ^{11}B. We

* Faculty of Science, Tohoku University

demonstrate the possible paths of nuclear contact of ^{6}Li projectile into 1) direct transfer of deuteron after a good separation into α + d state, 2) sequential transfer of two nucleons proceeding by each proton and hence neutron, vice versa. 3) characteristic population of ^{11}B excited state (Ex $\simeq$ 16.5 MeV) seen in (^{6}Li, α) spectrum which was also suggested as having extraordinary spin configuration of intruder $2s_{1/2}$ orbit indicated from the (^{3}He, p) and (d, γ) reactions on ^{9}Be nuclei. [7] Those two reports suggested the possible configuration of spin ($\Delta S = 1$) transfered feature lying on the basical sheme of $T_>$ (T=3/2) excitation which is caused by the distinct σ-binding split from it's lower counterpart of π-binding orbits. Further investigations on this relatively narrow and strong peak with more low background and also with more sofisticated DWBA analysis on it's angular distribution are needed.

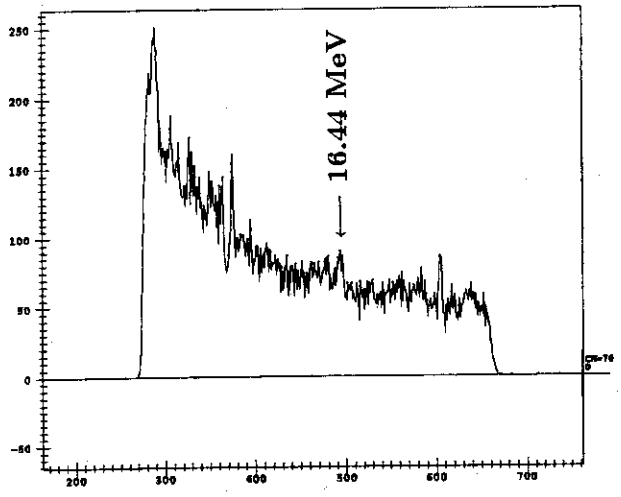

Fifure
Momemtum spectrum of ^{9}Be(^{6}Li, α)^{11}B reaction measured by ENMA-SWPC-Plastic Scintilator system. Horizontal axis corresponds to the particle momentum, approximately linear to the reaction Q-value at this angle θ=30°. Around Ex=16.44 MeV, relatively narrow and strong peak was seen which leads to the spin-flipped dipole resonance observed in (^{3}He, p) and (d, γ) reaction.

Refereces
1)W. von Oertzen, private communication, "Dimers based on the α+α Potential and Chain States of Carbon Isotopes, ^{12}C to ^{16}O" to be published.
W. von Oertzen, Z. Phys. A 354 (1996) 37. D.H. Wilkinson, Nucl. Phys. A 452 (1986) 296
2) S.L. Tabor, L.C. Dennis and K. ABDO, Nucl. Phys. A391 (1982) 458
M. Hugi, J. Lang, R. Müller, E. Ungricht, K. Bodek, L. Jarczyk, B. Kamys, A. Magiera, A. Strzałkowski and G. Willim, Nucl. Phys. A368 (1981) 173.
3) Claus E. Rolfs and William S. Rodney. *"Cauldrons in the Cosmos"* Chicago University Presse, 1988
4) N.De Takacsy et al. Phys. Lett. 33B (1970) 556. "Can the 7.65 MeV 0^{+} state in ^{12}C belong to a liner chain of α- clusters ?"
5) P. Descouvement. Nucl. Phys. A584 (1995) 532. Jingsheng Yan, F.E. Cecil, J.A. McNeil, M.A. Hofsee and P.D. Kunz, Phys. Rev. C55 (1997) 1890.
6)K. Arai et al. Phys. Rev. C54 (1996) 132
7)B. Zwieglinski et al. Nucl. Phys. A389 (1982) 301.
W. Del Bianco, S. Kundu and B. Rouben, Nucl. Phys. A232 (1974) 333.

3.10 STUDY OF PREEQUILIBRIUM (p,p') AND (n,n') REACTIONS FOR LOW INCIDENT ENERGIES

Y. WATANABE[1], S. YOSHIOKA[1], M. HARADA[1], K. SATO[1], Y. NAKAO[1], H. IJIRI[1], N. KOORI[2], S. CHIBA, T. FUKAHORI, S. MEIGO, and O. IWAMOTO

The statistical multistep reaction theory of Feshbach-Kerman-Koonin(FKK)[1] has been applied to analyze various experimental data for nucleon-induced preequilibrium reactions[2]. The FKK model reproduces those experimental data well by adjusting some model parameters, one of which is the strength V_0 of the effective N-N interaction used in the multistep direct (MSD) calculations. Since the strength V_0 determines the magnitude of MSD cross sections, it is crucial to study the systematic trends (i.e., the dependence on incident energy and mass number) from the viewpoints of nuclear data evaluation as well as nuclear physics. Recent analyses for low incident energies[3,4] have found that different V_0 values between (p,p') and (n,n') are necessary to fit both the experimental data for the same incident energies. However, a complete set of (p,p') and (n,n') data for the same targets and incident energies was not available in those analyses. Therefore, we have undertaken to measure preequilibrium (p,p') spectra for the same targets (^{56}Fe and ^{93}Nb) and incident energy (26 MeV) as in the previous (n,n') measurements[5] in order to see whether or not both (p,p') and (n,n') data can be described consistently well by the FKK model and to investigate the systematic trend of the extracted V_0 values.

The experiment was performed using a 26 MeV proton beam from the JAERI tandem accelerator. The experimental procedures were basically the same as those reported in Refs.[3,6]. The targets used (^{54,56}Fe, ^{90}Zr, and ^{93}Nb) were self-supporting metallic foils of about 500 μg/cm^2 thickness. We have used a stacked ΔE-E silicon detector counter telescope with an active collimator made of an NE102A plastic scintillator[7,8]. The thicknesses of ΔE and E silicon detectors were 30 μm, 200 μm, and 5000 μm. The active collimator played a role as a veto detector to reduce the continuum background component due to the edge-penetration which makes it difficult to measure continuum (p,p') spectra at small angles. Energy spectra of emitted protons were measured at angles in steps of 10° from 30° to 150°.

Both the data of ^{93}Nb(p,p') at 14.1 MeV[9] and 26 MeV were analyzed using the modified FKK-GNASH code[3,10] in which the FKK model for the preequilibrium process and the Hauser-Feshbach (HF) model for the compound process were used. The V_0 values were extracted using the same subtraction method as described in Ref.[3]. The other parameters used were same as those in Ref.[3]. In Fig.1, the extracted V_0 values are plotted as a function of the incident energy together with our previous results of (n,n') for ^{93}Nb and (p,p') for ^{98}Mo and ^{106}Pd[3]. There is found to be a systematic trend that the V_0 values for ^{93}Nb(p,p') are larger than those for (n,n') at low energies and both values become close with increasing incident energy. A possible explanation is given by a consideration of the local kinetic energy near the nuclear surface where the reaction takes place predominantly as discussed in Ref.[3]. Furthermore, the density-dependence of effective interaction might also be related to the difference in V_0, because the radial dependence of the first NN collision probabilities for (p,p') and (n,n') is different as discussed in Ref.[11].

Using each best fit V_0 value, we have calculated the angle-integrated (p,xp) and (n,xn) spectra for ^{93}Nb at 14.1 MeV and 26 MeV using the modified FKK-GNASH code and compared them with the experimental data. The result of 26 MeV is shown in Fig.2. The input parameters except the V_0 values were same for both (p,xp) and (n,xn). In the HF calculation of (p,p'), isospin was taken into account as an additional quantum number in the same way as the case (B) in Ref.[10]. The calculation provides satisfactory agreement with both experimental data of (p,xp) and (n,xn) in the continuum region of 12 to 20 MeV as shown in Fig.2.

[1] Department of Energy Conversion Engineering, Kyushu University
[2] Faculty of Integrated Arts and Sciences, The University of Tokushima

Further FKK analyses of the other nuclei are now in progress to see the mass number dependence of the strength V_0.

References

[1] H. Feshbach, A. Kerman, and S. Koonin, Ann. Phys. (N.Y.) **125** (1980) 429.
[2] E. Gadioli and P.E. Hodgson, Preequilibrium Nuclear Reactions, (Oxford University Press 1992).
[3] Y. Watanabe et al., Phys Rev. C **51** (1995) 1891.
[4] P. Demetriou et al., J. Phys. **G22** (1996) 629.
[5] A. Marcinkowski et al., Nucl. Sci. Eng. **83** (1983) 13.
[6] Y. Watanabe et al., Phys. Rev. C **36** (1987) 1325.
[7] M. Hayashi et al., Proc. of the 1994 Symp. on Nuclear Data, Nov. 17-18, 1994, JAERI, Tokai, JAERI-Conf 95-008 (1995), pp. 225.
[8] Y. Nakao et al., Kyushu University Tandem Accelerator Laboratory Report (1993-1994), KUTL report-5 (1995), pp. 115.
[9] S. Yoshioka, Proc. of the 1996 Symp. on Nuclear Data, Nov. 21-22, 1996, JAERI, Tokai, JAERI-Conf 97-005 (1997), pp. 301.
[10] Y. Watanabe, Proc. of Int. Symp. on Pre-Equilibrium Reactions, Smolenice, October 1995, acta physica slovaca **45** (1995) 749.
[11] M. Avrigeanu et al., Phy. Rev. C **54** (1996) 2538.

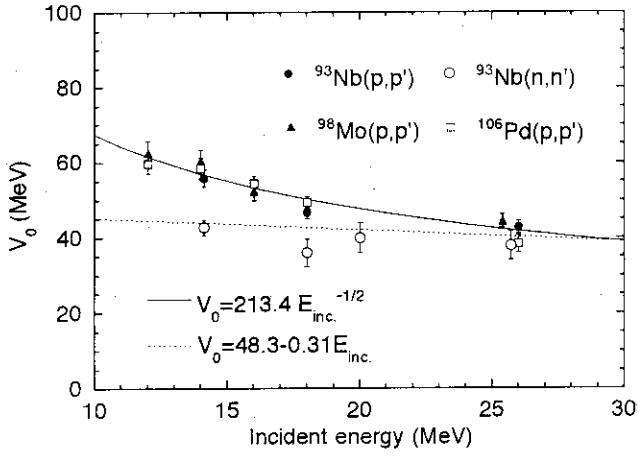

Fig.1 The extracted strength V_0 plotted as a function of the incident energy.

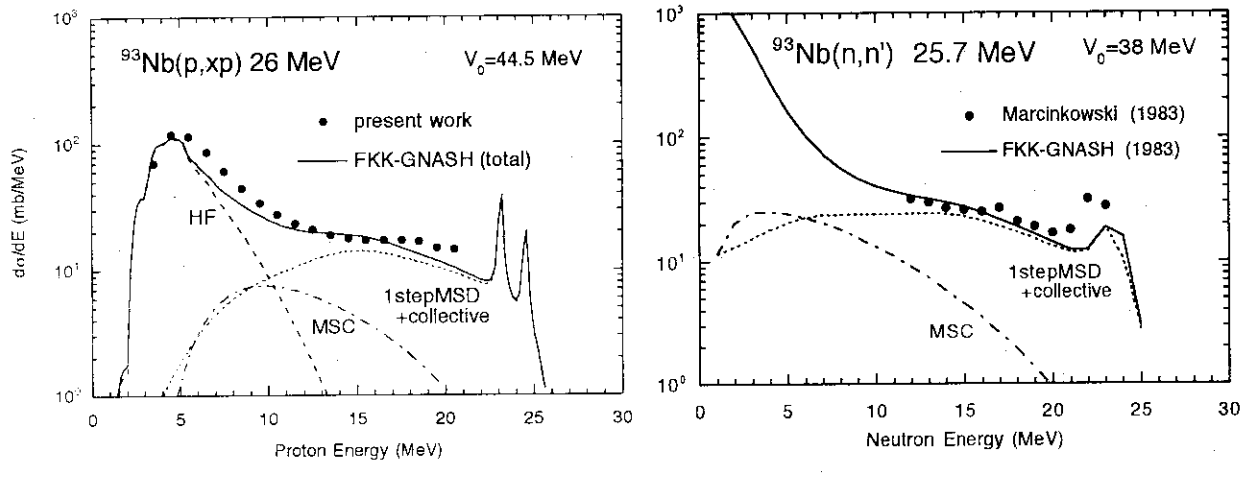

Fig.2 Comparison of the experimental angle-integrated (p,xp) and (n,xn) spectra for ^{93}Nb at 26 MeV with the modified FKK-GNASH calculations.

4. Nuclear Theory

4. 1 NUCLEAR DEFORMATION AND SUB-BARRIER FUSION CROSS SECTIONS

A. IWAMOTO and P. MÖLLER[1]

Sub-barrier fusion cross sections observed in experiments show enhancement over cross sections obtained in calculations based on the assumption of spherical projectile and target shapes and a corresponding one-dimensional fusion barrier. This enhancement has been studied both experimentally and theoretically for about 20 years. When both the projectile and the target are very heavy, however, it is rather hard to perform realistic coupled-channel calculations and to fit the measured cross sections.

We calculate here for a series of X + ^{154}Sm reactions, ^{16}O+^{186}W and ^{16}O+^{238}U fusion cross sections in a model that contains *no* free parameters, except for a simple shift in energy of the calculated cross section. These reactions involve a deformed nucleus and we attempt to investigate to what extent the subbarrier enhancement is accounted for by the concept of deformation. Deformation is related to the synthesis of the superheavy nuclides by hugging fusion mechanism [1] and this research might be the first step to that direction. The details of present study are given in [2].

To treat the simplest non-spherical configuration, namely a spherical projectile colliding with a deformed, axially- and mass-symmetric target we introduce the angle θ between the target symmetry axis and the beam direction. In a simple extension of the spherical formalism, a generalization that contains several approximations, we write for the fusion cross section $\sigma_{\rm f}$:

$$\sigma_{\rm f} = \int_{r_1}^{r_2} \sin\theta \, d\theta \sum_L \sigma_{\rm f}(L,\theta) \tag{1}$$

with the partial cross section $\sigma_{\rm f}(L,\theta)$ for a particular angular momentum L and orientation θ given by:

$$\sigma_{\rm f}(L,\theta) = \frac{\lambda^2(2L+1)T_L(\theta)}{4\pi} \tag{2}$$

The transmission probabilities $T_L(\theta)$ at various angles θ are obtained in WKB theory as

$$T_L = \frac{1}{1+e^{K_L(\theta)}} \tag{3}$$

where

$$K_L(\theta) = 2\int_{r_1}^{r_2} \left\{ \frac{2\mu}{\hbar^2} \left[V_{\rm p+c}(r,\theta,L) - E_{\rm cm} \right] \right\}^{1/2} dr \tag{4}$$

Here $V_{\rm p+c}(r,\theta,L)$ is the potential-plus-centrifugal energy of the projectile–target configuration as a function of the separation r between their centers of mass, the angle θ between the target symmetry axis and the beam direction, and the angular momentum L. For incident energies above the barrier we obtain the transmission probability in complete analogy with the spherical case.

Plotted in Fig.1 is the two-dimensional (ρ-z axes) potential energy surface for ^{16}O+^{238}U using the model of [3] based on the finite-range nuclear force. The deformation of the

[1] Permanent address: *P. Moller Scientific Computing and Graphics, Inc. P. O. Box 1440. Los Alamos, New Mexico 87544. USA*

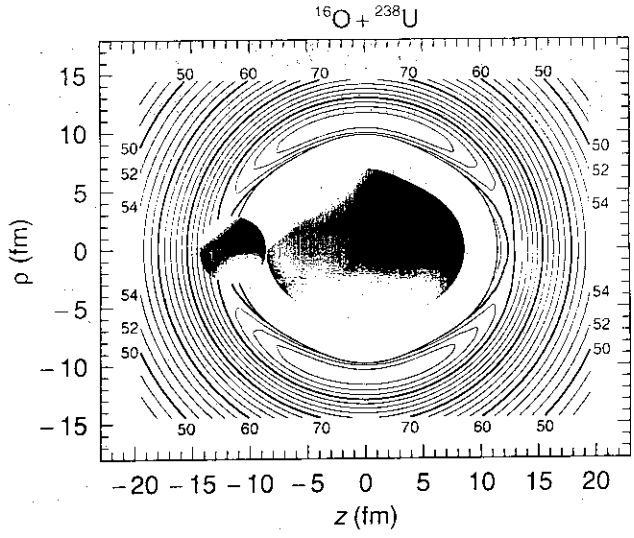

Fig.1. Interaction potential surface for $^{16}O+^{238}U$.

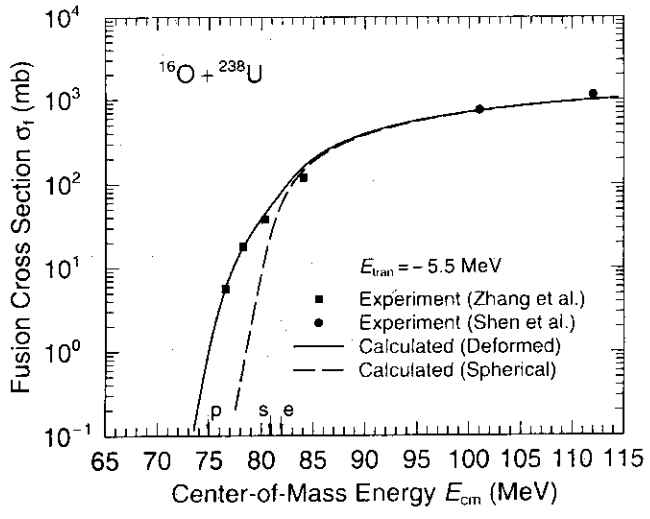

Fig.2. Fusion cross section for $^{16}O+^{238}U$.

ground state of ^{238}U was obtained by the shell correction calculation. Using this interaction potential, we calculated the fusion cross section of this system, which is shown in Fig.2. The symbols p,s,e on the abscissa mean the heights of the potential for long-axe direction, spherical nucleus and short-axe direction, respectively. The solid line calculated with the ground state deformationof ^{238}U reproduces the data well whereas the dashed line calculated with the spherical ^{238}U fails to fit the subbarrier data. We also calculated the barrier distribution of this system and got fairly good reproduction of the data.

Among other systems we tried, the reactions with projectiles lighter or equal to ^{28}Si were well reproduced by our calculations. For heavier projectiles of ^{32}S and ^{40}Ar, the calculated subbarrier cross sections underestimate the data. This discrepancy might be related to the increasing importance of the excitation of projectiles as their masses increase.

References

[1] A. Iwamoto, P. Möller, J.R. Nix and H. Sagawa, Nucl. Phys. **A596** (1996) 329.
[2] A. Iwamoto and P. Möller, Nucl. Phys. **A605** (1996) 334.
[3] P. Möller and A. Iwamoto, Nucl. Phys. **A575** (1994) 381.

4. 2 E1 TRANSITIONS IN RARE EARTH NUCLEI

M. SUGITA

Electric-dipole ($E1$) transitions between low-lying states of well deformed rare-earth nuclei are investigated using an SPDF boson model. The model can treat both the high-lying Giant Dipole Resonance (GDR) and the low-lying octupole vibrational bands. The p-boson is related to the GDR state while the f-boson is to the octupole vibration. The $E1$ operator $T(E1)$ consists of p and f boson terms; the two p boson terms are determined by the experimental data on the GDR states. The remaining $f \rightarrow d$ $E1$ transition charge is determined by fitting experimental $B(E1)$ values between low-lying collective states. The present method has been applied to ^{156}Gd, whose low-energy positive parity bands are well described by the SU(3) limit of IBM. It has been found that the $E1$ operator determined in this way gives the spin dependence of the $B(E1)$ branching ratios close to the experimental results, as has been shown in Ref. [1].

By using the same $E1$ operator, we calculated $B(E1 : 0_1^+ \rightarrow 1_1^-)$ of the Sm isotopes. The systematics of $B(E1)$ is well described by the calculation with the constant $E1$ operator, as shown in the figure. The current model does not include core particles below $Z = 50, N = 82$, which means that the semi-magic nucleus (Sm, $A = 144$ and $N = 82$) is beyond the scope of our model. The $E1$ transitions for $A = 148 \rightarrow 154$ are well reproduced, which indicates that, if many particles are outside the core, we can describe well the octupole and GDR states of such nuclei in a unified way by this SPDF model. We are now investigating microscopic foundation of the SPDF boson model.

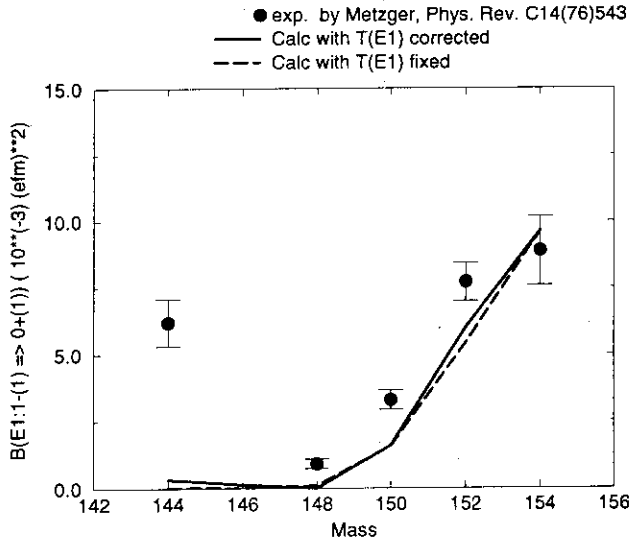

Figure 1: Mass dependence of B(E1) in the Sm isotopes

References

1) M. Sugita, T. Otsuka, and P. von Brentano, Phys. Lett. **B389** (1996) 642-648.

5. Atomic Physics, Solid State Physics and Radiation Effects of Materials

5. 1 ANGULAR SCATTERING OF HYDROGEN ACCOMPANIED WITH ELECTRON CAPTURE FROM RARE GAS ATOMS

M. Sataka, S. Kitazawa, K. Komaki[1], Y. Yamazaki[1], T. Azuma[1], H. Shibata[2]
K. Kawatsura[3], K. Kanai[4] and H. Tawara[5]

We are planning to study the correlation of electron production processes and charge changing processes. The electron emission processes in the collision of multi-charged ion and atoms and solids were investigated by means of 0 degree electron spectroscopy[1]. We started the measurement of the scattering angle in charge changing collision between fast ions and atoms.

The electron capture differential cross sections, differential in scattering angle of projectile ions, were measured 5 MeV H^+ ion impact on rare gases. H^+ was accelerated by the JAERI tandem accelerator. The ion beam was purified with use of three sets of dipole magnets, not to contaminate the beam with neutral hydrogen by collision of residual gas in the beam duct. The beam was introduced to collision cell and outgoing ions were separated using electro-static deflector and detected by Faraday cup. Neutral H atoms were detected by 2-dimensional position sensitive detector (multi-cannel plates with wedge and strip detector).

In Fig. 1, we show the 3-dimensional plots of scattered neutral H atoms after collisions of He, Ne, Ar, Kr and Xe target. In Fig. 2, we show angular distribution of neutral H atom. The nominal full width at half maximum was 0.22, 0.29 and 0.27 mrad for He, Ne and Ar targets, respectively. The ratio of total electron capture cross section (integrated cross sections of the differential cross sections) for He, Ne, Ar, Kr and Xe target is 1: 209: 463: 860: 955. The ratio is consistent as the results of the total capture measurements[2]. It is seen from the figure that the angular distribution of Ne target is almost same as that of Ar target. The width of the angular distribution is not likely to depend on the nuclear charge. In this energy region, H ions should capture the K-shell electrons for He and Ne target. The other hand, H ions capture L-shell electrons for Ar, Kr and Xe target. We suppose the angler scattering process accompanied with electron capture may depend on the effective charge and average radius of the active electron of the targets for take part in capture processes.

[1]Graduate School of Arts and Sciences, University of Tokyo,
[2]RCNST, University of Tokyo,
[3]Faculty of Engineering, Kyoto Institute of Technology,
[4]The Institute of Physical and Chemical Research(RIKEN),
[5]National Institute for Fusion Sciences.

References

1) M. Sataka, M. Imai, Y. Yamazaki, K. Komaki, K. Kawatsura, Y. Kanai, H. Tawara, D.R. Schultz and C.O. Reinhold, XIII Int. Conf on the Highly Charged Ions (Omiya, Japan 1997).

2) Y. Nakai, A. Kikuchi, T.Shirai, and M.Sataka, JAERI-M 83-143 (1983).

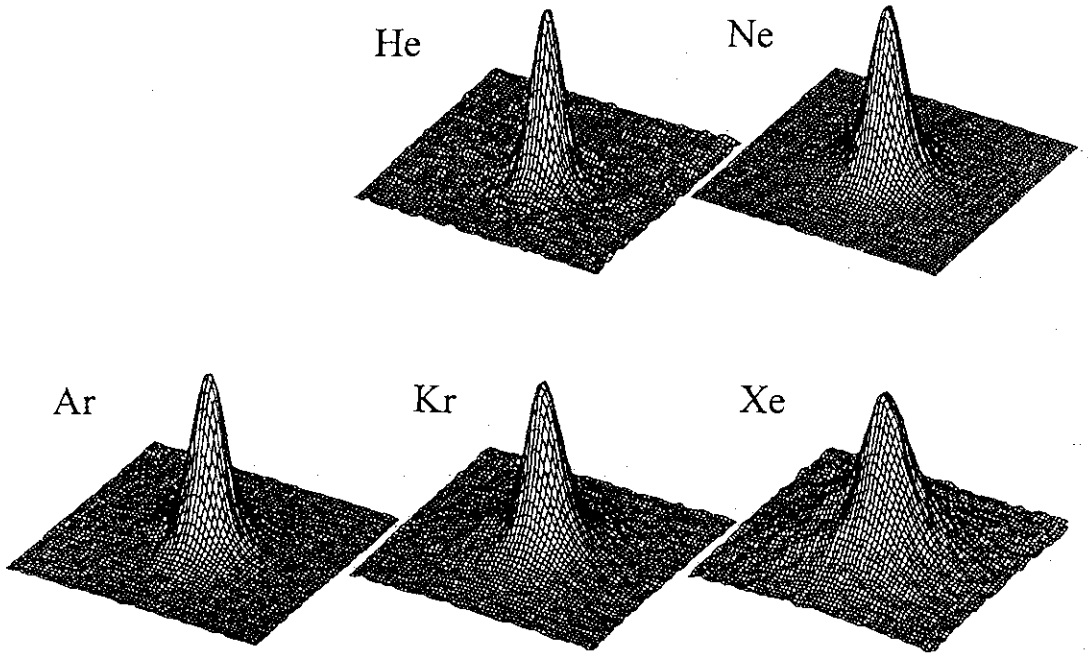

Fig.1 Three-dimensional plots of neutral H beam after collisions of rare-gas targets.

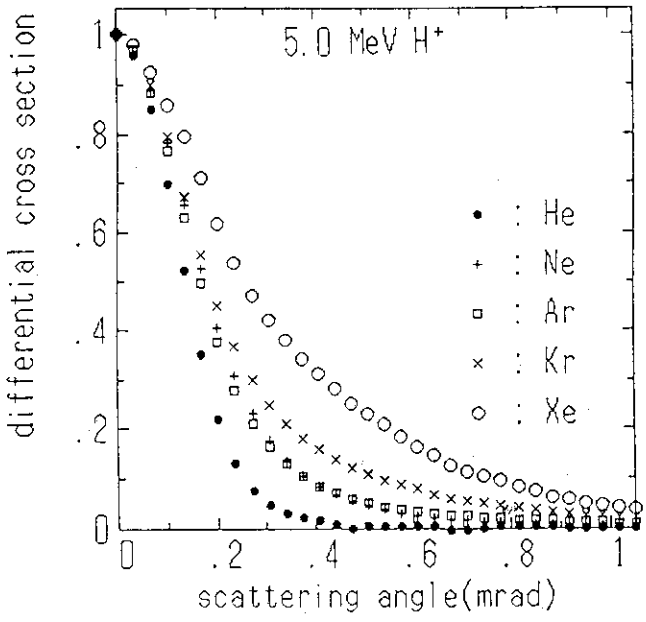

Fig. 2 Neutral beam profiles after collision of rare-gas targets.

5. 2 X-RAY DIFFUSE SCATTERING STUDY OF DEFECT CLUSTERS IN HEAVY ION-IRRADIATED COPPER

H. MAETA, H. OHTSUKA , N. MATSUMOTO, H.YUYA, H. SUGAI
T. SAOTOME[1], H.MOTOHASHI, K.YAMAKAWA[2] and F. ONO[3],

Irradiation of materials with energetic ions produces point defects and displacement cascades containing high local concentrations of vacancy -interstitial pairs, and at ambient temperature these vacancies and interstitials aggregated to form clusters such as dislocation loops, stacking fault tetrahedra, or voids. Transmission electron microscopy has provided a considerable amount of information on this process. However, additional quantitative information regarding small sizes , morphologies, internal defect densities and thermal evolution is needed for comparison with theoretical calculations and for obtaining a more complete picture of the physics of defect production and defect interaction. Even though scattering techniques do not offer direct imaging of defects as available through electron microscopy, x-ray diffuse scattering provides information complementary to that obtained by microscopy imaging in the sense that the defects are studied nondestructively in bulk with inherently good sampling statistics.

We have reported an " off-symmetry" x-ray diffuse measurements using the synchrotoron radiation source for the study of dislocation loops in heavy ion-irradiated copper single crystals. The specimens with <111> orientation were irradiated at 30 K with 150 MeV P(phosphorus) ions using the Jaeri Tandem Accelerator to fluence of 8.3 x 10^{14} ions/cm^2. Diffuse scattering experiments were performed on a four-circle diffractometer installed at BL-27B at the Photon Factory of the KEK in Tsukuba. The diffuse scattering near the 111 reflection was measured at room temperature. The measured diffuse scattering for P ion irradiated coppers is shown in the figure. These data are scaled by $q^4$and plotted as a function q along the 111 direction in reciprocal space. We note that the scattering magnitudes were found to be comparable for positive andnegative q for the irradiation, suggesting thepresence of substantial numbers of both vacancy and interstitial loops. We found sizedependence on ion dose for interstitial loops

The diffuse scattering intensities also depended with irradiation dose, suggesting that number of defects increased on ion doses.

No.1 8.3 x 10^{14} ions/cm^2
No.2 3.2 x 10^{14} ions/cm^2
No.3 1.3 x 10^{14} ions/cm^2

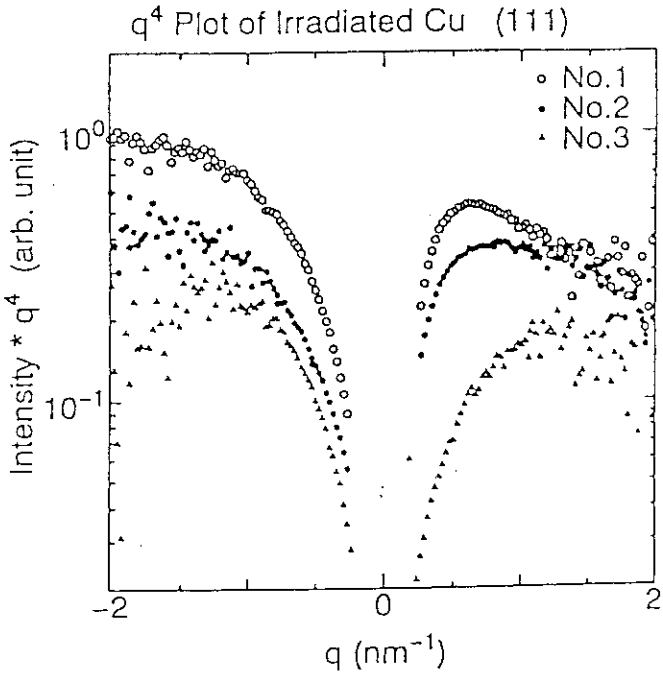

1 Faculty of Engineering, Tamagawa University,
2 Faculty of Engineering, Hiroshima University
3 Department of Science, Okayama University

5. 3 X-RAY DIFFRACTION STUDIES OF ION IRRADIATED SINGLE CRYSTAL DIAMOND

K. HARUNA [1], T. SAOTOME [1], T. SATOH[1], H. MAETA, H. SUGAI, N. MASUMOTO, F. ONO [2], H. OTSUKA and K. OHASHI [1]

Diamond based semiconductor devices may turn out to be of great technological importance due to the outstanding physical properties. It is very strong against radioactive rays and fits to the electronic devices in the high temperature region owing to the wide energy gap.
Ion implantation is a primary candidate technique for doping. There are many kinds of diamonds due to quantities of Nitrogen impurity and its form. But there are no reports for systematical X-ray diffraction studies on high energy ion doping into many type diamonds. We investigate the irradiation effects on many type diamonds by means of lattice parameter measurement by X-ray diffraction.

Investigated specimens were as follows, Natural I a, synthetic I b, synthetic II b diamonds. The synthetic single crystal diamonds were purchased from Sumitomo Denki Co.Ltd. The P and C-ion irradiations were carried out by the JAERI tandem accelerator. The ions of 150 MeV C and P were used in this study. The measurement of lattice parameter was done by Bond method in which two counters were placed symmetrically at room temperature. To attain the highest accuracy, a FeKβ beam was used, and the (400) reflection was measured at 2θ =160.01. The crystal size is (2.5-3.5)x(2.5-3.5)x0.3mm^3. Both sides of specimen were measured.

These results are shown in fig.1-5. These results show

1. natural diamond doesn't have sharp peak. It shows natural diamond is strained in process of crystal growth. 2. integrated intensities of measured X-ray diffraction profiles are different in specimen sides due to inhomgenity. 3. the remarkable increase of integrated intensities is seen after irradiation. These anomalous increase is due to the disappearance of extinction effects, which are associated with diffraction from planes strained by the point like defects and dislocation loops introduced by the ion irradiation.

In conclusion, the heavy ion irradiation into diamond distorted its crystal structure little due to strong covalent bond contray to Si with same diamond structure. This causes the disappearance of extinction effects of X-ray in diamond crystal.

---

[1] Faculty of Engineering, Tamagawa University

[2] Faculty of Science, Okayama University

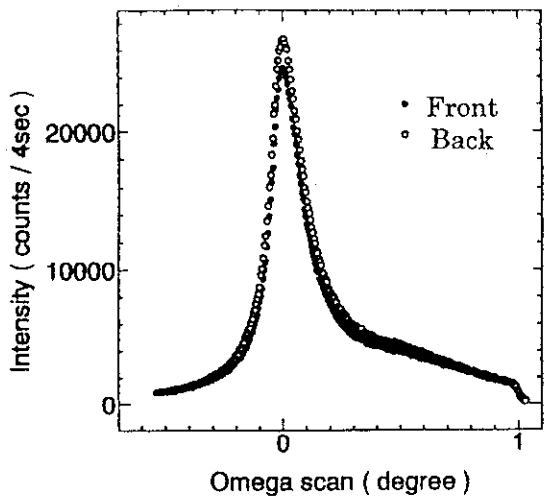

Fig.1 I b diamond

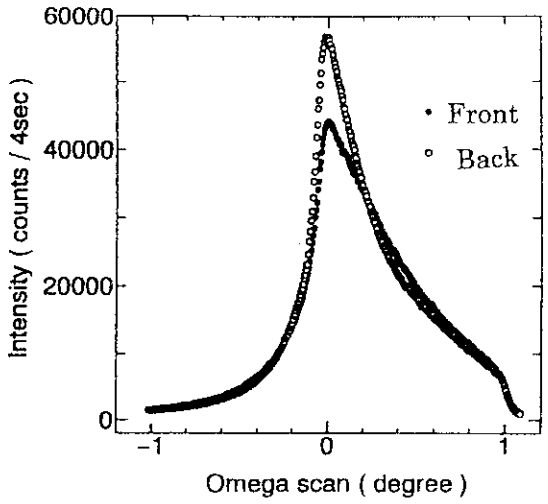

Fig.4 Natural I a diamond

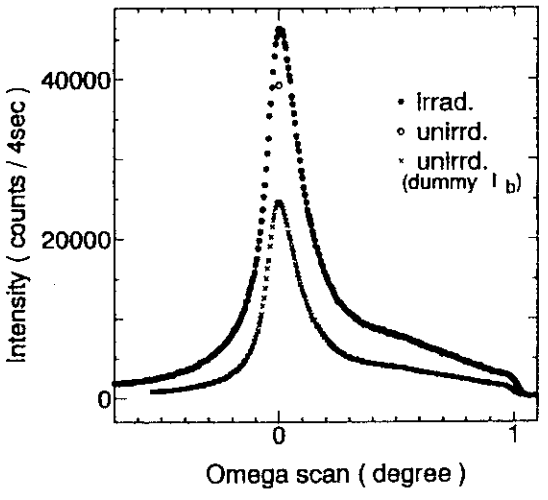

Fig.2 I b diamond irradiated C ion

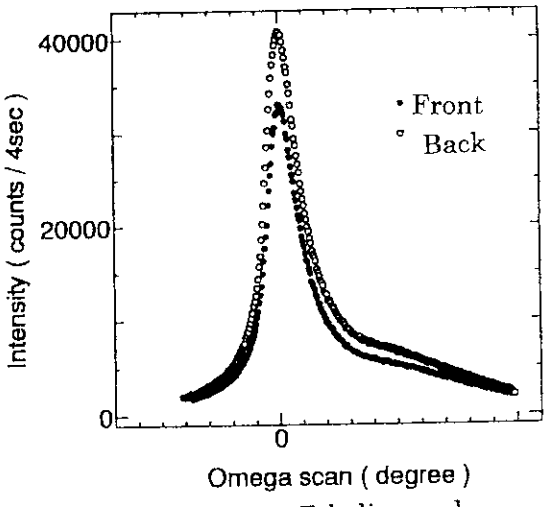

Fig.5 II b diamond

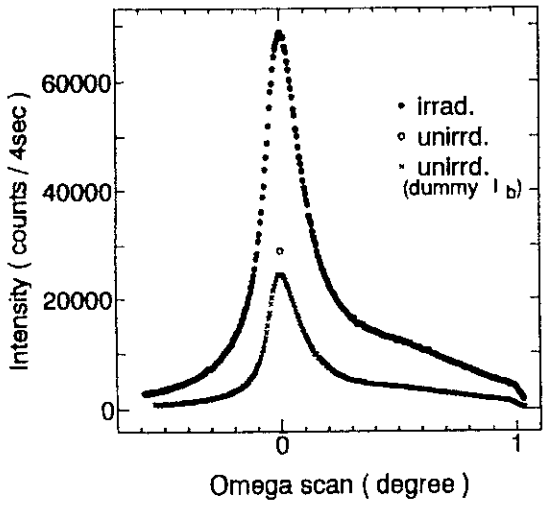

Fig.3 I b diamond irradiated P ion

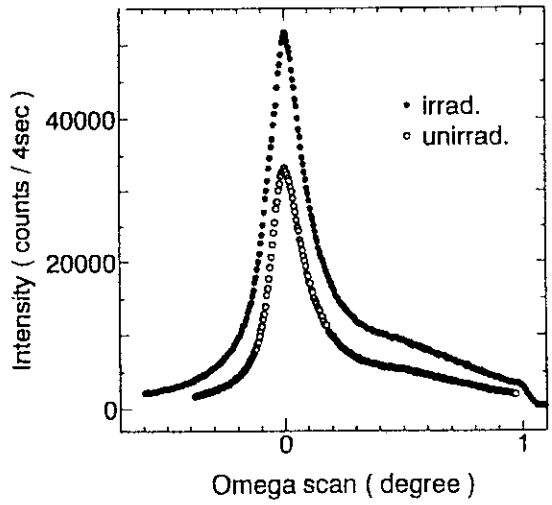

Fig.6 II b diamond irradiated P ion

5. 4 X-RAY STUDY OF IRRADIATION DEFECTS CAUSED BY MeV ION IMPLANTATION INTO Si PERFECT CRYSTALS V

M.KURIBAYASHI[1], K.TAKUMI[1], T.KANAMARU[1], H.KATOH[1], K.ISHIDA[1], K.AIZAWA, S.OKAYASU, H.TOMIMITU and H.MAEDA

We studied the nature of the irradiation defects caused by MeV ion implantation.[1-4] Ni, Cu and Au ions were implanted into silicon (111) wafers at accelerating energy of 80 - 230 MeV with doses of 0.1 -5.0 x 10^{14} atoms/cm^2. X-ray rocking curves from the wafers were investigated by the dynamical diffraction theory.

The following results were obtained.

(1) Taking the Split-type Peason VII function, the curve fitting between the observed and calculated curves was quite satisfactory (see Fig.1).

(2) Strain profiles obtained by the curve fitting were compared to the profiles of the loss energy per unit length (energy deposition) and stopping ions which were calculated by Aruga's code [5]. It was revealed that the former played a main role in expansion of the perpendicular lattice spacing and the latter played a sub-role.

(3)The height of the main peak of the strain profile in a crystal was proportional to the dose of ion implantation.

(4)In the case of Au ion implantation, an additional distortion near the crystal surface and a little uniform expansion of the perpendicular lattice spacing were observed.

(5) In the case of heavy dose of Ni and Cu ions, the uniform expansion was also observed.

Details of the results are to be published (M.Kuribayashi et al. (submitted to Jpn.J.Appl. Phys.)).

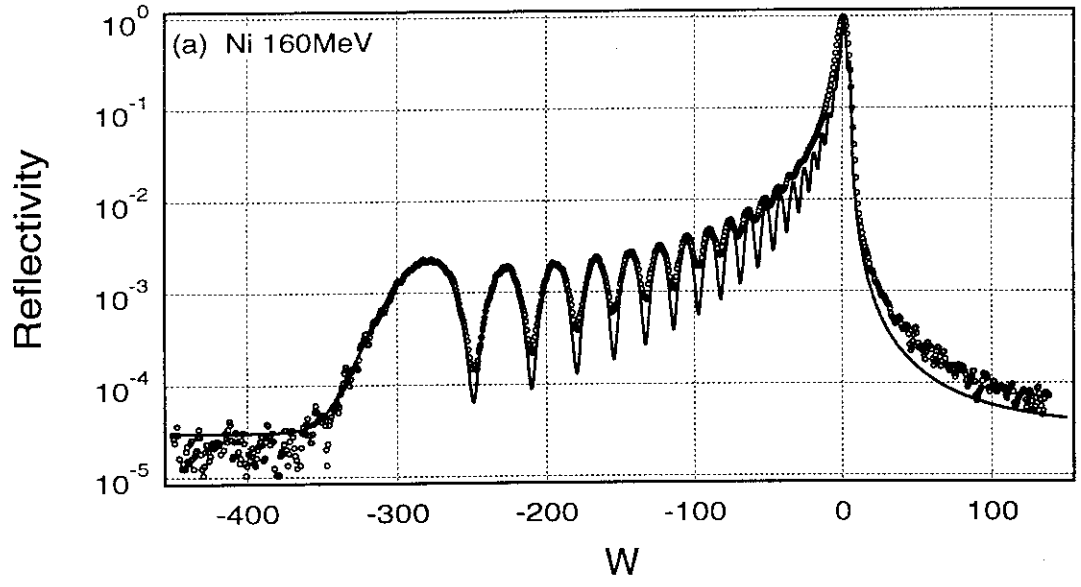

1)Dept. of Physics, Faculty of Science and Technology, Science Univ. of Tokyo

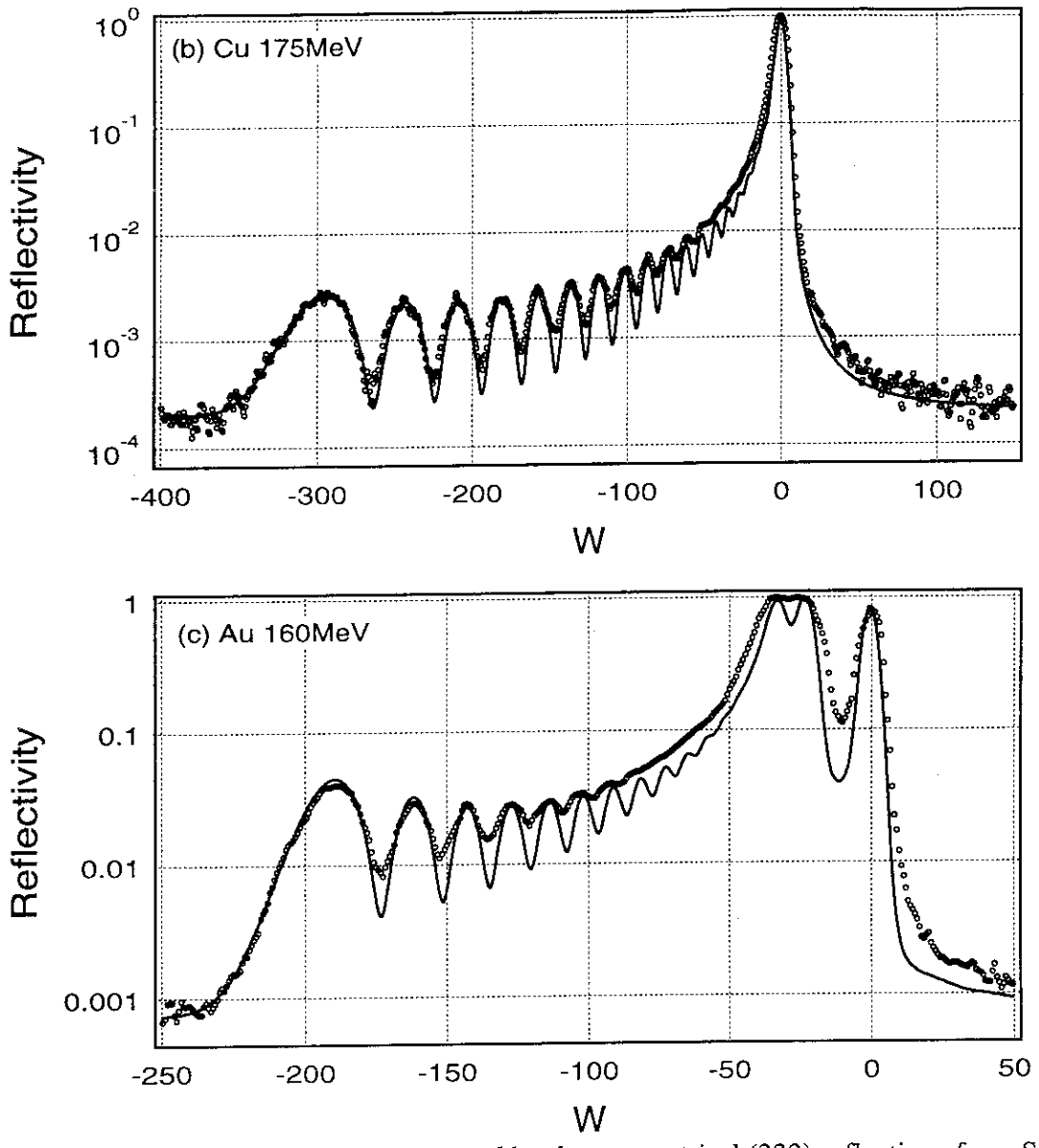

Fig.1 Experimental rocking curves measured by the symmetrical (333) reflections from Si wafers implanted with (a) Ni at 160 MeV and 1.6 x 10^{14} ions/cm^2, (b) Cu at 175 MeV and 1.6 x 10^{14} ions / cm^2, and (c) Au at 160 MeV and 8.4 x 10^{13} ions/cm^2. The solid lines are the calculated ones using the best fitting strain profiles .

References
1)H.Tanaka et al., JAERI TANDEM and V.D.G. Report 1992(1993)pp47-50.
2)M.Kuribayashi et al. JAERI TANDEM and V.D.G. Report 1993(1994)pp67-68.
3)M.Kuribayashi et al. JAERI TANDEM and V.D.G. Report 1994(1995)pp73-74.
4)M.Kuribayashi et al. JAERI TANDEM and V.D.G. Report 1995(1996)pp96-97.
5)T.Aruga, K.Nakata and S.Takamura: Nuch. Instr. and Meth.,B33(1988)748.

5. 5 ELECTRONIC EXCITATION EFFECT IN Fe IRRADIATED WITH ENERGETIC IONS

Y.CHIMI, A.IWASE and N.ISHIKAWA

Radiation effects in metals had been evaluated only by elastic interactions between incident ions and target atoms. It had been considered that electronic excitations hardly contribute to the radiation effects in metals due to the rapid motion of conduction electrons. However, on investigation of high energy (~100MeV) heavy ion irradiation effects in fcc metals, it has been found that electronic excitations contribute to radiation annealing, which means athermal annihilation of defects during irradiation, in Ni and Pt and to defect production in Cu and Ag [1]. On the other hand, through investigation in Fe, which is typical bcc metal, electronic excitations induced by GeV heavy ions contribute not only to radiation annealing but also to defect production [2]. However, in the range of electronic stopping power in which electronic excitations mainly contribute to the radiation annealing (S_e<40keV/nm), defect production curves don't saturate enough to observe the radiation annealing clearly, because the defect production rates caused by elastic interactions on the GeV heavy ion irradiation are relatively low. We performed irradiation of Fe with ~100MeV and ~1MeV heavy ions which give higher defect production rate than those for the GeV heavy ions, and we have investigated the effect of the electronic excitations on behavior of defect induced by irradiation.

Fe thin films ~200nm thick were deposited on α-Al_2O_3 single crystal substrates by rf magnetron sputtering with an Fe target (99.99%) using Ar gas. These films were irradiated at ~80K with 90~200MeV ^{35}Cl, ^{58}Ni, ^{79}Br and ^{127}I ions using the JAERI tandem accelerator and 0.5~2.0MeV ^{1}H, ^{4}He, ^{12}C, ^{20}Ne and ^{40}Ar ions using the JAERI 2MV Van de Graaff accelerator. We have measured the electrical resistivity of the specimens before, during and after irradiation, and obtained the defect production curves and the defect recovery behavior in the annealing process.

Fig.1 shows the defect production curves for ^{127}I ion and ^{1}H ion irradiations. We can see strong saturation of the resistivity change, $\Delta\rho$, for the high energy ion irradiations compared with the low energy ion irradiations. It indicates that in the high energy ion irradiation the radiation annealing occurs intensely. The cross-sections for the defect production and the defect annihilation have been derived from the analysis of the defect production curve. The cross-sections for the defect annihilation in the high energy ion irradiations are extremely larger than those in the low energy ion irradiations and increase with the electronic stopping power. It suggests that high density electronic excitation caused by the high energy ion irradiation enhances the radiation annealing. On the other hand, the defect recovery behavior after irradiation is shown in Fig.2. The fraction of stage-I recovery, which is observed around 120K, in the high energy ion irradiations are much smaller than those in the low energy ion irradiations. It implies that in the high energy ion irradiation the defects which can move at the recovery stage-I have already been annihilated during irradiation. This phenomenon also supports the result from the defect production curve.

References

1) A.Iwase and T.Iwata, Nucl. Instrum. Methods B90 (1994) 322.
2) A.Dunlop, D.Lesueur, P.Legrand, H.Dammak and J.Dural, Nucl. Instrum. Methods B90 (1994) 330.

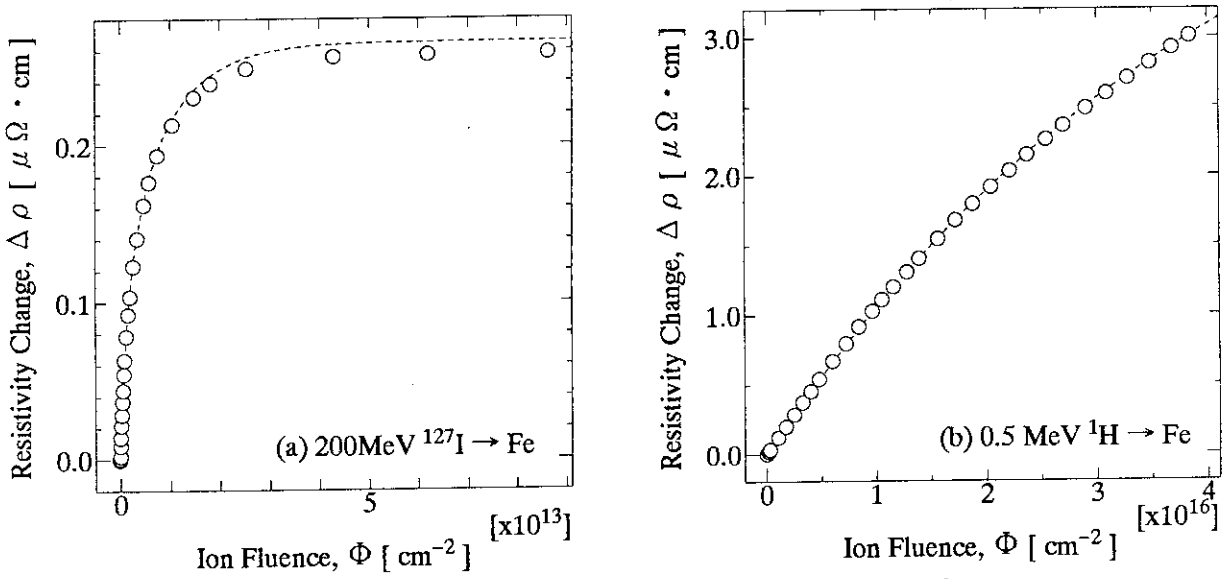

Fig. 1. Defect production curves for (a) 200MeV ^{127}I and (b) 0.5MeV ^{1}H ion irradiations.

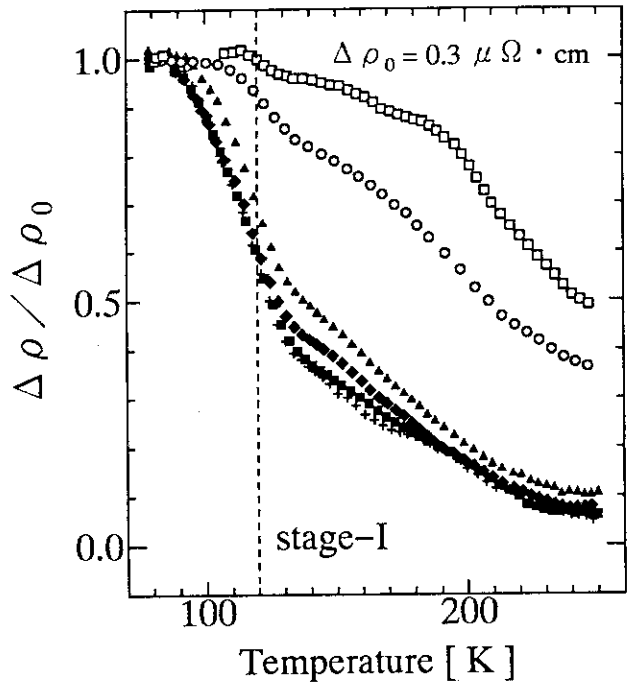

Fig. 2. Defect recovery behavior for several ion irradiations: (+) 0.5MeV ^{1}H, (■) 1MeV ^{4}He, (◆) 1MeV ^{12}C, (▲) 1MeV ^{20}Ne, (○) 120MeV ^{35}Cl and (□) 200MeV ^{127}I.

5. 6 EMISSION OF SECONDARY IONS FROM A FOIL BOMBARDED WITH HEAVY IONS

T.SEKIOKA[1], M.TERASAWA[1], M.SATAKA and S.KITAZAWA

The electron transport property of high temperature superconductors (HTSC) can be improved remarkably by irradiation of high energy heavy ions at low ion fluence [1,2,3]. This is due to the pinning effect of the columnar defects which hinder the easy motion of the magnetic flux vortices, so that the critical current density in a high magnetic field is drastically enhanced. High electronic excitations play an important role in the damage process by high energy heavy ions. However, the conversion mechanism of the energy of the excited electrons into kinetic energy for the target atoms is not well understood. In the Coulomb explosion model, a radial kinetic energy is transferred to the highly ionized atoms by which cascade collisions are induced. The columnar defects may be interpreted as an assemblage of such cascades along the incident ion path. It is reported that above a certain threshold value of approximately 2keV/Å of electronic stopping power, the electronic excitation contributes remarkably to the defect production in HTSC [2,4]. In order to investigate the fundamental process of the irradiation effects of high energy heavy ions in solids, we have been studying the secondary ions mass spectra from solid targets irradiated by heavy ion beams at the energy regions where the stopping power is in the neighborhood of the threshold value (2keV/Å) and far below this threshold, respectively for comparison.

The C, Cu and Au foil targets are irradiated by a high energy heavy ion beam from the tandem accelerator or the Van de Graaff accelerator. The secondary ions ejected from the front surface of the target are collected by a time of flight (TOF) mass spectrometer by applying an acceleration voltage of –500V and detected by an electron multiplier. Secondary electrons from the back side of the target are detected by another electron multiplier and this signal is used for the start signal of the TOF. The projectiles are I^{7+} ions with energies of 80, 100 MeV and Au^{12+} ions with 200 MeV energy from the tandem accelerator and 0.5, 0.8, 1.0 MeV C^+ ions from the Van de Graaff accelerator. The targets are carbon (30μg/cm^2 C-foil), gold (about 200Å thickness Au evaporated on a 30μg/cm^2 C-foil) and copper (about 400Å thickness Cu evaporated on a 30μg/cm^2 C-foil). The Cu target was irradiated by 200 MeV Au^{12+} ions only.

Figure 1 shows the yield of the secondary ions of C^+, Cu^+ and Au^+ normalized by the counts of secondary electrons signal as a function of the electronic stopping power. The values of an electronic stopping power are obtained from ref.[5]. In the figure, the secondary ion yield increases remarkably above an electronic stopping power of 2keV/Å, where the contribution of the electronic excitation to the defect production in HTSC and some metallic materials becomes remarkable. On the contrary, in the region of electronic stopping power of 100eV/Å, the dependence of the secondary ions yield on the stopping power is weak. This is the first observation of a sputtering enhancement in conductor materials due to high electronic excitation by high energy heavy ions.

This result suggests that the behavior of the yield of the secondary ions in C, Cu and Au targets is very similar to the behavior of the defect formation in HTSC by heavy ion irradiation, and the same threshold mechanism works. To confirm this suggestion, it is important to study secondary ions mass spectroscopy in a wide range of electronic stopping power with various combinations of projectiles and targets. Bulk specimens must be used for the study of the irradiation effect in HTSC, so that we need to reform the method of mass spectroscopy.

---

[1] Faculty of Engineering, Himeji Institute of Technology

References
1) M.Terasawa, T.Mitamura, T.Kohara, K.Ueda, H.Tsubakino, A.Yamamoto, Y.Awaya, T.Kambara, Y.Kanai, M.Oura and Y.Nakai, Physica C **235-240** (1994) 2805
2) V.Hardy, J.Provost, D.Groult, Ch.Simon, M.Hervieu, S.Bouffard and B.Raveau, Radiation Effects and Defects in Solids, **126** (1993) 137
3) M.Kraus, P.van Hasselt, J.P.Strobel, S.Peehs, M.Leghissa, G.Kreiselmeyer, B.Holzapfel, W.Gerhauser, B.Hensel, S.Klaumunzer, S.Bouffard and G.Saemann-Ischenko, Radiation Effects and Defects in Solids, **126** (1993) 147
4) C.Houpert, M.Hervieu, D.Groult, F.Studer and M.Toulmonde, Nucl. Instrum. Methods. **B32** (1988) 393
5) L.C. Northcliffe and R.F. Schilling, Nucl. Data Tables **A7** (1970) 233

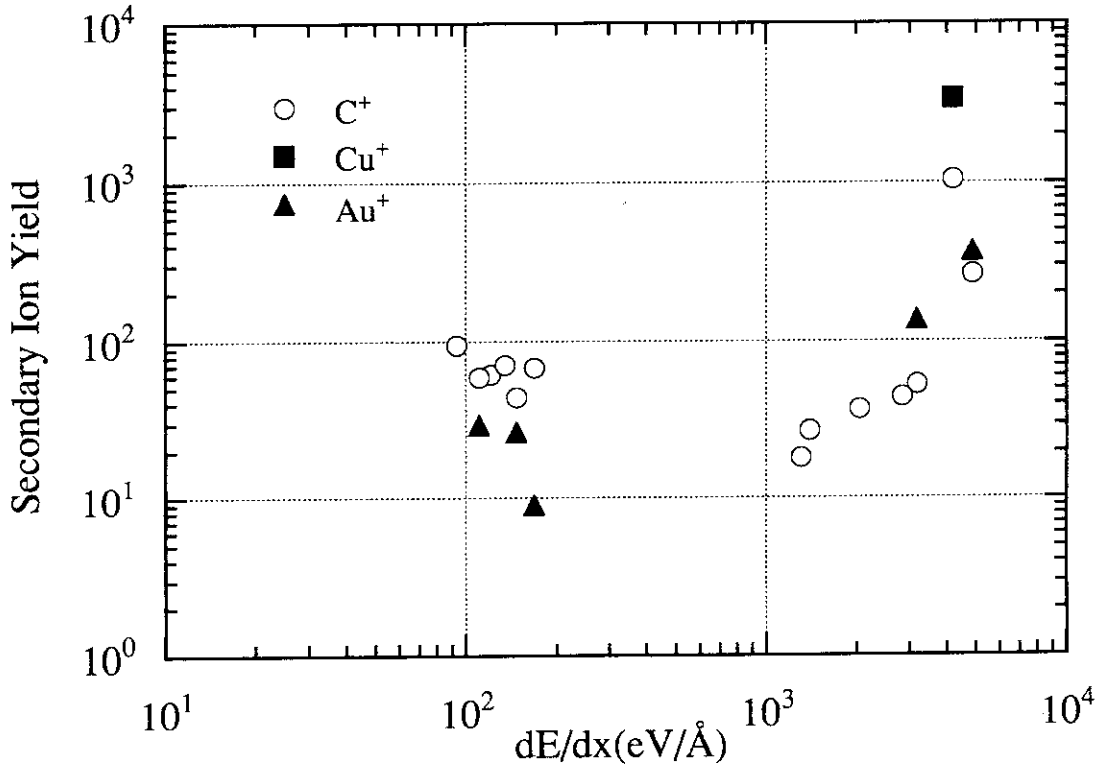

Fig. 1. The yield of the secondary ions of C^+, Cu^+ and Au^+ normalized by the counts of secondary electrons signal as a function of the electronic stopping power. The values of the electronic stopping power are obtained from ref.[5].

5. 7 DEFECT RECOVERY IN Fe UNDER STRONG MAGNETIC FIELD

A. IWASE, Y. CHIMI and N. ISHIKAWA

Much experimental work on defect recovery in irradiated metals shows that the stage-I recovery in Fe appears at much higher temperature (~100 K) than in other typical metals (Ni, Cu, Al and so on). Ono, Maeta and Kittaka have proposed a new model to explain this anomalous property of defects in Fe[1]. According to their model, the interstitial atom in the dumbbell configuration is pressed by the other member of dumbbell, and the orbits of the 3d-electrons are distorted to minimize the total free energy. This distortion leads to a decrease of the local magnetic moment and a high stability of interstitial atoms in Fe. If this model is correct and the stability of interstitials can be changed by the external magnetic field, the behavior of defect recovery under a magnetic field will be different from without a magnetic field.

In order to study the possibility of changing the stability of interstitial atoms in Fe by the external magnetic field, we performed the following experiment; Fe film about 200 nm thick, which was deposited on Al_2O_3 substrate by using rf magnetron sputtering, was irradiated with 2-MeV Ar ions at liquid nitrogen temperature. After the irradiation, the specimen temperature was held at 120K and the change in electrical resistivity was measured as a function of time. During the measurement, we applied a magnetic field of 3T to the specimen at some intervals.

Figure 1 shows the change in the resistivity of irradiated Fe at 120K as a function of time. A large decrease of the resistivity can be explained as due to the defect recovery through the migration of interstitials to vacancies. The figure indicates that the behavior of defect recovery at 120K under a magnetic field of 3T is just the same as without a magnetic field. From the present experimental result, we conclude that the magnetic field up to 3T does not have any effect on the stability of interstitial atoms in Fe.

[1] F. Ono, H. Maeta and T. Kittaka, J. Phys. Soc. Jpn, 53(1984) 920.

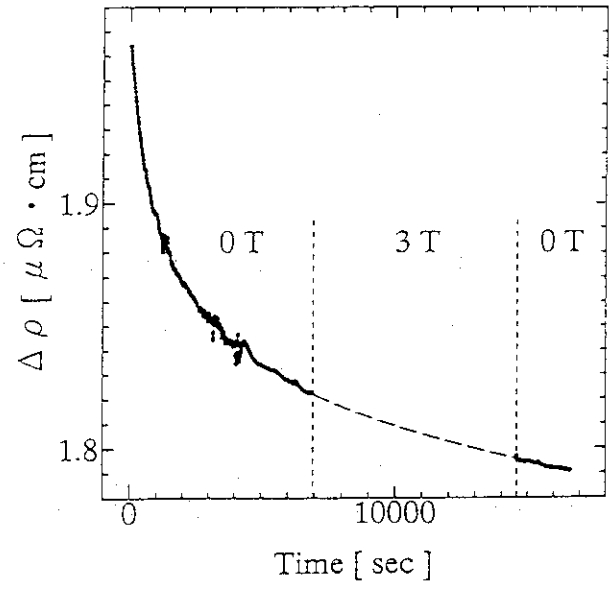

Fig.1 Change in electrical resistivity of Ar-irradiated Fe as a function of time. Measurement temperature is 120 K. During the measurement, magnetic field of 3T was applied to the specimen at some intervals.

5. 8 ELECTRONIC EXCITATION AND DEFECT PRODUCTION IN $EuBa_2Cu_3O_y$ IRRADIATED WITH HIGH ENERGY IONS

N.ISHIKAWA, Y. CHIMI, A. IWASE, H.MAETA, K. TSURU[1], O. MICHIKAMI[2]

Ion-irradiation induced defects especially columnar amorphous tracks have been an object of study for their effectiveness in increasing J_c. Since columnar amorphous tracks are created due to electronic excitation induced by ion-irradiation, it has been considered that electronic stopping power,S_e, may play an important role in creating columnar defects. Several papers have reported there is a correlation between the size of irradiation-induced columnar defects and S_e[1]. For other ion-irradiated insulotors ion-velocity dependence of defect production when Se is same has been found[2], but for ion-irradiated high-Tc superconductors it has not been observed yet. It is necessary to investigate whether Se is really a good parameter to explain the defect production and to test which available defect production models are valid for a consistent description of defect production process.

In our previous work[3], we suggested that increase rate of c-axis against ion-fluence, $(\Delta c/c_0)/\Phi$, is a useful quantity to explain the defect production rate, where Δc is the increment of c-axis lattice parameter, c_0 is the c-axis lattice parameter for pre-irradiated sample, and , Φ is ion-fluence. We showed defect production rate can be separated into two contribution; one is the effect due to elastic displacement and the other is the effect due to inelastic interaction of ions and electrons, namely electronic excitation. When S_e is high enough, former effect can be neglected. However, as Se decreases and the former effect become comparable to the latter effect, separation of two effects becomes necessary for the accurate estimation of both effects. In this study, we have performed irradiation of $EuBa_2Cu_3O_y$ superconductor with various ions from He to Au changing the energy from 0.85 MeV to 3.80GeV and have measured the increase rate of c-axis lattice parameter against ion-fluence for each irradiation. Fig.1 shows some of the data illustrating the linear increase of c-axis lattice parameter as a function of ion-fluence. The slope of these figures, $(\Delta c/c_0)/\Phi$, can be regarded as a quantity proportional to defect production rate, which is separated into two effects as stated above. By subtracting the effect due to elastic displacement from the total effect of defect production, the effect via electronic excitation can be precisely estimated. In order to investigate the effect of energy deposition by electronic stopping, the effect via electronic excitation, $((\Delta c/c_0)/\Phi)_{inelastic}$, is plotted against Se in Fig.2. However, we could not observe clear correlation between $((\Delta c/c_0)/\Phi)_{inelastic}$, and Se. This means another parameter which determines the defect production rate should be introduced. We propose introduction of a related quantity called primary ionization rate, dJ/dx, which is a number of ions produced per unit path length[4] We found dJ/dx gives a good fit to the experimnetal data. This can be seen in Fig.3 where $((\Delta c/c_0)/\Phi)_{inelastic}$ varies as a function of single parameter $(dJ/dx)^4$. The $(dJ/dx)^4$-dependent irradiation effect can be also observed in UF_4 and ice irradiated with ions when ion-energy dependence on sputtering yield is measured[5].

[1]Device Physics Research Laboratory, NTT Basic Research Laboratories
[2]Faculty of Engineering, Iwate University

References
1)Y.Zhu, Z.X.Cai, R.C.Budhani, M.Suenaga, and D.O.Welch, Phys.Rev. B 48 (1993) 6436.
2)Z.G.Wang, Ch. Dufour, B.Cabeau, J.Dural, G.Fuchs, E.Paumier, F.Pawlak, and M. Toulemonde, Nucl. Instrum. Methods in Phys. Res. B 107 (1996) 175.
3)N.Ishikawa, A. Iwase, Y. Chimi, H.Maeta, K. Tsuru, and O. Michikami, Physica C 259, 54 (1996).
4)V.H.Bethe, Ann.Phys. 5 (1930) 325.
5)L.E.Seiberling, C.K. Meins, B.H.Cooper, J.E.Griffith, M.H.Mendenhall, and T.A.Tombrello, Nucl. Instr. and Meth. 198 (1982) 17.

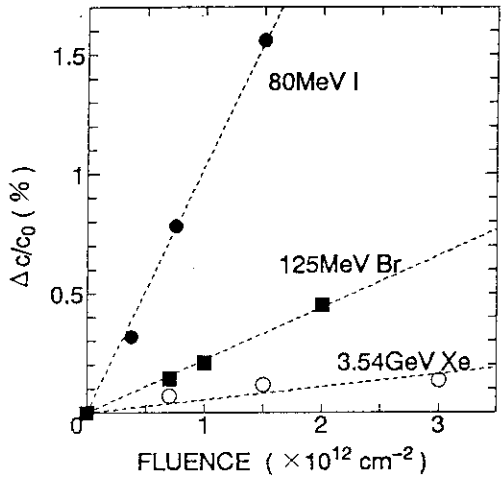

Fig.1 $\Delta c/c_0$ plotted against ion-fluenceΦ for $EuBa_2Cu_3O_y$ irradiadiated with 80MeV I, 125MeV Br, and 3.54GeV Xe, where Δc is the increment of c-axis lattice parameter, c_0 is the c-axis lattice parameter for pre-irradiated sample.

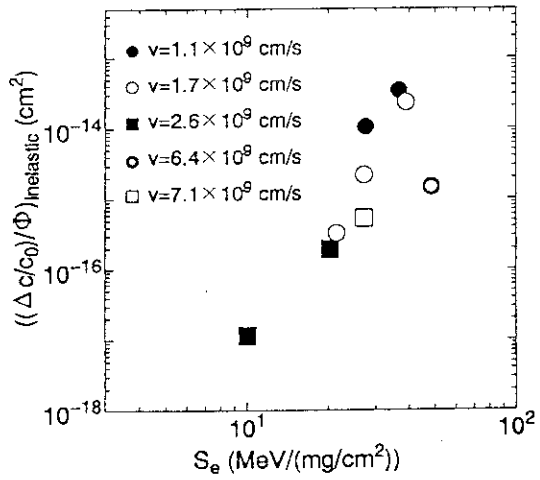

Fig.2 $((\Delta c/c_0)/\Phi)_{inelastic}$, plotted against S_e. The velocity of incident ions are shown for reference.

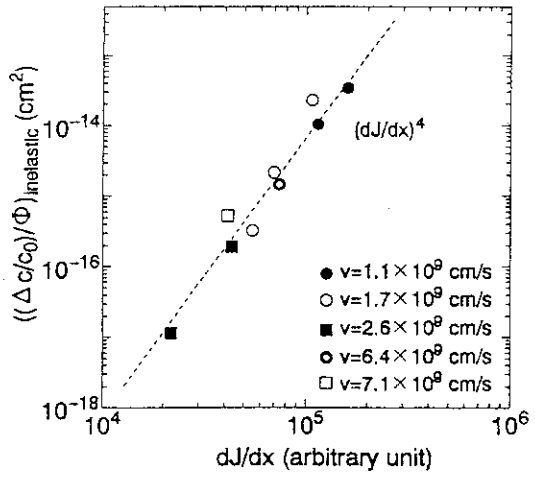

Fig.3 $((\Delta c/c_0)/\Phi)_{inelastic}$, plotted against dJ/dx. The velocity of incident ions are shown for reference.

5. 9 EFFECTS OF Au^{24+} ION IRRADIATION ON SUPERCONDUCTIVE PROPERTIES AND MICROSTRUCTURE OF $EuBa_2Cu_3O_x$ THIN FILMS

M. SASASE, S. OKAYASU and K. HOJOU

Large enhancement in critical current density(Jc) was observed in single crystal, thin films and bulk cuprates irradiated with high-energy heavy ions that produced a suitable density and size of columnar defects[1]. To clarify the relationship between superconductive properties and structures of the defects, we have investigated effects of irradiation with energetic ions of Au^{24+} using transmission electron microscopy(TEM) and SQUID magnetometer

Specimens used in this study were $EuBa_2Cu_3O_x$ thin films(300 nm) - sputter - coated MgO(100) plates. The specimens were irradiated with Au^{24+} ions which were accelerated to 300 MeV with the fluence of 1.9×10^{10} ions/cm^2 at the room temperature using a Tandem accelerator at JAERI. In order to obtain the wide range irradiation energies, some irradiations were performed with the ions which were transmitted through thin aluminum foils mounted in front of the specimens. In this case, the energies were estimated from the range-energy relations obtained from the calculated stopping powers by J. F. Ziegler[2].

Magnetization hysteresis loops of the specimens before and after irradiation were measured with SQUID magnetometer. Crystalline structures of the $EuBa_2Cu_3O_x$ films were measured by X-ray diffraction (XRD). The specimens were observed with TEM and electronic energy loss spectroscopy(EELS).

Fig.1 shows the energy dependence of Jc in typical conditions of temperature and magnetic field. We found that Jc increased with an increase in the Au^{24+} ion energy and reached a maximum value of 3.5×10^6 A/cm^2 (5K, 1T) at 24 MeV. This value was about two times as high as that for no irradiation. The Jc decreased with an increase in ion energy and reached at 2.0×10^6 A/cm^2 at 208 MeV.

The dependences of Jc and critical temperature(Tc) on ion energy were similar and both parameters had a maximum at 24 MeV. This tendency is explained by their defect structure including the size, the shape and the distribution of radiation - induced defects.

We will observe the microstructure and electric structure of defects in the irradiated films by using both TEM image and EELS spectrum.

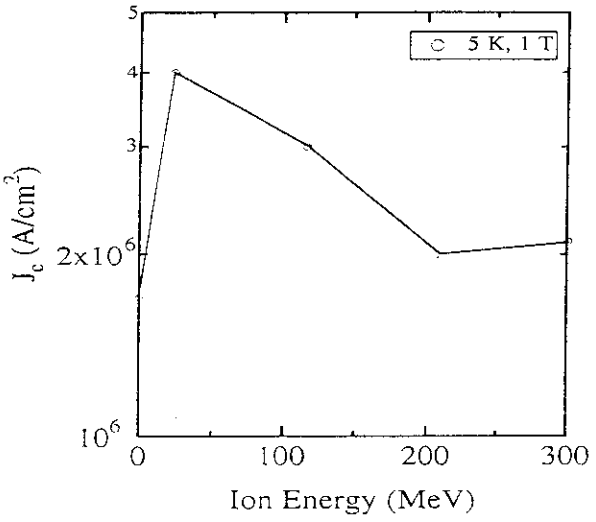

Fig. 1 Energy dependence of Jc for the $EuBa_2Cu_3O_x$ thin films

Reference

1) Y. Zhu, M. Suenaga and D. O. Welch, Phys. Rev. B48(1993)6436.

2) J. F. Ziegler : Handbook of Stopping cross Sections for Energetic Ions in All Element(Pergamon Press, New York, 1980).

5.10 EFFECTS OF HIGH-ENERGY HEAVY-ION IRRADIATION ON THE HIGH-T_c SUPERCONDUCTOR

T.TERAI[1], T.KOBAYASHI[1], S.OKAYASU and K.HOUJYOU

High-*T*c superconductors are expected to be applied for various systems such as fusion reactors. In order to use these materials practically, enhancement of *J*c is essential. We have been studying *J*c enhancement of Bi-2212 single crystals by particle beam irradiation using ions, electrons and neutrons. By these experiments, it turned out that columnar defects induced by high-energy heavy-ions are quite effective for flux pinning. In this report, we show the changes in *J*c and *F*p due to 240 MeV Au ion irradiation in comparison with other kinds of particle irradiation.

It is necessary to use well-characterized specimens to make irradiation effects clear. In this study, we prepared Bi-2212 single crystal specimens by Floating-Zone (FZ) method in oxygen atmosphere (1atm). Thin film specimens (1.5x1.5x0.06 mm^3) were obtainded by cutting from the rod-shaped specimen thus prepared. The largest face of the films was perpendicular to c-axis.

Gold ion irradiation was carried out parallel to the c-axis in vacuum at room temperature with a the JAERI tandem Accelerator. The doses were from $5.0x10^{10}$ to $1.0x10^{12}$ions/cm^2.

Magnetization hysteresis curves of the specimens before and after irradiation were measured with a vibrating sample magnetometer (VSM) at 20K, 40K and 60K as a function of applied magnetic field parallel to the c-axis. The critical current density and the pinnnig force density were calculated from the difference of hysteresis curve by Bean's model [1].

A comparison of *J*c increase at optimal fluence with other kinds of particle irradiation is shown in Fig.1. Though the optimal fluence was not clarified for Xe irradiation yet, we assumed that $5x10^{10}$ions/cm^2 was the optimal fluence, taking the results in Kr and Au irradiaiton into account.

According to Leghissa et al[2]., the threshold value of electronic energy transfer to produce columnar defects in Bi-2212 is 16 keV/nm. In our cases, the calculated values of the energy transfer from Bethe's and Firsov's formulas were 30keV/nm for Au, 25keV/nm for Kr and 24keV/nm for Xe, respectively.

Macroscopic pinning force density ($F_p = J_c \times B$) is more essential parameter than *J*c in discussing the effects of shape of defects on the flux pinning. In Fig.2, we show *F*p values as a function of applied field at optimal fluence. The columnar defects did not penetrate the specimen, the *F*p values were converted to the case of perfect penetration. The columnar defects induced by high-energy heavy-ion irradiation are more effective for flux pinning than the point defects induced by electron irradiation or the isotropic cascade defects induced by fast neutron irradiation.

The *F*p values as a function of magnetic field at the same fluence are shown in Fig.3. For high-energy heavy-ion irradiation which makes columnar defects, there is a close connection between the *F*p values and the diameter of defects. The calculated electronic energy transfer for 240MeV Au irradiation is 30keV/nm, which makes bigger defects than the other kinds of ions. It is concluded that thicker defects are more effective for flux pinning.

References
[1] E.M.Gyorgy et al., Appl.phys.Lett. **55**,283(1989).
[2] M.Leggissa et al., Europhys.Lett. **19**,323(1992).

[1]Engineering Research Institute, School of Engineering, Univeristy of Tokyo.

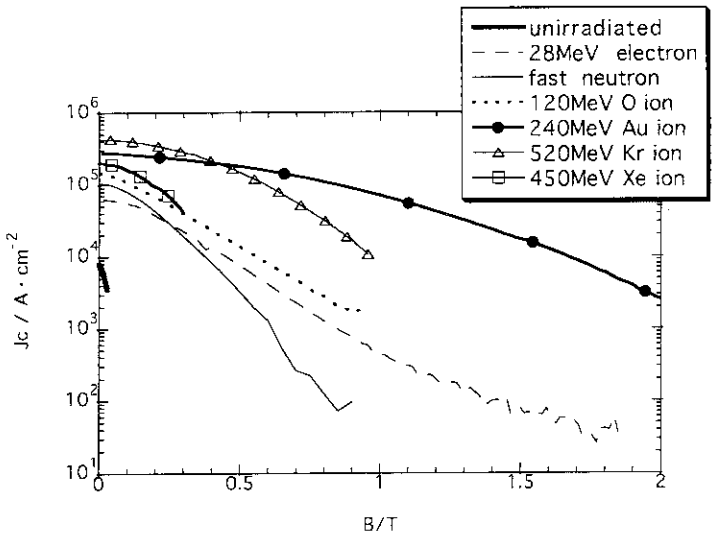

Fig.1 Critical current densities of various particle irradiation at optimal fluence (40K).

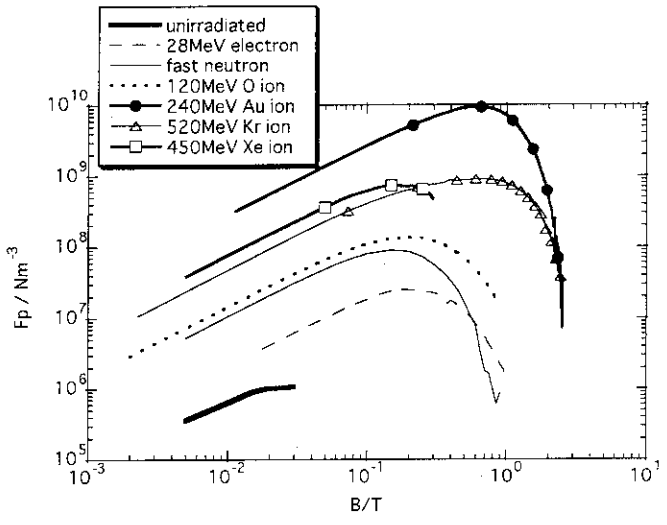

Fig.2 Pinning force density at optimal fluence (40K)

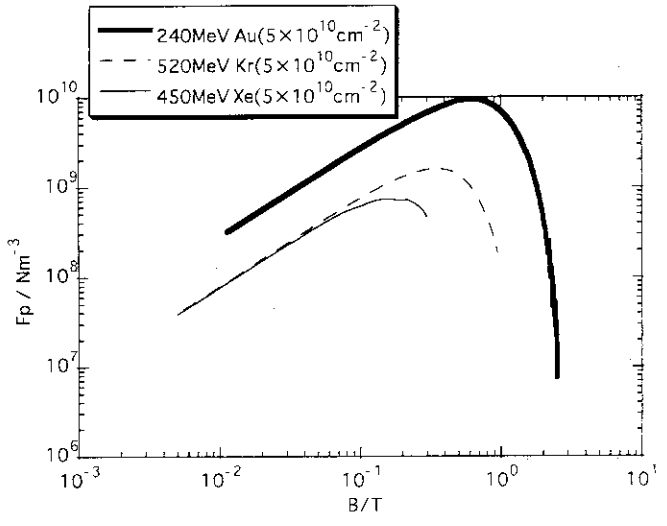

Fig.3 Pinning force density for columnar defects at the same fluence.

5.11 PARALLEL AND CROSSED COLUMNAR DEFECTS IN Bi-2212 TAPES

Y. KAZUMATA[1], S. OKAYASU, H. KUMAKURA[2] and K. TOGANO[2]

Two Bi-tapes were irradiated with 180 MeV Cu^{11+} ions by the two processes. At the first process, the surfaces, perpendicular to the c-axis, of the tapes were inclined to -45 ° to the Cu^{11+} ion beams and both tapes were irradiated at a dose of 5.8×10^{10} Cu^{+}/cm^2 at the same time. On the next, one of the tapes was rotated by 180° so that the angle between the c-axis and the beam direction became +45° , and both tapes were irradiated again to a dose of 2.7×10^{10} Cu^{+}/cm^2. Therefore, the total fluence of both tapes was exactly the same; one of the tapes had parallel columnar defects to the amount of $1.35 \times 10^{11}/cm^2$, which corresponded a dose equivalent matching field B_ϕ =2.8 T, to the direction of -45° (this direction is defined as 135° as shown in Fig.1(a) for the angle between the direction of the defects and the ab-plane) away from the c-axis, and the other had crossed columnar defects with B_ϕ =1.2 T to +45° and 1.8 T to -45° , respectively.

Angular dependence of irreversibility field (H_{irr}) at 55 K is shown in Fig.1(b) for the three specimens, prior to irradiation, with the parallel and crossed columnar defects. The angle θ is defined in Fig.1(a) as the angle between the applied field and the ab-plane of the tapes. H_{irr} was estimated from the hysteresis loop measured and defined as the field at critical current density $Jc=1 \times 10^2$ A/cm^2. As already shown in ref.[1], remarkable enhancement of H_{irr} by irradiation is observed at 55 K. For the specimen prior to irradiation, two maxima are seen at 0° and 180° in Fig.1(b), which is caused by intrinsic pinning between CuO_2 layers. The angular dependence of H_{irr} can be written in eq.(1),

$$H_{irr}(T,\theta)=H_{90}(T)/\varepsilon(\theta) \quad (1)$$

$$\varepsilon(\theta)=[\gamma^{-2}\cos^2\theta+\sin^2\theta]^{1/2}$$

where γ is the anisotropy parameter, $(m_c/m_{ab})^{1/2}$. By applying above eq.(1) to the experimental curve, γ prior to irradiation was estimated to be 10, which is much smaller than those for single crystals, 50-200.

For the parallel columnar defects(PCD), a peak beside the peaks due to

1. Nihon Advanced Technology Co.
2. National Research Institute for Metals

intrinsic pinning is observed at the direction of the columnar defects, 135° , and H_{irr} in all directions of the applied field are enhanced. The crossed columnar defects (CCD) are much effective for the enhancement of H_{irr} as seen in Fig.1(b). The peak at 125° due to these defects deviates from the direction of the defects, 45° and 135° . A bulge is observed at 90° (H//c-axis) in the breast of the peak. The bulge is recognized as a peak for the ϕ -rotation (see Fig.1(a)) as shown in Fig.1(c). This peak is not only a peculiar feature of CCD but also a definite evidence of the breaks of line vortices since such a peak can not be expected by the pancake vortices and also is not observed in PCD.

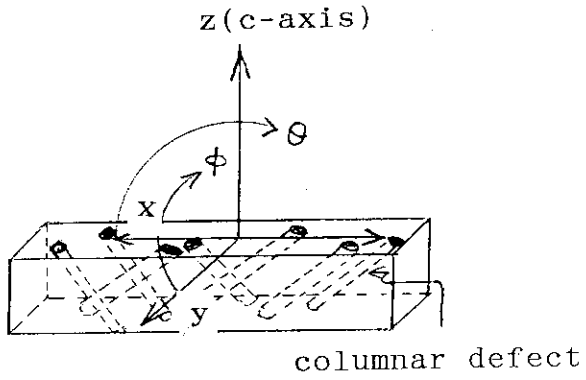

Fig.1(a). Definition of the rotation
θ-rotation: Rotation in the xz-plane.
ϕ-rotation: Rotation in the yz-plane.

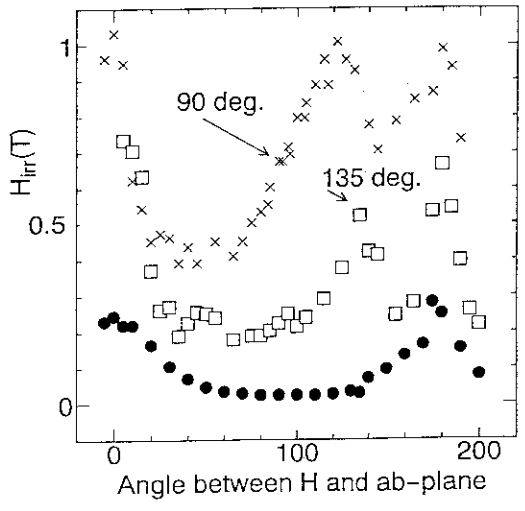

Fig.1(b). H_{irr} for θ-rotation

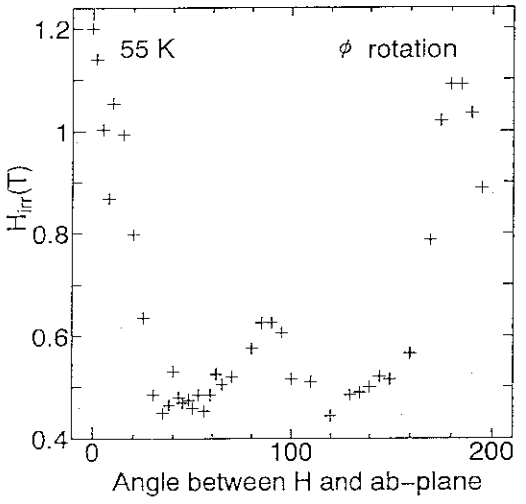

Fig.1(c). H_{irr} for ϕ-rotation

●:Prior to irradiation, □:Parallel columnar, ×&+:crossed columnar

Reference

1) Y. Kazumata et al. Phys. Rev. B54(1996)16206; Surface & Coating Technol. 84(1996)348

5.12 COLUMNAR DEFECTS WITH STAIR SHAPE GENERATED BY B ION IRRADIATION IN Bi2Sr2CaCu2Ox SINGLE CRYSTAL

Y. SASAKI[1], D.X. HUANG[1], K. HOJHO and S. OKAYAU

$Bi_2Sr_2CaCu_2O_x$ superconductors were irradiated with B ions or Fe ions for introduction of flux pinning centers. The irradiation effect was also confirmed by measurements of magnetic property. Electron microscopy studies revealed that columnar defects with the structure of stair shape along a direction of <100> and <001> in $Bi_2Sr_2CaCu_2O_x$ crystal. The internal structure of defect was found to be amorphous. In the previous studies, it was thought that columnar defects were generated in $Bi_2Sr_2CaCu_2O_x$ by the ion irradiation with energy loss rate (stopping power) more than 16keV/nm. This irradiation condition did not agree with the threshold value of energy loss rate. However, columnar defects were observed in this irradiation sample.

Thin pieces of $Bi_2Sr_2CaCu_2O_x$ single crystals for irradiation experiment were cut out from a sample rod (FZ sample) prepared by floating zone melting method[1]. The shape of samples used for ion irradiation experiment is a plate approximately 1x2mm in cross section and approximately 20mm thick. The ion irradiation was performed using a tandem-type ion injection system. Ions of B with an irradiation energy of 11MeV were used. The orientation of ion irradiation was set parallel to the c-axis. The irradiation effect on the superconductivity was evaluated by changes in magnetic moment ΔM at 50K before and after irradiation using a superconducting quantum interference device (SQUID; QUANTUM DESIGN). Irradiation damages were observed perpendicular to the axis of ion irradiation using a high-resolution transmission electron microscope (EM 002B; TOPCON Corporation).

Figure 1 shows irradiation effects with 11MeV B ions on the critical current density in this experiment condition. The critical current density was enhanced according to the increase of fluence in the range of $1x10^{11}$ - 10^{13} ions/cm^2. In the irradiation with 11MeV B ions, the irradiation effect is not saturated with fluence of $1x10^{13}$ ions/cm^2 either. Then, it is expected that the structure and spatial distribution of the irradiation defects generated by B ion irradiation are different from the defects generated by Fe ion irradiation at lower energy (18MeV) [2]. To make clear this point, cross section observations of the sample were performed using transmission electron microscope (TEM). TEM image observed at low magnification is show in Figure 2. Within the whole specimen, some white contrast parts with a stair shape were observed. A High resolution TEM image of the stair shape shows that the white contrast is a columnar defect (Figure 3). This defect is an amorphous phase instead of a crack. This columnar defect has a stair shape structure along the crystallographic directions of <100> and <001>, is different from columnar defects generated by irradiation using heavy ions with the high energy [3]. However, this

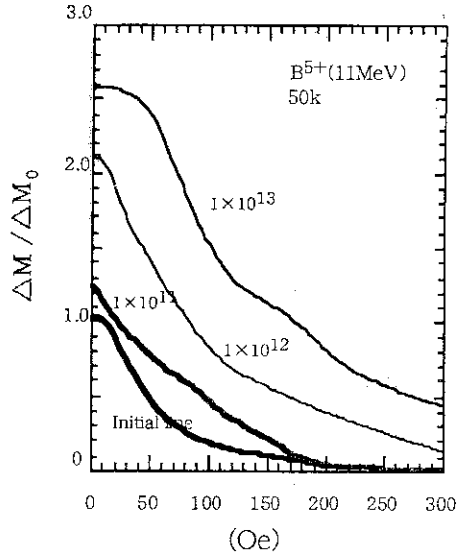

Fig. 1 Ion irradiation effects on hysteresis of magnetization under the magnetic field parallel to the c-axis at 50K.

Research and Development Lab., Japan Fine Ceramics Center

defect is a kind of column defect.

Generally, the structure of defect formed by ion irradiation is decided by energy loss rate (stopping power) of the ions (-dE/dx). In order to introduce usual columnar defects in $Bi_2Sr_2CaCu_2O_x$, it had been assumed that over 16keV/nm is necessary as the energy loss rate [4]. A energy loss rate in this experimental condition is much smaller than that value. Then, we can conclude that two kinds columnar defects exist and one in two kinds things can be made by ion irradiation with 11MeV B ions. The other is a general columnar defect which generated with heavy ions at several hundred MeV. This experimental study showed for the first time that the columnar defects were generated by the irradiation with a light element at low energy. This result is prospective as a first step of new technique development for introduction of flux pinning centers into the $Bi_2Sr_2CaCu_2O_x$.

Fig. 2 Low magnified cross-sectional TEM image. Within the whole specimen, some areas with white contrast with a stair shape were observed.

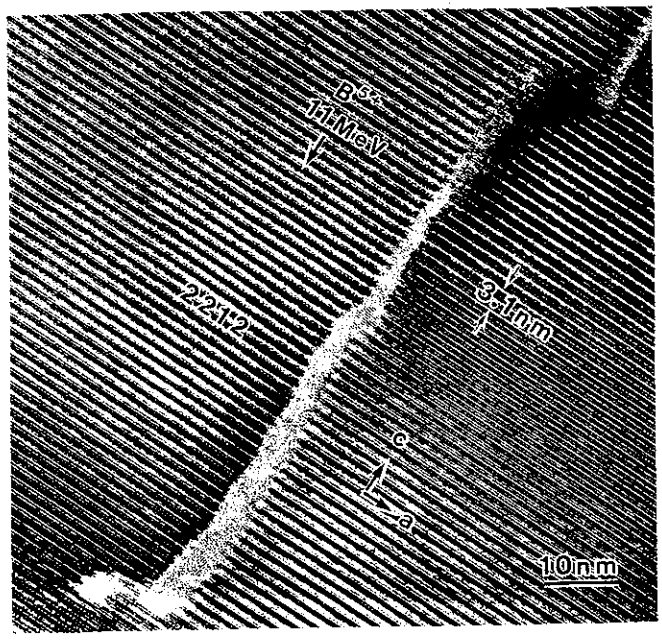

Fig. 3 Cross-sectional TEM image observed along [010] direction. The internal structure of the columnar defect is amorphous in most areas, but one part was crystallized

The internal structure of the columnar defects is amorphous in most areas, but one part was crystallized as shown in figure 3 (marked with a triangle). To create a such small crystal mean that recrystallization occurred. It suggests that this defect was formed by thermal damage.

REFERENCE

1. Y. Kubo, K. Michishita, Y. Higashida, M. Mizuno, H. Yokoyama, N. Shimizu, E. Inukai, N. Kuroda and H. Yosida Jap. J. Appl. Phys. 28 (1989) L6061.
2. Y. Sasaki, W.L, Zhou and Y. Ikuhara, J. Ceram. Soc. Japan, 103 (1995) 195-198
3. L. Cival, A.D. Marwick, T.K. Worthington, M.A. Kirk, J.R. Thompson, L. Krusin-Elbaum, Y. Sun, J.R. Clem and F. Holtzberg, Phys. Rev. Lett., 67 (1991) 648-651
4. T. Terai and Y. Kusagaya Proc. Int. workshop on Superconductivity, Kyoto (1994) 55-58

5.13 PROTON IRRADIATION EFFECTS ON PINNING PROPERTIES OF QMG-YBCO

S. OKAYASU and Y. KAZUMATA

It is well known that critical current density Jc flowing within high-Tc superconducting materials exhibits a large long-time decay. This phenomenon is related to pinning properties of vortices. Many studies have been done to improve the pinning at temperature of liquid nitrogen. Ion-irradiation is one possible way to investigate the vortex dynamics in high-Tc superconductors. We focused attention on the pinning forces of QMG(Quenched and Melt-Growth)-YBCO, which is known as a large Jc material, to understand its origin of large critical currents.

The QMG-YBCO materials were synthesized with the quenched and melt-growth method in Advanced Research Institute, Nippon Steel Co. Samples contain small grains (d$\sim$1 μ m) of nonsuperconducting Y-211 phase as inclusions about 30 mol-%. The sample was cut into two pieces, one was for the proton irradiation and the other for a reference. The irradiation at liquid nitrogen temperature was accomplished at the Tandem accelerator in Tokai Research Establishment, JAERI. The energy of the proton ions was 30MeV and the irradiation dose was up to 1×10^{16} ions/cm^2. To investigate the pinning properties of the QMG-materials, comparisons of some superconducting properties, such as critical current densities (Jc), activation energies (U_{eff}) and pinning forces (Fp) between 16MeV proton-irradiated and unirradiated QMG-YBCO material have been accomplished. We focus our attention to the pinning forces in this report.

The transition temperature decreased with the irradiation from 92K to 89K. The amount of the defects introduced by the irradiation is estimated about 20ppm from our previous works[1,2]. The average defect size is also calculated as d$\sim$10Å. Therefore, the defects of unit cell sizes distribute in the sample randomly with the distance about 100Å. These defects act as pinning centers. From the comparison of the critical current densities between proton-irradiated and unirradiated sample, one can find a remarkable enhancement of Jc around 1 Tesla in entire temperature range. The enhancement is characteristic for the proton irradiation. Similar enhancement of superconducting properties at 1T field can be seen with the effective activation energies as reported previously[2]. Usually, pinning energies of these small defects are not so high, and pinning properties should be improved only in lower temperature range which thermal activation is smaller than the pinning. Proton irradiation, however, brings a result of enhancement of pinning force even at 77K. This is because that the core size of vortices is comparable to the that of defects and vortices are effectively pinned by these defects.

It is well known that two empirical power laws are found with the high-Tc superconductors. One is the relation between the irreversibility temperatures and field, $H_{irr}=A(1-T/Tc)^{\alpha}$. The other is the

relation between the irreversibility fields and the maximum value of the pinning forces, $F_{p\text{-}max}$. The latter relation, $F_{p\text{-}max}=B\cdot H_{irr}{}^{\beta}$, is obtained only for the above 60K in our case. It is difficult to determine the $F_{p\text{-}max}$ at lower temperatures because samples have a large pinning force at that temperature and we were not able to apply such a large magnetic field. Using these two relations, $F_{p\text{-}max}$ can be expressed as $F_{p\text{-}max}=B\cdot A^{\beta}(1\text{-}T/Tc)^{\alpha\beta}$. The field dependence of $F_{p\text{-}max}$ is expressed empirically as $Fp/F_{p\text{-}max}=b^{m}(1\text{-}b)^{n}$, where $b=B_{ext}/B_{irr}$. Therefore, $F_{p\text{-}max}$ should be written with the following expression, $$Fp=B\cdot A^{\beta}(1\text{-}T/Tc)^{\alpha\beta}\cdot b^{n}\cdot(1\text{-}b)^{m}. \quad (1)$$

Using the values obtained the above two power-law fittings with appropriate n and m, the calculated values of Fp's can be compared with the data. The results are shown in Fig.1-(a) and (b). Both cases, the value of n is 1 and m is 4. The agreement of the calculated values to the real data above 60K is excellent except the region around the second peak for the unirradiated sample. This indicates that the second peak has a different its origin with the usual pinning. The irradiation does not change this formula. It does not change the pinning forces qualitatively, just enhance. The pinning forces of the QMG-materials are originated from the inclusions randomly distributed in the sample. The irradiation also introduces random pinning centers. Thus the pinning forces does not change qualitatively with the irradiation. This fact suggests the pinning is originated from the random pinning centers for both two cases.

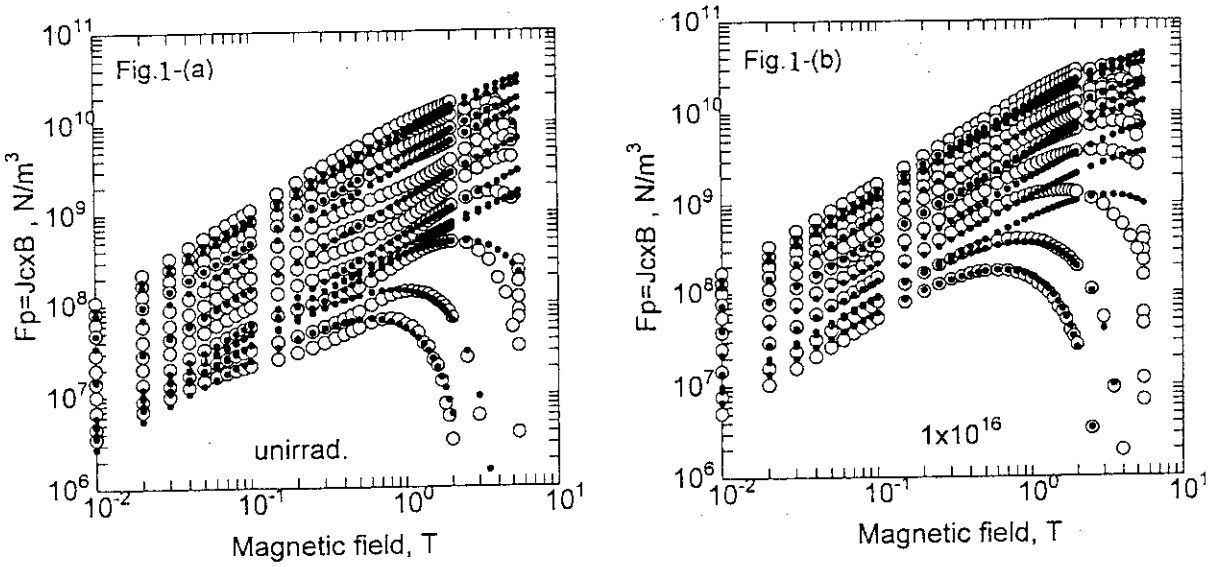

Fig.1 The field dependence of pinning forces at different temperatures, (a) for unirradiated and (b) for proton irradiated case. Open circles are obtained data and small solid circles are calculated values from eq.(1). Measured temperatures are 5,10,20,30,40,50,60,70,77 and 80K, respectively.

References

1)S.Okayasu and Y. Kazumata, Czech. J. Phys., 43,(1996) 1645

2)S.Okayasu and Y. Kazumata, to be published

5.14 STUDY ON FRACTURE PROCESS IN POLYCRYSTALLINE SILICON CARBIDE IRRADIATED BY HIGH ENERGY IONS

S. BABA, J. AIHARA, M. ISHIHARA and T. ARAI

It is well known that deformation and fracture properties in polycrystalline ceramics depend highly on their microstructure, especially on mesoscopic pore/grain structures. The authors are interested in analyzing physical processes controlling bulk mechanical properties by means of micromechanics relevant to mesoscopic flaws, i.e., micropores in engineering ceramics. The physical process under mechanical loading is governed by mesoscopic spacial and statistical distributions of mesoscopic flaws.

In the present study the thin rectangular specimens (0.5mm wide, 1.0mm thick and 20mm long) made of pressureless sintered polycrystalline silicon carbide(α -SiC) were prepared. The statistical distribution of grain size was characterized by a quantitative image analysis and shown in Fig.1 together with its morphology. The specimens were irradiated by high energy ions of gold and nickel using the TANDEM facility to generate microdefects distributed nonuniformly along the thickness. After irradiation they were subjected to three-point bending to measure a degradation in bending strength.
Preliminarily two different types of irradiated specimens were available: One irradiated by 180MeV Au ions to a fluence of about 2.5×10^{12} ions/mm^2 (surface) and the other by 90MeV Ni ions to about 2.3×10^{13}/mm^2(surface). Those heavy ion induced damages are represented typically by the maximum dpa(displacement damage per atom) of 3.9 at 12.6 μm deep and 14.1 at 11.2 μm deep, respectively, according to the calculation by the TRIM-95 code.

The results of the bending tests with those specimens are shown in Fig. 2 by plotting the bending strengths in a normal distribution scheme. It indicates the reduction in bending strength of the irradiated specimens as compared to the unirradiated ones. It is however apparent that those less heavily irradiated specimens have more reduced strengths. We assume that the estimated displacement damages should not correspond all to those physical defects which are responsible for micromechanics in SiC. It should be noted also that an accurate bending strength could be calculated by considering a nonuniform distribution in governing microdefects along the thickness. To characterize quantitative nature of induced defects we will examine the concurrently irradiated tiny disks by an electron microscopy.

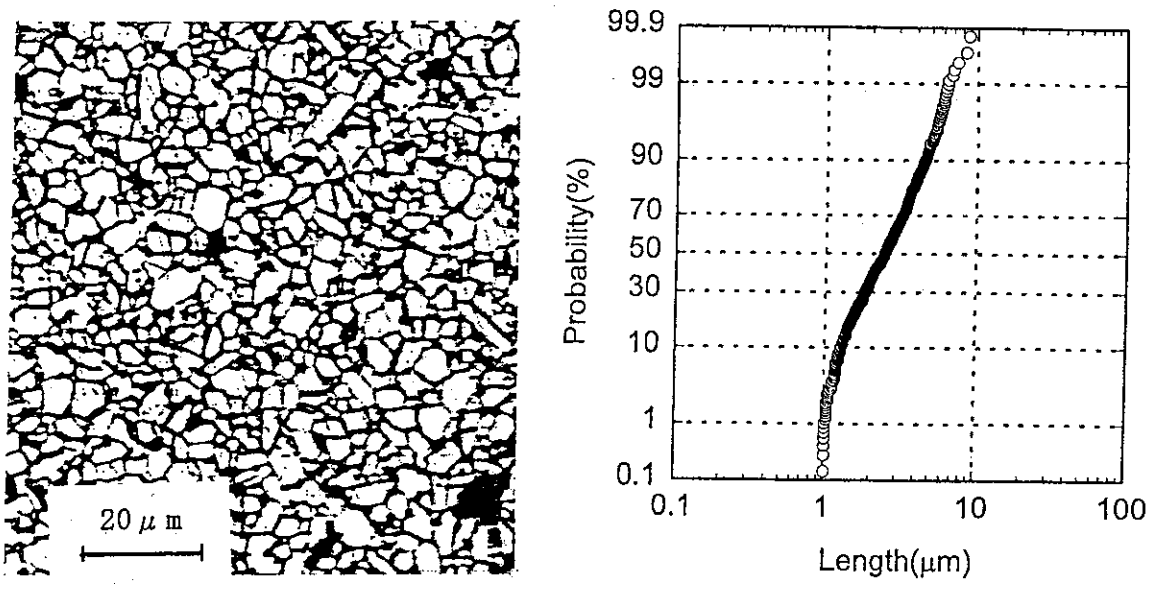

a) Mesoscopic pore/grain structure b)Statistical distribution of grain size

Fig. 1. Results of of the quantitative image analysisof polycrystalline α —SiC.

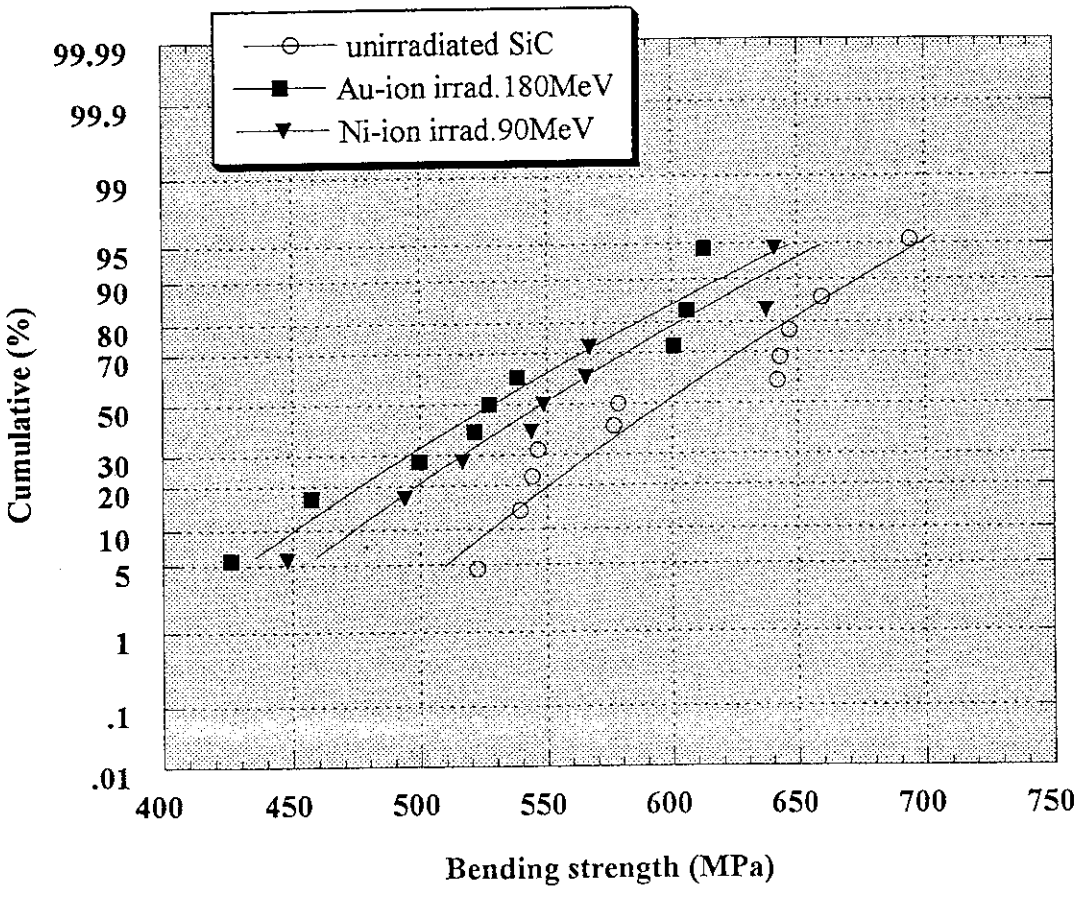

Fig. 2. Statistical distribution of measured bending strengths of unirradiated and irradiated SiC specimens.

5.15 RADIATION EFFECTS OF OXIDE CERAMICS BY HEAVY-IMPLANTATION IN TANDEM ACCELERATOR

K.FUKUDA, S. KASHIMURA,T. SHIRATORI and T. OHMICHI

In the framework of a program for developing the rock-type fuel[1] at the Japan Atomic Energy Research Institute(JAERI) , which is envisaged to incinerate the excess plutonium, followed by disposition without any reprocessing(once-through cycle), we have investigated radiation stability on several ceramic oxides, alumina(Al_2O_3), spinel($MgAl_2O_4$) and zirconia(ZrO_2), all of which are major components of the rock-type fuel. In the rock-type fuel alumina and spinel are expected to act as a getter phase for the fission products such as alkali metal and alkali earth, meanwhile zirconia is expected to act an inert matrix for actinides and a getter phase for rare earth.

The present experiment carried out in 1996 is aimed to investigate recovery of radiation-induced defects of these three ceramics after heavy-ion implantation with 70-80MeV, which is simulated to fission-fragment irradiation. The recovery of defects is investigated with combination of the electron beam diffraction and the Raman spectroscopy.

The implantation was conducted by the heavy-ion TANDEM accelerator at JAERI. I^{+6} or I^{+7} ion irradiation have been carried out on these oxides with ion energy of 70-80 MeV, and fluence ranging from $1.0x10^{15}$ to $1.0x10^{16}$ ions/cm^2 . Highlights previously reported in this journal[2,3] were that the Raman spectroscopy defined clear difference in the spectrum of the bombarded and non-bombarded $MgAl_2O_4$ samples, where one spectrum at the wave number of 400 cm^{-1} remained unchanged in the bombarded $MgAl_2O_4$, although other spectra almost disappeared. Also, all of the spectra of Al_2O_3 completely disappeared in the bombardment. From the Raman spectroscopy we deduced that bombarded area of $MgAl_2O_4$ is disordered, but not amorphous, meanwhile the area of Al_2O_3 became amorphous.

For investigation on recovery of radiation-induced defects in the oxides, the Raman spectroscopy was conducted after heat-treatment of the implanted oxides in air at two different temperatures. The spectra from heat-treated oxides were compared with those of as-implanted ones. Comparison of those spectra indicated different recovering natures of the defects in the oxides. For Al_2O_3 as shown in Fig. 1, a typical feature indicating raised background in as-implanted sample was disappearing with annealing time at 590℃ and any peaks in the spectra, not clear in the as-implanted one appeared after 5 min and increased rapidly, on the contrary. This seems that amorphous formed in Al_2O_3 by implantation is recovered by annealing. The heat-treatment at 800℃ indicated enhanced recovering feature.

as-implanted ZrO_2 no peaks was detected, but very short time annealing for only 5 min at 480℃ recover peaks of the spectrum as same as those of un-implanted one. From this behavior it is deduced that defects introduced in ZrO_2 by implantation are a disorder of atomic arrangement in ZrO_2 lattice.

References

[1] H.Akie, et al.,"A new fuel material for once-through weapons plutonium burning", Nucl. Technol., 107(1994) 182-192.

[2] S.Kashimura, et al., "Physical property changes of aluminum constituent oxides by bombardment with 70MeV iodine ions", JAERI-Review 95-017(1995).

[3] S.Kashimura, et al., "On Amorousness and Disordering in Oxide Ceramics by Heavy-Ion Bombardment", JAERI-Review 96-011(1996).

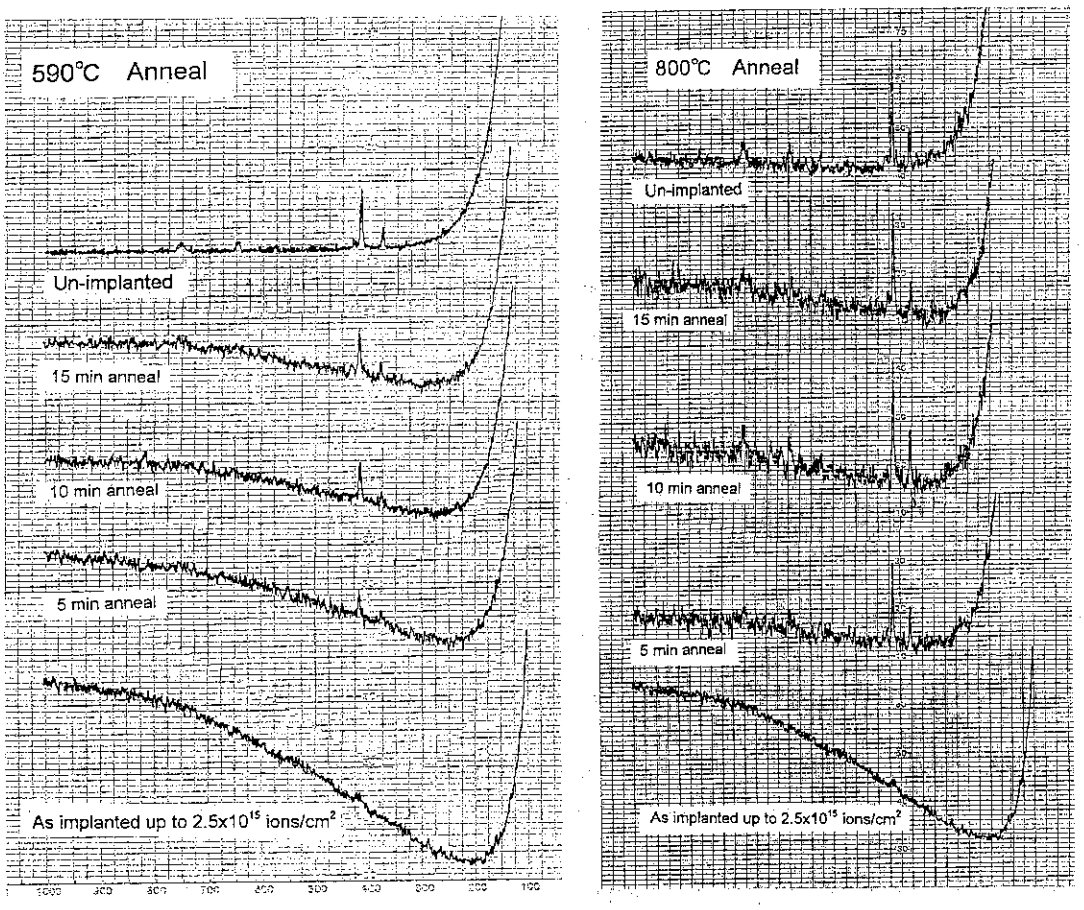

Fig. 1 Typical recovery of defects in Al_2O_3 by heat-treatments.

5.16 RADIATION DAMAGE ANALYSIS FOR RELATING NUCLEAR ENERGY DEPOSITION AND LATTICE PARAMETER CHANGE OF UO_2

K. HAYASHI, H. KIKUCHI and K. FUKUDA

A series of high-energy ion irradiation works [1-3] has been made on UO_2 by using the tandem accelerator of the Tokai Research Establishment of JAERI. The works are relevant to the "rim effect" [4], or a microstructural change, in high-burnup fuels for light water reactors.
In the previous work, the effect of the incident energy on the lattice parameter change of UO_2 was studied, and the possibility of defect formation due to the electronic energy deposition was proposed [2,3]. Thereafter, additional experiments with 70 and 150 MeV iodine ions were performed to confirm the possibility. The results of the experiment are under analysis.

Besides the experimental works, radiation damage calculation has been made, as follows. As a first step, the partitioning of the nuclear energy deposition between uranium and oxygen target atoms was focused using the SRIM-96 code, which is a revised TRIM code [5].

In the previous calculation, the EDEPJR-87 code [6] was used to determine the nuclear energy deposition to the target atoms in total. Unfortunately, this code cannot calculate the partitioning of the nuclear energy deposition between the constituent U and O atoms. Therefore, the partitioning fractions derived by Soullard et al. [7] had been adopted [3]. The referred fractions correspond to those for the nuclear fission of uranium, in which light and heavy fission fragments with energies around 70 and 90 MeV, respectively, are implanted into the UO_2 matrix. The fractions are expected to apply to the case of iodine ions with energies around 100 MeV, because the heavy fission fragments, such as iodine, have energies comparable to this value. However, in the case of higher energy up to 300 MeV, it is not clear whether the fractions after Soullard et al. can be applied in a reasonable approximation.

On the other hand, the monte carlo code, SRIM-96, can calculate the partitioning fractions easily, although much longer calculation time is needed for the full calculation determining the partition fractions. On this background, the revised damage calculation was made with the SRIM-96 code for UO_2 (100%TD) irradiated by iodine ions with different energies. The displacements per atom (dpa) for U and O target atoms at the incident surface were evaluated by a least-squares fitting using the calculated depth profiles adjacent to the surface, since the depth profiles had some scattering.

The results of the calculation are listed in Table 1. It is noted in this table that the dpa ratio of O and U atoms at the surface, which reflects the partition of the nuclear energy deposition between U and O target atoms, can be reasonably approximated by the ratio evaluated by Soullard et al. [7]. It is also noted that the mean projected range and the dpa values for uranium at the surface, which were calculated by the SRIM-96 code, are somewhat larger than those calculated by the EDEPJR-87 code. It is considered that these differences come from those in the electronic and nuclear stopping powers used in each code. At this moment, however, it is difficult to discuss the validity of the stopping power equations used in these codes, because reliable experimental data are not available to the present authors for the case

of UO_2 target and heavy ions.
The above-calculated results are leading to analyses of the relation between the surface dpa values and the lattice parameter changes measured by X-ray diffractometry.

Table 1 Results of radiation damage analysis by the SRIM-96 code for UO_2 irradiated with iodine ions with different energies.

Ion Energy (MeV)	Mean Projected Range (μm)		Surface U-dpa at 10^{15}ions/cm^2		Surface dpa Ratio dpa(O)/dpa(U)	
	EDEP	SRIM	EDEP	SRIM	Ref.[7]	SRIM
70	5.4	6.2	0.14	0.29	1.36	1.37
100	6.5	7.6	0.10	0.20	1.36	1.34
150	7.9	9.4	0.074	0.14	1.36	1.29
200	9.0	11.0	0.059	0.11	1.36	1.31
300	10.9	14.0	0.042	0.064	1.36	1.27

The authors are grateful to Drs. A. Iwase, Y. Chimi, and N. Ishikawa of Advanced Science Research Center of JAERI for guidance and assistance in the SRIM-96 code calculation. They are also indebted to S. Kashimura, T. Shiratori, K. Tsukada and S. Ichikawa of Department of Fuels and Chemistry and members of Accelerators Division of JAERI for their assistance in the tandem accelerator irradiation experiments.

References

1) K.Hayashi, H.Kikuchi and K.Fukuda, J. Alloys Compo. 213/214 (1994) 351.
2) K.Hayashi, H.Kikuchi and K.Fukuda, JAERI-Review 96-011 (1996) p.107.
3) K.Hayashi, H.Kikuchi and K.Fukuda, Intern. Workshop on Interfacial Effects in Quantum Engineering Systems, IEQES-96 (August 21-23, 1996, Mito, Japan) PB-01; to be published in J. Nucl. Mater. (1997).
4) e.g. J.O.Barner, M.E.Cunningham, M.D.Freshley and D.D.Lanning, Proc. Intern. Topical Mtg. on LWR Fuel Performance (Avignon, France, April 21-24, 1991) p.538.
5) J.P.Biersack and L.G.Haggmark, Nucl. Inst. Meth. 174 (1980) 257.
6) T.Aruga, K.Nakata, and S.Takamura, Nucl. Instr. Meth. in Phys. Res. B33 (1988) 748.
7) J.Soullard and A.Alamo, Rad. Effects 38 (1978) 133.

5.17 LUMINESCENCE CHARACTERISTICS OF PHOTO-STIMULABLE PHOSPHOR WITH HEAVY CHARGED PARTICLES

C. MORI [1], T. SUZUKI [1], H. SAKAI [1], A. URITANI [1],
M. YOSHIDA, F. TAKAHASHI

Photo-stimulable phosphor BaFBr:Eu^{2+} is used for two-dimensional position sensitive detectors known as imaging plate (IP). The IP is useful to measure extremely low level radioactivity [1], because of its high sensitivity and storage effect of the image (F-centers and Eu^{3+} ions) formed by incident particles. Owing to the storage effect, however, it is usually impossible to identify the kind and energy of incident particles. We proposed a repeated reading method for the identification [2]. In this method, the decrease of PSL (Photo-Stimulated Luminescence) intensities with the number of reading times depends on the kind and energy of incident particles as shown in Fig. 1 and also the preservation time between the exposure and the reading operations [3]. The purpose of this study is to obtain some information to make the PSL mechanism clear by measuring prompt luminescence intensity and PSL intensity as a function of the number of repeated reading times for high-energy heavy charged particles which have large stopping power and long ranges. Adding it, we began to examine the improvement of quantitative precision in the determination of latent image intensity by means of the repeated reading method.

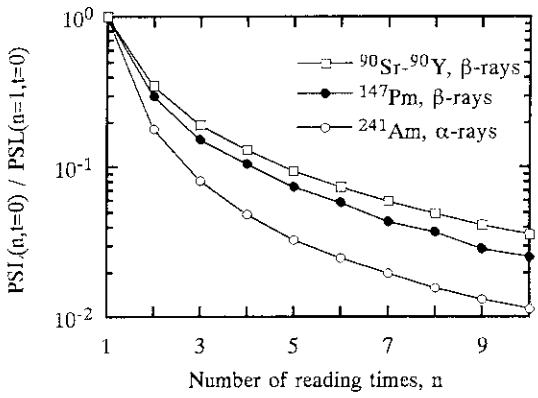

Fig. 1 The multiple successive reading method in the case of α-particle and ß-particle incidences.

Figure 2 shows the fading of the first reading as a function of the preservation time between the 5 minute exposure and the reading operation for

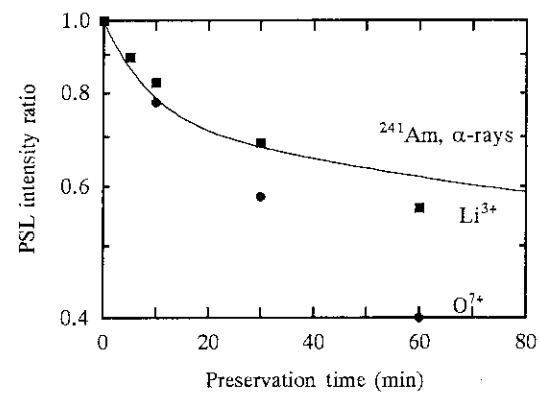

Fig. 2 The fading of the first reading PSL intensity in the case of α-ray, O^{7+} ion Li^{3+} ion incidences.

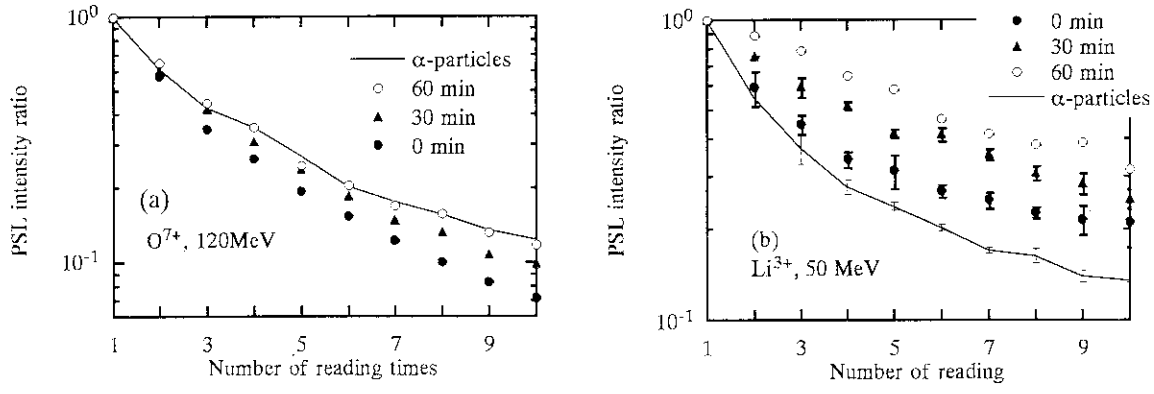

Fig. 3 The multiple successive reading method in the case of (a) O^{7+} ion (b) Li^{3+} ion and α-particle incidences. The preservation time between the exposure and the first reading was changed to 0, 30 and 60 minutes.

[1] Department of Nuclear Engineering, Nagoya University

O^{7+} 120 MeV ions and Li^{3+} 50 MeV ions incidences, respectively. Figure 3 shows the decrease of the PSL intensities as a function of the number of reading times where the preservation time between the exposure and the first reading changed into 0 min, 30 min or 60 min, for the (a) O^{7+} ion and (b) Li^{3+} ion incidences. Because experimental conditions are different between (a) and (b), these figures cannot be compared directory with each other. But the results of heavy ion and α-particle incidences, for which the preservation time is 0 min, in the same figure can be compared. For the O^{7+} ion incidences, whose stopping power is larger than that of α-particle and whose range is longer than that of α-particle, the decrease of PSL intensity is more rapid than that for α-particle. For the Li^{3+} ion incidences, which have a stopping power close to that of α-particle and a range longer than that of α-particle, the decrease of PSL intensities with the number of reading was more gradual than α-particle. The tendencies of the decrease of PSL intensity with the number of reading time become gradual with increasing the preservation time, which have been shown for α-particle and ß-particle incidences because of the decrease of the densities of trapped holes and electrons by the diffusion [3].

There is a probability that an electron excited by a laser photon recombines with a trapped hole and causes PSL or it is trapped by an F^+-center and becomes an F-center. The probability of emission depends on the density of trapped holes. If holes distribute densely, the probability of the recombination will be large and many electrons will cause luminescence. Therefore, the tendency of the decrease with the number of reading times becomes gradual both with decreasing the stopping power of incident particle and with increasing the preservation time. Furthermore, the probability of the excitation of trapped electrons depends on the depth from the surface of IP because of the attenuation of laser beam. Therefore, it is difficult to read out the image for the long range particle with a single reading operation. The explanation is supported by the experiments carried out using the tandem accelerator.

To obtain a high precision in radiation measurement with IP, PSL intensity must be intense. To get the large intensity, we tried to read IP repeatedly and to add each read intensity. Figure 4 shows the improvement of the precision by the method of repeated readings. The normalized standard deviation of the sums of the PSL intensities decreased with the number of reading times. Details were measured for α-particle and ß-particle incidences and it was found that repeated readings with long time interval of more than 1 hour between the readings improve the precision drastically [4].

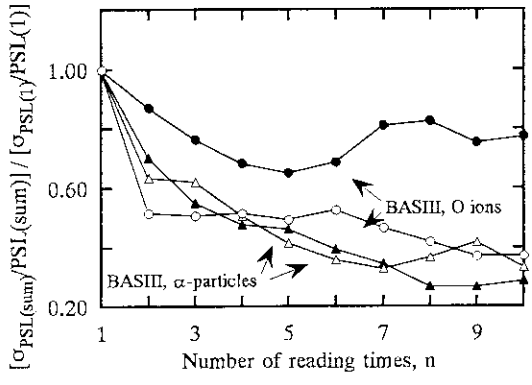

Fig. 4 Improvement of the precision with repeated reading method.

References

[1] C. Mori, T. Suzuki, S. Koido, A. Uritani, H. Miyahara, K. Yanagida, Y.Wu, K.Nishizawa, M.Yoshida, F. Takahashi, J. Miyahara, J. Radioanal. Nucl. Chem., **206** (1996) 263.

[2] C. Mori, T. Suzuki, S. Koido, H. Miyahara, A. Uritani and K. Nishizawa : Nucl. Instrum. and Methods., **A353** (1994) 371.

[3] T. Suzuki, C. Mori, K. Yanagida, A. Uritani, H. Miyahara, M. Yoshida, F. Takahashi, J. Nucl. Sci. Technol., **34** (1997) 461.

[4] T. Suzuki, C. Mori, H. Miyahara, A. Uritani, M. Yoshida, K. Takahashi, International Committee for Radionuclide Metrology 1997 in NIST, Gaithersburg MD USA (May 19, 1997)

5.18 SINGLE EVENT GATE RUPTURE IN POWER MOSFETS BY INCIDENCE OF HIGH-ENERGY IONS

S. SHUGYO[1], T. HIRAO, S. MATSUDA[1], I. NASHIYAMA
K. SUGIMOTO[1], M. NAKAMURA[1], M. YONEMARU[1]
A. MATSUMOTO[1], T. SUZUKI[1], T. HIROSE[2], H. OHIRA[2]
Y. NAGAI[2]

Power MOSFETs exhibit low power losses and fast turn-on/turn-off switching time and are desirable devices for space system application. However, Power MOSFETs are susceptible to Single Event Phenomena(SEP). At first, Single Event Burnout(SEB) have been found and a lot of tests were performed on SEB, and the mechanism is getting clear. But lately, another failure mode surfaced. This failure mode was identified as Single Event Gate Rupture(SEGR) and was recognized to be serious problem, resulting in catastrophic device failure. SEGR is caused by heavy-ion-induced charge accumulation in a silicon and localized dielectric breakdown of the gate oxide. Subsequent gate and drain current results in a thermal runaway condition melting a permanent short between the gate and drain rendering the MOSFET useless. The occurrence of SEGR depends on the gate-drain voltage (Vds) , LET and temperature [1-2]. The susceptibility to SEGR increases with increasing Vds or LET or temperature. Consequently SEGR tolerance of Power MOSFETs for Vds and LET must be studied.

At the present irradiation test, the scattered ion beam by a Au scatterer is used. Changing the scattered ion energy is to change LET. To control LET, changing the scattering angle was considered. Thus, the apparatus to move the devices testing SEGR was made, and the scattering angle dependence of the scattered ion beam energy was investigated. As a result(Fig.1), the test results agree with the calculated result well, so it is possible to control LET by changing the scattering angle.

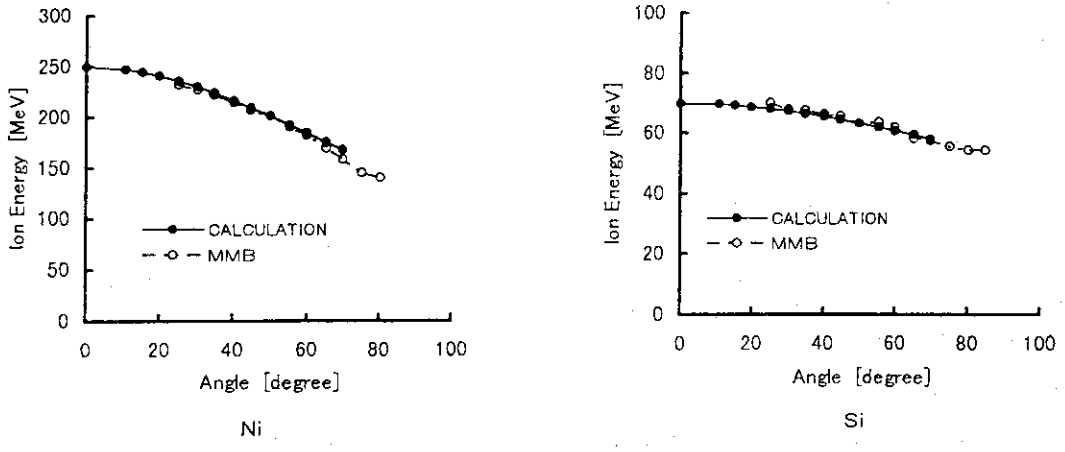

Fig 1. The characteristics of the scattered ion energy—the scattering angle for Ni and Si.
In this figure, CALCULATION plots are a calculated result as a perfect elastic collision between Ni or Si and Au. MMB plots are a measurement result using Multi Parameter Analyzer, and normalized by the calculation result for 50°

[1]Electronic and Information Technology Laboratory, Office of Research and Development, National Space Development Agency of Japan.
[2]Components Engineering Section, Engineering Dept., RYOEI TECHNICA Corporation.

To investigate the occurrence of SEGR(NASDA 2SK2271), the SEGR measurements on two angles (25° and 45°) used Ni ion was performed(Table.1). Its results differ from our estimate that it is more susceptible to SEGR on the condition of 45° angle rather than that of 25° angle under the same Vds condition. Because the LET on the condition of 45° (approximately 29 MeV -cm^2-mg^{-1}) is big compared with that of 25° (approximately 28 MeV -cm^2-mg^{-1}). SEGR occurred on the condition under Vds=300[V] for 25° and didn't occur on the condition under the same Vds for 45° . The reason is not clear yet, but one possibility is that the scattered ion beam used for this test includes gold particles from Au scatterer. Fig.2 shows that the scattered ion beam includes gold particles. Thus, it is possible that the test results were affected by such gold particles. The estimation of SEGR tolerance of NASDA 2SK2271 for space application was studied. But, the experimental procedure should be improved, and the influence of gold particles would be verified.

Table 1. The occurrence of SEGR (the Au scatterer angle of 25° and 45°)

V ds [V]	the angle of 25°	the angle of 45°
250	×	×
275	×	—
300	○	×

○ : SEGR occur, × : SEGR not occur

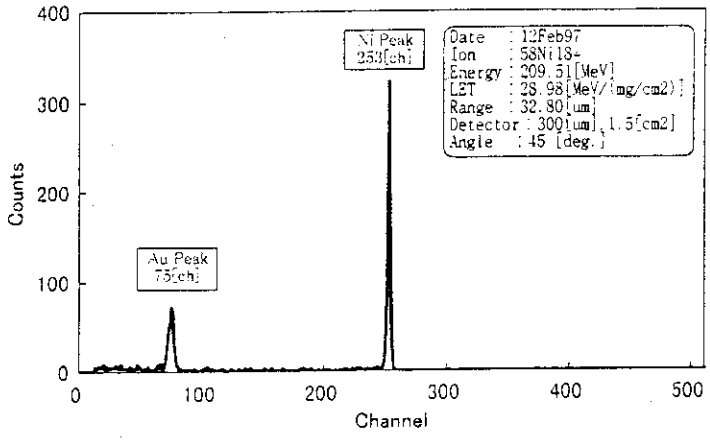

Fig 2. The measurement result of irradiation spectrum.

Reference

1)C.Frank Wheatley, Jeffrey L.Titus, Dnald I.Burton, and Donald R. Carley, IEEE Trans.Nucl.Sci. Vol.43,No.6,(1996),pp.2944-2951

2) I.Mouret, M.-C.Calvet, P.Calvel, P.Tastet, M.Allenspach, K.A.LaBel, J.L.Titus, C.F.Wheatley, R.D.Schrimpf, and K.F.Galloway, IEEE Trans.Nucl.Sci. Vol.43,No.43,(1996),pp/936-943

5.19 IMPROVEMENTS OF IN-SITU RESISTIVITY MEASUREMENT SYSTEM AT LOW TEMPERATURE

H. SUGAI, H. MAETA, and H. OHTSUKA

Recently, semiconductor materials are destined for use in high radiation environments such as nuclear facilities and the artificial satellites. However, the relations between radiation defects and electrical properties in semiconductors are not clear [1]. In the previous works [2-4], we studied the resistivity and the structural changes for doped diamond and silicon irradiated with heavy ions at low temperatures. We report here improvements of an in-situ resistivity measurement system, which is installed at the H-1 beam-line of JAERI tandem accelerator, for semimetals and semiconductors irradiated with heavy ions at low temperature.

A new sample holder is composed of the four tungsten probes, a pyrolytic boron nitride (P-BN), and a Cu plate as shown in Fig. 1. We selected P-BN to insulate the sample from the Cu plate, because P-BN has good thermal conductivity and machinability. The Cu plate is connected to the bottom of a liquid helium vessel and cooled by liquid helium in a vacuum chamber. Since the cooling power of the cryostat was increased owing to the improvements of thermal contact and radiation shield, the minimum temperature of the sample decreased from 18 K to 6 K.

Our apparatus is composed of a current source (Keithley 238), a voltage meter (Keithley 182), a switching system (Keithley 7001 with 7012-S card), and a temperature controller (Lake Shore 340 with silicon diodes sensor). The instruments are controlled by a personal computer through the GPIB-bus extenders from the control room. Small pieces of indium were inserted between the tungsten probes and specimen to make the Ohmic contacts. The maximum value of the resistivity measured by the van der Pauw method [5] was 1.9 MΩcm at the current of 0.5 μA. The method does not need the specimen dimension except the thickness. The maximum is limited by the isolation of resistance in the switching system.

If you need a sample of program (N88-BASIC) for the van der Pauw method, please contact one of the authors (sugai@popsvr.tokai.jaeri.go.jp).

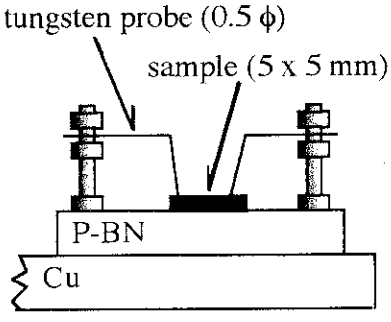

Fig. 1. Schematic side view of a sample holder.

References **1)** For example, S. Ishino, Oyo buturi, 46 (1977) 458 [in Japanese]. **2)** K. Haruna, H. Maeta, H. Sugai, T. Sato, T. Otsuki, F. Ono, H. Ohtsuka, and K. Ohashi, JAERI-Review-96011 (1996) 98. **3)** H. Maeta, K. Haruna, Lu Bang and F. Ono, Nucl. Instr. and Meth., B80/81 (1993) 1477. **4)** H. Sugai, H. Maeta, H. Ohtsuka, N. Matumoto, K. Haruna, and F. Ono, Fall Meeting of the Physical Society of Japan in Yamaguchi (Oct. 2, 1996). **5)** For example, H. Ryssel and I. Ruge, Ion Implantation (John Wiley and Sons, New York and Toronto, 1986) p. 188.

5.20 A NEW IRRADIATION CHAMBER INSTALLED IN THE BOOSTER LINE

M. SATAKA, Y. KAZUMATA[1] S. OKAYASU and T. Shoji

When high energy ions are bombarded to solids, radiation effects are caused by two mechanisms; that is , nuclear collisions and electron excitations. Current studies for radiation damage are focused on the latter mechanisms although lots of the study are already accumulated in reports for both mechanisms. Recent discovery of columnar defects produced by high energy heavy ions in high T_c superconducting materials particularly stimulated the study of radiation effects due to electron excitations, since the critical current density in the materials was remarkably enhanced by the introduction of the defects. The interaction between the defects and magnetic flux lines is a currently central problem for the improvement of the critical current density in high T_c materials. For pushing forward the problem, we fabricated a new irradiation chamber. By using this chamber, we can take a new step for the study using 3-4 times higher energy ions, compared with the study having done so far. Higher energy ion beams can produce well-tailored columnar defects and also enable us to perform the experiments with single crystals in 3-4 times thicker than the thickness of thin films used so far.

The new chamber followed the instrument for nuclear physics at the backward is installed at the B1 line (booster line) in the tandem accelerator. The vacuum of the chamber is better than $1x10^{-8}$ torr., and is free from oil contamination because a magnetically suspended turbo-molecular pump is used for the evacuation. The irradiation temperature of a specimen can be controlled from 15 K to room temperature by a refrigerator. Without breaking down the vacuum, the number of 24 specimens can be set on an experiment. The irradiation angle between the beam direction and the surface of a specimen can cover the range from -180 to +180 deg. Very homogeneous beams passing through the apparatus of 15 or 20 mm in the diameter are led to a specimen. The beam current is monitored by a Faraday cup and the profile of the beams can be adjusted by the image from a TV camera which observes the light emitted from a quartz-viewer by high energy ion bombardments.

---

1. Nihon Advanced Technology. Co.

Figure 1 depicts a rough sketch of the part of the sample-holder of the chamber. The first experiment was performed with high T_c materials at the end of the last fiscal year and proved the performance as expected. The beam current at the experiment is about 10 nA for 400 MeV Au^{24+} ions. Many experiments with the use of the chamber are in our future plans.

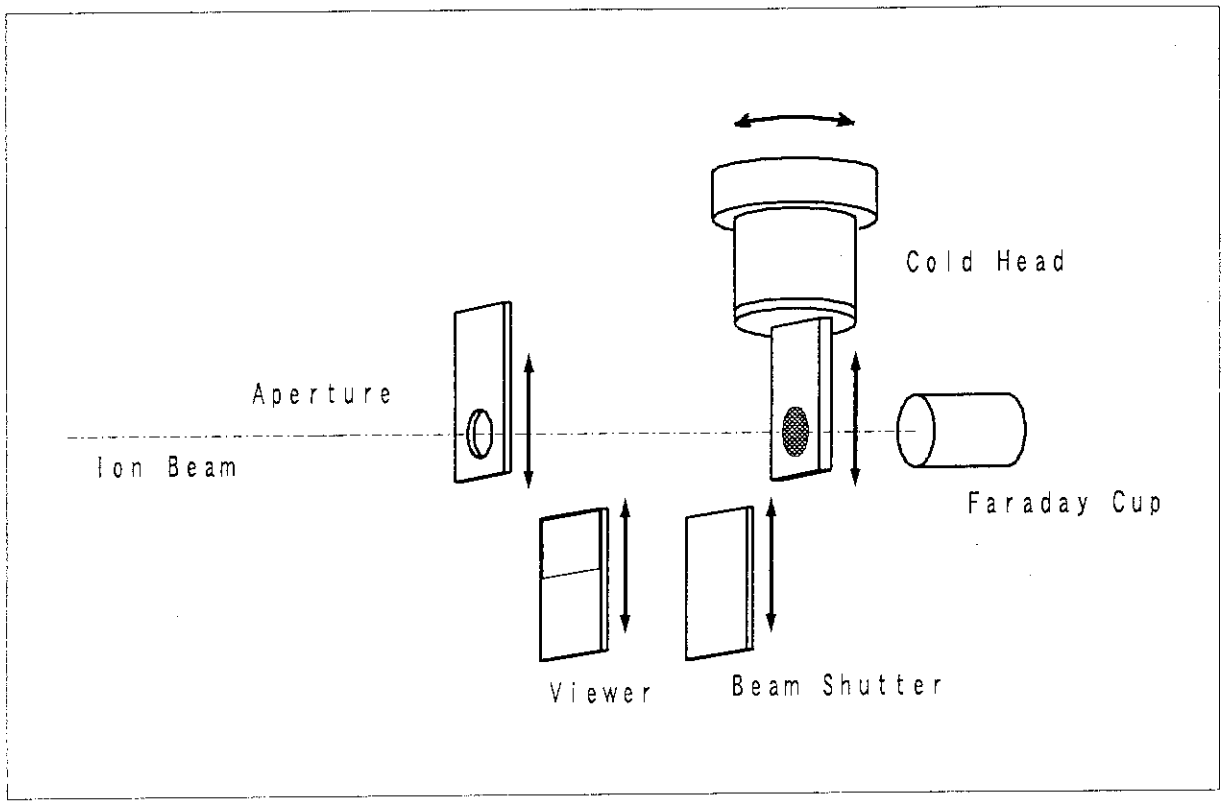

Fig.1. A rough sketch of the part of the sample-holder of the chamber installed in the booster line.

6. Publication in Journal and Proceedings, and Contributions to Scientific Meetings

ACCELERATOR OPERATION AND DEVELOPMENT

Journal/Proceedings

Takeuchi, S., Ishii, T., Matsuda, M., Zhang, Y. and Yoshida, T.
Acceleration of heavy ions by the JAERI tandem superconducting booster
Nucl. Instr. and Methods **A 382**(1996)153.

Takeuchi, S., Matsuda, M., Kanazawa, S., Yoshida, T., Ohuchi, I. and Shoji, T.
Status of thr JAERI tandem superconducting booster
Proc. of the 9th workshop on tandm accelerators and associated technology, Tokai,
July 4-5(1996)pp42-44.

Yoshida, T., Kanda, S., Takeuchi, S., Hanashima, S., Shouji, T., Ohuchi, I., Horie, K.,
Tsukihashi, Y., Abe, S., Kanazawa, S., Ishizaki, N., Tayama, H., and Masuda, M.
The Status of the JAERI Tandem Accelerator
Proc. Of the 9th Workshop of the Tandem Acclerator and their Associated
Technorogy
(JAERI Tokai, July, 4-5, 1996)

Meetings

Yoshida, T., Kanda, S., Takeuchi, S., Hanashima, S., Shouji, T., Ohuchi, I., Horie, K.,
Tsukihashi, Y., Abe, S., Kanazawa, S., Ishizaki, N., Tayama, H., and Masuda, M.
The Status of the JAERI Tandem Accelerator
9th Workshop of the Tandem Acclerator and their Associated Technorogy
(JAERI Tokai, July, 4, 1996)

NUCLEAR STRUCTURE

Journal/Proceedings

Asai, M., Tsukada, K., Ichikawa, S., Osa, A., Kojima, K., Shibata, M., Yamamoto, H., Kawade, K., Shinohara, N., Nagame, Y., Iimura, H., Hatsukawa, Y., Nishinaka, I.,
Identification of a New Isotope ^{166}Tb
J. Phys. Soc. Japan **65** (1996) 1135.

Baba, H., Yokoyama, A., Takahashi, N., Nitani, N., Kasuga, R., Yamaguchi, T., Yano, D., Takamiya, K., Shinohara, N., Tsukada, K., Hatsukawa, Y. and Nagame Y.
Abrupt Changes of the Characteristics of the Proton-Induced Fision of ^{238}U around 14-MeV Excitation
Z. Phys. **A356**(1996) 61.

Hashimoto, N., Saitoh, T., Lu, J., Komatsubara, T., Furuno, K., Oshima, M., Hatsukawa, Y., Hayakawa, T., Furutaka, K., Kidera, M., Ishii, T.
Static Magnetic Moments of the ground state rotational band in ^{181}Ta
Contrib. to the Conf. on Nuclear Structure at the Limits July 22-26, 1996, ANL

Ichikawa, S., Asai, M., Tsukada, K., Osa, A., Ikuta, T., Shinohara, N., Iimura, H., Nagame, Y., Hatsukawa, Y., Nishinaka, I., Kawade, K., Yamamoto, H., Shibata, M. and Kojima, Y.
Mass Separation of Neutron-Rich Isotopes Using a Gas-Jet Coupled Thermal Ion Source
Nucl. Instrum. Methods **A374**, (1996) 330.

Iimura, H., Katakura, J., Kitao, K.and Tamura, T.
Nuclear Data Sheets for A=124
Nucl. Data Sheets **80**(1997)895.

Kidera, M., Oshima, M., Hatsukawa, Y., Furutaka, K., Hayakawa, T., Matsuda, M., Iimura, H., Kusakari, H., Igari, Y., and Sugawara, M.
Coulomb Excitation of ^{155}Gd
J. Phys. Soc. Jpn, **66**(1997)285-287

Magara, M., Shinohara, N., Hatsukawa, Y., Tsukada, K., Iimura, H., Usuda, S., Ichikawa, S., Suzuki, T., Nagame, Y., Kobayashi, Y. and Ohshima, M.
Decay Properties of ^{245}Cf
Radio Chim. Acta. **72** (1996) 39-43

Nagame, Y., Nishinaka, I., Tsukada, K., Oura, Y., Ichikawa, S., Ikezoe, H., Zhao, Y.L., Sueki, K., Nakahara, H., Tanikawa, M., Ohtsuki, T., Kudo, H., Hamajima, Y.,

NUCLEAR STRUCTURE

Journal/Proceedings

Asai, M., Tsukada, K., Ichikawa, S., Osa, A., Kojima, K., Shibata, M., Yamamoto, H., Kawade, K., Shinohara, N., Nagame, Y., Iimura, H., Hatsukawa, Y., Nishinaka, I.,
Identification of a New Isotope ^{166}Tb
J. Phys. Soc. Japan **65** (1996) 1135.

Baba, H., Yokoyama, A., Takahashi, N., Nitani, N., Kasuga, R., Yamaguchi, T., Yano, D., Takamiya, K., Shinohara, N., Tsukada, K., Hatsukawa, Y. and Nagame Y.
Abrupt Changes of the Characteristics of the Proton-Induced Fision of ^{238}U around 14-MeV Excitation
Z. Phys. **A356**(1996) 61.

Hashimoto, N., Saitoh, T., Lu, J., Komatsubara, T., Furuno, K., Oshima, M., Hatsukawa, Y., Hayakawa, T., Furutaka, K., Kidera, M., Ishii, T.
Static Magnetic Moments of the ground state rotational band in ^{181}Ta
Contrib. to the Conf. on Nuclear Structure at the Limits July 22-26, 1996, ANL

Ichikawa, S., Asai, M., Tsukada, K., Osa, A., Ikuta, T., Shinohara, N., Iimura, H., Nagame, Y., Hatsukawa, Y., Nishinaka, I., Kawade, K., Yamamoto, H., Shibata, M. and Kojima, Y.
Mass Separation of Neutron-Rich Isotopes Using a Gas-Jet Coupled Thermal Ion Source
Nucl. Instrum. Methods **A374**, (1996) 330.

Iimura, H., Katakura, J., Kitao, K.and Tamura, T.
Nuclear Data Sheets for A=124
Nucl. Data Sheets **80**(1997)895.

Kidera, M., Oshima, M., Hatsukawa, Y., Furutaka, K., Hayakawa, T., Matsuda, M., Iimura, H., Kusakari, H., Igari, Y., and Sugawara, M.
Coulomb Excitation of ^{155}Gd
J. Phys. Soc. Jpn, **66**(1997)285-287

Magara, M., Shinohara, N., Hatsukawa, Y., Tsukada, K., Iimura, H., Usuda, S., Ichikawa, S., Suzuki, T., Nagame, Y., Kobayashi, Y. and Ohshima, M.
Decay Properties of ^{245}Cf
Radio Chim. Acta. **72** (1996) 39-43

Nagame, Y., Nishinaka, I., Tsukada, K., Oura, Y., Ichikawa, S., Ikezoe, H., Zhao, Y.L., Sueki, K., Nakahara, H., Tanikawa, M., Ohtsuki, T., Kudo, H., Hamajima, Y.,

Takamiya, K. and Chung, Y.H.
Phys. Lett. **B387**(1996)26.

Nagame, Y.
Heaviest Elements-Synthesis and Chemical Properties
Chemistry and Education, **44**(1996)712

Oshima, M.
Coulomb excitation of ^{155}Gd
Proc. of the Joint Symposium on Nuclear Physics in the 21st Century opened by
Gamma-ray Spectroscopy at Saitama(1996)p.104.

Saitoh, T., Hashimoto, N., Lu, J., Komatsubara, T., Furuno, K., Oshima, M.,
Hatsukawa, Y., Hayakawa, T., Furutaka, K., Kidera, M.and Ishii, T.
E2/M1 mixing ratio of the transition from the 11/2-to 9/2-state in ^{193}T1
Contrib. to the Conf. on Nuclear Structure at the Limits July 22-26, 1996, ANL

Takeuchi, S., Ishii, T., Matsuda, M., Zhang, Y. and Yoshida, T.
Acceleration of Heavy Ions by the JAERI Tandem Superconducting Booster
Nucl. Instrum. Methods **A382**(1996)153.

Yokoyama, A., Takahashi, N., Nitani, N., Baba, H., Kasuga, R., Yamaguchi, T.,
Yano, D., Takamiya, K., Shinohara, N., Tsukada, K., Hatsukawa, Y. and Nagame, Y.
Precision Determination of Charge Dispersion and Distribution in the Proton-Induced Fission of
^{238}U at 13.9MeV Excitation
Z. Phys. **A356**(1996)55.

Zhang, C.T., Bhattacharya, P., Daly, P.J., Broda, R., Grabowski, Z,W., Nisius, D.,
Ahmad, I., Ishii, T., Carpenter, M.P., Morss, L.R., Phillips, W.R., Durell, J.L.,
Leddy, M.J., Smith, A.G., Urban, W., Varley, B.J., Schulz, N., Lubkiewicz, E.,
Bentaleb, M. and Blomqvist, J.
Yrast Excitations around Doubly Magic ^{132}Sn from Fission Product
γ -Ray Studies
Phys. Rev. Lett. **77**(1996)3743.

Meetings

Furutaka, K.
The High-spin Spectroscopy at A=60 region
RIKEN symposium (Dec. 27-28, 1996)

Furuno, K., Lu, J., T., Saitoh, T., Hashimoto, N., Komatsubara, T., Shizuma, T.,
Uchiyama, K., Oshima, M., Kidera, M., Furutaka, K., Hayakawa, T., Hatsukawa, Y.,
Ishii, T. and Matsuda.

Rotational band structures in ^{131}Cs.
Fall meeting of the Physical Society of Japan, October 8, 1996,

Hashimoto, N., Saitoh, T., Komatsubara, T., Lu, J., shizuma, T., Uchiyama, K., Furuno, K., Oshima, M., Kidera, M., Furutaka, K., Hayakawa, T., Hatsukawa, Y., Ishii, T. and Matsuda, M.
The measurement of g factors of s-band in ^{134}Ce.
Joint symposium on "Nuclear Physics in 21th century opened up by means of γ -ray spectroscopy", December 25-26, 1996.

Hatsukawa, Y., Hayakawa, T., Furutaka, K., Kidera, M., Ishii, T., Oshima, M., Shizuma, T., Mitarai, S., Morikawa, T., Gono, Y., Kusakari, H., Sugawara, M. and Nakada, H.
High spin states in ^{61,63}Cu
1996 Annual meeting of Physical Society of Japan (Oct. 8, 1996)

Hayakawa, T.
High spin states of Zn isotopes
The 4th International Conference on Radioactive Nuclear Beams
June 4, 1996, Omiya, Japan

Hayakawa, T.
Signature inversion of π h11/2 $\otimes$ ν h11/2 band in odd-ddd 132Cs Symposium
"Nuclear Physics and γ ray spectroscopy in 21th century"
Dec 26, 1996, Riken, Saitama

Hayakawa, T., Lu, J., Furuno, K., Furutaka, K., Komatsubara, T., Shizuma, T., Hasimoto, N., Saitoh, T., Matsuda, M., Hatsukawa, Y. and Oshima, M.
Shape coexistence of ^{132}Cs
Spring Meeting of the Physical Society of Japana
Mar 29, 1997, Nagoya, Japan

Ichikawa, S., Tsukada, K., Asai, M., Osa, A., Oura, Y., Iimura, H., Kojima, Y., Nishinaka, I., Hatsukawa, Y., Nagame, Y. and Kawade, K.
Search for Unknown Isotopes Using the JAERI-ISOL
13th International Conference on Elecrtomagnetic Isotope Separators and Techniques Related to Their Applications. Bad Durkhime (Germany)

Ichikawa, S., Tsukada, K., Asai, M., Osa, A., Kojima, Y., Kawade, K., Nagame, Y., Oura, Y., Iimura, H. and Yamamoto, H.
Identification of a New Isotope ^{165}Gd
Fall Meeting of the Japan Physical Society in Saga (Oct. 8, 1996)

Ideguchi, E., Gono, Y., Mitarai, S., Morikawa, T., Odahara, A., Kidera, M., Shibata, M., Tuchida, H., Kishida, T., Ishihara, M., Oshima, M., Hatsukawa, Y., Hamada, S., Iimura, H. and Ishii, T.
High-spin states in ^{146}Eu
Autumn meeting of Japan Physical Society of Japan (Saga, October 8, 1996)

Iimura, H., Ichikawa, S., Oshima, M., Katakura, J., Shinohara, N., Magara, M., Osa, A., Tamura, T., Asai, M. and Yamamoto, H.
Level Scheme of ^{127}La Fed by the ^{127}Ce Beta-Decay
Ninth Int. Symp. on Capture Gamma-Ray Spectroscopy and Related Topics in Budapest (Oct. 8, 1996)

Iimura, H., Ichikawa, S., Oshima, M., Katakura, J., Shinohara, N., Magara, M., Osa, A., Asai, M. and Yamamoto, H.
Level Scheme of ^{127}La Fed by the ^{127}Ce Beta-Decay
52nd Annual Meeting of the Physical Society of Japan in Nagoya (Mer. 29, 1997)

Ishida, Y., Iimura, H., Ichikawa, S. and Horiguchi, T.
Isotope Shifts of Optical Transitions in Ce Ⅱ by Collinear Laser-Ion-Beam Spectroscopy
Fall Meeting of the Physical Society of Japan (Oct. 3, 1996)

Itoh, M., Ishii, T., Ishii, M., Makishima, A,, Kohno, T., Hayakawa, T. and Ogawa, M.
In-Beam γ -Ray Spectroscopy of Neutron-Rich Nuclei through Deep Inelastic Scattering
Fall Meeting of the Physical Society of Japan in Fukuoka (Oct. 8, 1996)

Kidera, M., Oshima, M., Hatsukawa, Y., Furutaka, K., Hayakawa, T. and Gono, Y.
Multiple Coulomb Excitation of ^{155}Gd
Spring meeting of Japan Physical Society of Japan (Nagoya, March 29, 1996)

Komatsubara, T., Lu, J., Hayakawa, T., Saitoh, T., Hashimoto, N., Takahashi, H., Uchiyama, K., Furuno, K., Mukai, J., Oshima, M., Kidera, M., Furutaka, K., Hatsukawa, Y., Ishii, T., Matsuda, M. and Mitarai, S.
Nuclear structure of the odd-odd Nucleus ^{126}Cs
Spring meeting of the Physical Society of Japan, April 2, 1996,

Komatsubara, T., Hashimoto, N., Saitoh, T., Lu, J., Hayalawa, T., Takahasi, H., Uchiyama, K., Furuno, K., Mukai, J., Oshima, M., Kidera, M., Furutaka, K., Hatsukawa, Y., Ishii, T. and Matsuda, M.
M1 bands in nuclei with the mass number around A=130.
Joint symposium on "Nuclear Physics in 21th century opened up by means of γ -ray

spectroscopy", December 25-26, 1996.

Nagame, Y., Nishinaka, I., Tsukada, K., Oura, Y., Ichikawa, S., Ikezone, H.,
Zhao, Y. L., Sueki, K., Nakahara, H., Tanikawa, M., Ohtsuki, T., Kudo, H.,
Hamajima, Y., Takamiya, K. and Chung, Y. H.
Bimodal Nature in Low Energy Fission of Light Actinides
4th International Conference on Nuclear and Radiochemistry, St. Malo, France (Sep. 8, 1996)

Nagame, Y., Nishinaka, I., Tsukada, K., Oura, Y., Ichikawa, S., Ikezoe, H.,
Zhao, Y. L., Sueki, K., Nakahara, H., Tanikawa, M., Ohtsuki, T., Kudo, H.,
Hamajima, Y., Takamiya, K. Nakanishi, K., Inoue, T., Baba, H. and Chung, Y. H.
Correlation between Mass Division Modes and Two Deformation Paths in Low Energy
Fission of Actinides
The 40th Symposium on Radiochemistry, Wako (Oct. 22, 1996)

Nakanishi, K., Takamiya, K., Inoue, T., Yokoyama, A., Saito, T., Baba, H.,
Nishinaka, I., Tsukada, K., Oura, Y., Nagame, Y., Zhao, Y. L. and Tanikawa, M.
Study of Proton Induced Fission of ^{238}U by Counter Method
The 40th Symposium on Radiochemistry, Wako (Oct. 24, 1996)

Ohyama, T., Zhao, Y. L., Sueki, K., Nakahara, H., Tsukada, K., Ichikawa, S.,
Oura, Y., Hatsukawa, Y., Hata, K., Nishinaka, I., Nagame, Y., Asai, M.,
Hirose, T., Kojima, Y., Yamamoto, H. and Kawade, K.
Search for New Actinide Isotopes using the Gas-jet coupled JAERI-ISOL
The 40th Symposium on Radiochemistry (Oct. 23, 1996)

Oshima, M.
Coulomb excitation of ^{155}Gd
The Joint Symposium on Nuclear Physics in the 21st Century opened by Gamma-ray spectroscopy
(Saitama, December 25th, 1996).

Oshima M., Hayakawa, T., Hatsukawa, Y., Frutaka, K., Katakura, J., Matsuda, M.,
Iimura, H., Kidera, M., Kusakari, H., Sugawara, M. and Shizuma, T.
Interpretation of Anomalous Coulomb excitation of ^{155}Gd
Spring meeting of Japan Physical Society of Japan (Nagoya, March 29, 1996)

Oura, Y., Tsukada, K., Hatsukawa, Y., Ohyama, T., Zhao, Y. L., Sueki, K., Shinohara,
N., Nishinaka, I., Hata, K., Nagame, Y. and Ichikawa, S.
Radiochemical Identification of ^{236}Am
The 40th Symposium on Radiochemistry, Wako (Oct. 24, 1996)

T., Saitoh, T., Hashimoto, N., Komatsubara, T., Lu, J., Hayakawa, N., Takahasi,
H., Ushiyama, K., Furuno, K., Mukai, J., Oshima, M., Kidera, M., Furutaka, K

K., Hatsukawa, Y., Ishii, T., Matsuda, M. and Mitarai, S.
The measurement of internal-conversion electrons and the shape coexistence in ^{193}Tl.
Spring meeting of the Physical Society of Japan, April 2, 1996,

Sugawara, M., Kusakari, H., Igari, Y., Terui, K., Myojin, K., Nishimiya, D.,
Mitarai, S., Oshima, M., Hayakawa, T., Kidera, M., Furutaka, K. and Hatsukawa, Y.
Study on the nuclear structure of ^{142}Gd by using the GENKEN-TSUKUBA ball
Fall Meeting of the Physical Society of Japan in Saga (Oct. 8, 1996)

Sugawara, M., Kusakari, H., Igari, Y., Terui, K., Myojin, K., Nishimiya, D.,
Mitarai, S., Oshima, M., Hayakawa, T., Kidera, M., Furutaka, K. and Hatsukawa, Y.
M1 Bands in ^{142,143}Gd
Riken Joint Symposium on "Nuclear physics in the 21st century through γ-ray spectroscopy"
(Dec. 25, 1996)

Sugawara, M., Kusakari, H., Igari, Y., Terui, K., Myojin, K., Nishimiya, D.,
Mitarai, S., Oshima, M., Hayakawa, T., Kidera, M., Furutaka, K. and Hatsukawa, Y.
Nuclear structure of ^{143}Gd
Spring Meeting of the Physical Society of Japan in Nagoya (March 29, 1997)

Zhao, Y. L., Sueki, K., Nakahara, H., Nagame, Y., Nishinaka, I., Tsukada, K. and Tanikawa, M.
Complete and Incomplete Fusion Fission at the Energy Range Near and Sub Coulomb Barrir
The 40th Symposium on Radiochemistry, Wako (Oct. 22, 1996)

NUCLEAR REACTIONS
Journal/Proceedings

Futami, Y., Yuasa-Nakagawa, K., Nakagawa, T., Lee, S. M., Furutaka, K., Matsuda, K., Yoshida, K., Jeong, S. C., Fujiwara, H., Mizota, T., Honjo, Y., Tomita, S., Heusch, B., Ieki, K., Kasagi, J., Shen, W. Q. and Matsuse, T.
Decay Mechanism of a Highly Excited Nucleus Produced in the Reaction $^{84}Kr+^{27}Al$ at 10.6 MeV/nucleon
Nucl. Phys. **A607**(1996)85-104

Hamada, S., Yasue, M., Kubono, s., Tanaka, M. H. and Peterson, R. J.
Cluster structures in 10Be from the $^{7}Li(\alpha,p)^{10}Be$ reaction.
Phys. Rev. **C49**(1994)

Ikezoe, H., Ikuta, I., Mitsuoka, S., Hamada, S., Nagame, Y., Nishinaka, I., Tsukada, Y., Oura, Y. and Ohtsuki, T.
The Feature of the JAERI Recoil Mass Separator.
Nucl. Instr. & Meth. **B125**(1997)1.

Ikezoe, H., Ikuta, I., Mitsuoka, S., Hamada, S., Nagame, Y., Nishinaka, I., Tsukada, Y., Oura, Y. and Ohtsuki, T.
14th International Conference on the Application of Accelerators in Research and Industry Nov. 6-9, 1996, Denton, Texas, USA.

Mitsuoka, S., Ikezoe, H., Ikuta, T., Nagame, Y., Tsukada, K., Nishinaka, I., Oura, Y., and Zhao, Y. L.,
α -decay properties of the New Neutron Deficient Isotope ^{212}Pa
Phys. Rev. **C55**(1997)1555.

Sugiyama, Y., Tomita, Y., Yamanouti, Y., Hamada, S., Ikuta, T., Fujita, H. and Napoli, D. R.
Elastic Two-Neutron Transfer Reactions of $^{58}Ni+^{60}Ni$ and $^{62}Ni+^{64}Ni$ around the Coulomb Barrier.
Phys. Rev. **C55**(1997)5R.

Sugiyama, Y.
Elastic and Inelastic Scattering in Heavy-Ion Collisions around the Coulpmb Barrier Proc. Intern. workshop on Physics with Recoil Separators and Detector Arrays, New Delhi, India, 1995, p3-11

Sugiyama, Y.
New approach to resonance spin determinations
Proc. to Joint Japan-U. S. Seminar on Clustering Phenomena in Nuclear and

Mesoscopic Systems, Honolulu, Hawaii, 1996

Yoshioka, S., Watanabe, Y., Harada, M., Sato, K., Nakao, Y., Ijiri, H., Chiba, S., Fukahori, T., Meigo, S., Iwamoto, M. and Koori, N.
A Consistent Analysis of (P, P') and (n,n') Reactions using the Feshbach-Kerman-Koonin Model
Proc. of the 1996 Symp. on Nuclear Data, Nov. 21-22, 1996,
JAERI, Tokai, JAERI-Conf 97-005(1997), pp.301.

Meetings

Hamada, S., Sugiyama, K., Ikuta, T., Yamasaki, A.
On the cluster structure studied by ^{6}Li induced transfer reaction on ^{9}Be nuclei.
Similarities and Differences between Atomic-Nuclri and-Clusters, University of Tsukuba, Jul. 1-4. 1997.

Ideno, K., Hamada, S., Sugiyama, Y., Yamanouchi, Y., Ikezoe, H. and Tomita, Y.
Search for Collective States of ^{12}C from the 100MeV ^{16}O + ^{12}C Reaction
Annual Meeting of the Physical Society of Japan in Kanazawa (April 1, 1996)

Mitsuoka, S., Ikezoe, H., Ikuta, T., Nagame, Y., Tsukada, K., Nishinaka, I., Oura, Y., and Zhao, Y. L.,
α -decay properties of the New Neutron Deficient Isotope ^{212}Pa
Spring Meeting of Physical Society of Japan in Nagoya (Mar. 28, 1997)

Nishinaka, I., Nagame, Y., Tsukada, Y., Oura, K., Ichikawa, S., Ikezoe, H., Zhao, Y., Sueki, K., Nakahara, H., Tanikawa, M.
Correlation between Mass Division Modes and Neutron Multiplicity in Fission of Actinides.
The 40th Symposium on Radiochemistry, RIKEN (Oct., 22-24, 1996).

Sugiyama, Y., Tomita, Y., Yamanouti, Y., Hamada, S., Ikuta, T., Ideno, K., Ikezoe, H. and Fujita, H.
Elastic Two-Neutron Transfer Reactions of 58Ni+60Ni and 62 Ni+64Ni around the Coulomb Barrier.
Annual Meeting of the Physical Society of Japan in Kanazawa (April 1, 1996)

Sugiyama, Y.
Elastic two-nuetron transfer reactions around the Coulomb barrier
Intrn. Conference on "Nuclear Dynamics at Long and Short Distances", Angra dos Reis, Brazil, (Apr. 8-12, 1996)

Sugiyama, Y., Tomita, Yamanouti, Y., Hamada, S., Ikuta, T., Ideno, K., Ikezoe, H., Fujita, H. and Kondo, Y.

Airy Oscillation observed in Excitatio Function at $q_{cm}=90^{\circ}$ for $^{16}O+^{16}O$ Elastic Scattering
Fall Meeting of the Physical Society of Japan in Saga (October 6, 1996)

Sugiyama, Y., Tomita, Y., Yamanouti, Y., Hamada, S., Ikuta, T. and Yamazaki, A.
Elastic two-neutron transfer reactions in $^{58}Ni+^{60}Ni$ and $^{62}Ni+^{64}Ni$ around the Coulomb barrier
Intern. Workshop on Heavy-Ion Collisions at Near-Barrier Energies, South Durras, Australlia, (March 20, 1997)

Sugiyama, Y., Tomita, Y., Yamanouti, Y., Hamada, S., Ikuta, T., Fujita, H. and Yamazaki, A.
Elastic Two-Neutron Transfer Reaction of $^{58}Ni+^{60}Ni$ and $^{62}Ni+^{64}Ni$ around the Coulomb Barrier and Nuclear Josephson Effect
Annual Meeting of the Physical Society of Japan in Nagoya (March 28,1997)

Yamanouchi, Y., Sugiyama, Y., Ideno, K. and Tomita, Y.
$^{50}Ti(^{12}C, ^{12}C')$ Reaction at E=115MeV
Annual Meeting of the Physical Society of Japan in Kanazawa (April 1, 1996)

Yamanouchi, Y., Sugiyama, Y., Ideno, K. and Tomita, Y.
Isospin character of transitions to the excited states of intermediate unclei
Fall Meeting of the Physical Society of Japan in Saga (October 6, 1996)

Yoshioka, S., Watanabe, Y., Harada, M., Sato, K., Nakao, Y., Ijiri, H., Chiba, S., Fukahori, T., Meigo, S., Iwamoto, M. and Koori, N.
A Consistent Analysis of (p, p') and (n, n') Reactions using the Feshbach-Kerman- Koonin Model
The 1996 Nuclear Data Symposium, JAERI, Tokai, Ibaraki (Nov. 21-22, 1996)

Watanabe, Y., Yoshioka, S., Harada, M., Sato, K., Nakao, Y., Ijiri, H., Chiba, S., Fukahori, T., Meigo, S., Iwamoto, M. and Koori, N.
Measurement of Continuum Spectra of (p, p') Scattering at 14.1 and 26 MeV
The 52nd Annual Meeting of the Physical Society of Japan, Meijo University, Nagoya (Mar. 28-31, 1997)

NUCLEAR THEORY

Journal/Proceedings

Chiba, S., Iwamoto, O., Fukahori, T., Niita, K., Maruyama, Toshiki, Maruyama, Tomoyuki and Iwamoto, A.
Analysis of Proton-Induced Fragment Production Cross Sections by the Quantum Molecular
Dynamics Plus Statistical Decay Model
Phys. Rev **C54**(1996)285-290.

Iwamoto A., M6ller, P., Nix, J. R., and Sagawa, H.
Collisions of Deformed Nuclei and Superheavy-Element Production
Proc. 2nd Japan-Italy Joint Symp "Perspectives in Heavy Ion Physics", World Scientific(1996)88-102.

Maruyama, Tomoyuki, Niita, K., Maruyama, Toshiki, Chiba, S., Nakahara, Y., and Iwamoto, A.,
Relativistic Effects in the Transverse Flow in the Molecular Dynamics Framework
Prog. Theor. Phys. **96**(1996)263-268.

Iwamoto, A. and Moeller, P.
Nuclear Deformation and Sub-Barrier Fusion Cross Sections
Nucl. Phys. **A605**(1996)334-358.

Bonasera, A. and Iwamoto, A.
Spontaneous Fission: A Kinematic Approach
Phys. Rev. Lett. **78**(1997)187-190

Maruyama, Toshiki, Niita, K. and Iwamoto. A.
Extended QMD and Low Energy Heavy-Ion Reactions
Proc. Second. Int. Symp. "Heavy Ion Physics and Its Applications", World Scientific(1997)141-150.

Sugita, M., Otsuka, T., and von Brentano, P.
E1 Transitions in Rare Earth Nuclei and the SPDF Boson Model
Phys. Lett. **B389**(1996)642-648

Sugita, M.
Applications of IBM-3 to the Z～N～40 Nuclei
Phys. Lett. **B394**(1997)235-241

Meetings

Nitta, K., Maruyama, Tomoyuki, Oyamatsu, K., Maruyama, Toshiki and Iwamoto, A.
Sub-Saturated Nuclear-Matter in the QMD Simuration and Application to the Astrophysics
Spring Meeting of the Physical Society of Japan, Kanazawa (Apr. 1, 1996)

Bonasera, A. and Iwamoto, A.
Many-body Approach to the Spontaneous Fission
Spring Meeting of the Physical Society of Japan, Kanazawa (Apr. 1, 1996)

Iwamoto, A., Maruyama, Toshiki., Maruyama, Tomoyuki. and Niita, K.
Multi-Fragmentation in Au + Au Collisions
Spring Meeting of the Physical Society of Japan, Kanazawa (Apr. 2, 1996)

Maruyama, Tomoyuki., Niita, K., Chiba, S., Maruyama, Toshiki. and Iwamoto, A.
Photo-Meson Production in the QMD Simulation
Spring Meeting of the Physical Society of Japan, Kanazawa (Apr. 2, 1996)

Iwamoto, A. and Moeller, P.
Barrier Distributions and Nuclear Deformation in Subbarrier Fusion
Fall Meeting of the Physical Society of Japan, Saga (Oct. 7, 1996)

Maruyama, Toshiki., Nitta, K., Maruyama, Tomoyuki. and Iwamoto, A.
Multifragmentation in Au + Au Scattering
Fall Meeting of the Physical Society of Japan, Saga (Oct. 7, 1996)

Nitta, K., Maruyama, Tomoyuki., Maruyama, Toshiki. and Iwamoto, A.
Study on the Subbarier Fusion between Neutron Rich Nucleus and Stable Nucleus by Using QMD
Fall Meeting of the Physical Society of Japan, Saga (Oct. 7, 1996)

Maruyama, Tomoyuki., Niita, K., Chiba, S., Maruyama, Toshiki. and Iwamoto, A.
Study on Photo Nuclear Reaction by Using QMD
Fall Meeting of the Physical Society of Japan, Saga (Oct. 7, 1996)

Maruyama, Tomoyuki., Niita, K., Chiba, S., Otsuka, N., Maruyama, Toshiki. and Iwamoto, A.
Analysis of the Quasi Free Peak in (p, p) and (p, n) Reactions by Using QMD
Fall Meeting of the Physical Society of Japan, Saga (Oct. 7, 1996)

Iwamoto, A.
Spontaneous Fission: A Kinetic Approach Int. Symp. on Large Scale Collective Motion of Atomic

Nuclei, Brolo (Oct. 17, 1996)

Iwamoto, A.
Spontaneous Fission: A Many-Body Approach
Frontier in Nuclear Fission Research, Kumatori (Oct. 29, 1996)

Iwamoto, A.
Vlasov Approach to the Spontaneous Fission of Heavy Nuclei
1996 Konan Workshop on Nuclear Physics, Kobe (Dec. 9, 1996)

Iwamoto, A.
Tunneling in Many-Body System-Spontaneous Fission
2'nd Symp. of the Advanced Science Research Center, Tokyo (Mar. 18, 1997)

Iwamoto, A.
Hugging Fusion and Related Topics
Scientific Meeting on the Fusion-Fission of Heavy Elements, Tokai (Mar. 24, 1997)

Maruyama, Toshiki., Oyamatsu, K., Niita, K., Maruyama, Tomoyuki. and Iwamoto A.
Study on the Properties of Nuclear Matter and Its Shape Change in Subsaturation
Density by Using QMD Model
Spring Meeting of the Physical Society of Japan, Nagoya (Mar. 29, 1997)

Sugita, M., Otsuka, T., and von Brentano, P.
The spdf Boson Model and E1 Transitions
Annual Meeting of the Physical Society of Japan in Kanazawa(Apr. 1. 1996)

Sugita, M.
Applications of IBM-3 to N～Z～40 Nuclei
International Workshop on Spectrum Generating Algebras and Dynamical Symmetries,
Trento, Italy (Jul. 22-Aug. 2 1996)

Sugita, M.
Applications of the O(18) Limit of the IBM-3 to the Z～N～40 Nuclei
9th International Symposium on Capture gamma Ray Spectroscopy, (Oct. 2-8, 1997)

ATOMIC PHYSICS, SOLID STATE PHYSICS AND RADIATION EFFECTS OF MATERIALS

Journal/Proceedings

Harada K., Kasai, H., Kamimura, O., Matsuda, T., Tonomura, A., Okayasu, S. and Kazumata, Y.
Obervation of Dynamic Flux-Line Relaxation in Ion-Irradiated $Bi_2Sr_2CaCu_2Ox$
Phys. Rev. **B53**(1996)9400

Ishikawa, N., Chimi, Y., Iwase, A., Maeta, H., Tsuru, K. and Michikami, O.
Irradiation Effects on c-axis Lattice Parameter in $EuBa_2Cu_3Oy$ Irradiated with Energetic Ions
Proc. 7th Int. Symp. on Advanced Nuclear Energy Research Recent Progress in Accelerator Beam Application (Mar. 18-20, 1996, Takasaki, Japan)406.

Iwase, A.
Defect Production and Annihilation in Metals through Electronic Excitation by Energetic Heavy Ion Bombardment
Proc. 7th Int. Symp. on Advanced Nuclear Energy Research Recent Progress in Accelerator Beam Application (Mar. 18-20, 1996, Takasaki, Japan)109.

Kazumata, Y., Gao, X., Kumakura, H. and Togano, K.
Effect of 230 MeV Au14+ Irradiation on $Bi_2Sr_2CaCu_2Ox$
Surface & Coatings Technology **84**(1996)348

Kazumata, Y., Kumakura, H. and Togano, K.
Vortex Pinning in $Bi_2Sr_2CaCu_2Ox$ Tapes Irradiated by Ions
Phys. Rev. **B54**(1996)16206

S. Okatasu and Y. Kazumata
Effective Activation Energy of 16MeV Proton Irradiated QMG-YBCO
Czech. J. Phys., **43**,(1996)1645

Suzuki, T., Mori, C., Yanagida, K., Uritani, A., Miyahara, H., Yoshida, M. and Takahashi, F.
Characteristics and Correction of the Fading of Imaging Plate
J. Nucl. Sci. Technol., **34**(1997)461-465.

Tolstikhina, I. Yu, Tawara, H., Safronova, U. I., Imai, M., Sataka, M., Kawatsura, K., Komaki, K. and Yamazaki, Y.
Coster-Kroning Electron Spectra from the Singlet and Triplet $1s^2$ 2pnl(n=9-20) States
Physica Scripta **54** (1996) 88

Terai, T. and Ito, Y.
Enhancement in Critical Current Density of High-Tc Superconductor $Bi_2Sr_2CaCu_2O7$-y by Particle Beam Irradiation
Material Chemistry in Nuclear Environment(1996)829.

Meetings

Chimi, Y., Ishikawa, N. and Iwase, A.
Effect of High Energy Heavy Ion Irradiation in Iron
1996 Fall Meeting of the Physical Society of Japan in Yamaguchi (Oct. 3, 1996)

Fukuda K., Kashimura S., Ohmichi T. and Muromura T.
Radiation Effects of Ceramic Oxides Bombarded with Heavy Ions
Atomic Energy Society of Japan, Fall Meeting in Tohoku University, Sept. 23, 1996

Hada, T., Aoki, S., Nakamura, M., Matsuda, S., Hirao, T., Nashiyama, I.,
Hirose, T., Ohira, H., Nagai, Y.
Single Event Burnout by Incident of High-Energy Ions.
The Fifth TIARA Research Reviw Meeting (June 24-25, 1996)

Hada, T., Aoki, S., Nakamura, M., Matsuda, S., Hirao, T., Nashiyama, I.,
Hirose, T., Ohira, H., Nagai, Y.
Use of TANDEM Accelerator for the Study of Single Event Burn-out.
The Ninth TADEM Research Review Meeting (July 4-5, 1996)

Hayashi, K., Kikuchi, H. and Fukuda, K.
Radiation damage of UO_2 by high-energy heavy ions
Intern. Workshop on Interfacial Effects in Quantum Engineering Systems, IEQES-96 (August 21-23, 1996, Mito, Japan) PB-01.

Hayashi, K.
Radiation damage of UO_2 by heavy ions with energies around 100 MeV Symposium on Electron Excitation Effects and Low Temperature Properties in Solids
Irradiated with Energetic Particles (Nov. 7-8, 1996, JAERI-Tokai, Japan)

Imai, M., Sataka, M., Yamazaki, Y., Komaki, K., Kawatusra, K. and Kanai, Y.
Electron Spectra from Highly Excited Si Ions
8Th Int. Conf. on the Physics of Highly Charged Ions (Omiya, Japan)

Ishikawa, N.
Defect Production by Low-Temperature Irradiation in High-Tc Superconductors
Fall Meeting of the Physical Society of Japan in Yamaguchi (Oct. 3, 1997)

Ishikawa, N., Chimi, Y., Iwase, A., Maeta, H., Tsuru, K., Michikami, O.,
Kambara, T., Mitamura, T., Awaya, Y. and Terasawa, M.
Velocity Effects on Defect Production in Ion-Irradiate High-Tc Superconductors
Spring Meeting of the Physical Society of Japan in Nagoya (Mar. 29, 1997)

Iwase, A., Iwata, T., Ishikawa, N. and Chimi, Y.
Heavy-Ion Irradiation Effects in Metals and High-Tc Superconductors
13th RIKEN Symp. on Atomic Physics Using Accelerators -Heavy-Ion Irradiation Eff ects- (Nov. 27, 1996)

Iwase, A., Iwata, T., Ishikawa, N. and Chimi, Y.
Heavy-Ion Irradiation Effects in Metals and High-Tc Superconductors
13th RIKEN Symp. on Atomic Physics Using Accelerators -Heavy-Ion Irradiation Eff ects- (Nov. 27, 1996)

Kawatusra, K., Sataka, M., Imai, M., Yamazaki, Y., Komaki, K., Kanai, Y.,
Kuroki, K. and Stolterfoht, N.
Low Energy Projectile Rydberg Electron Spectra from 2MeV/u Sq+ -He, C Collisions
using Zero-degree Electron Spectroscopy
6th Workshop on Fast Ion-Atom Collisions

Kato, T., Maeta, H., Ohtsuka, H., Matsumoto, N., Yuya, H. and Sugai, H.
X-ray Diffraction Cryostat for Heavy Ion Irradiation
Fall Meeting of Cryogenics Engineering in Osaka (Nov, 8, 1997)

Matsumoto, N., Ohtsuka, H., Maeta, H., Sugai, H., Saotome, T., Kato, T., Yuya H. and
Motohashi, H.
X-ray Diffuse Scattering from Radiation Defects in FCC Metals Fall Meetings of
Japan Physical Society in Yamaguchi (April, 3, 1997)

Matsumoto, A., Pesce, A., Aoki, S., Hada, T., Nemoto, N., Akutsu, T. and Matsuda, S.
Comparison of BBSEM & Heavy Ion SEU Test on NASDA's 64kbit SRAMs.
NSREC (July 15-19, 1996)

Matsumoto, A., Pesce, A., Aoki, S., Hasa, T., Nemoto, N., Akutsu, T. and Matsuda, S.
Comparison of Beam Blanking SEM and Heavy Ion SEU Tests on NASDA's 64kbit SRAMs.
The Institute of Electronics, Information and Communication Engineering
(Dec. 13, 1996)

Nakamura, M., Kimoto, Y., Ohira, H. and Matsuda, S.
The Evaluation of PMOS Dosimeter (2)
The Institute of Electronics, Information and Communication Engineering
(Sep. 27, 1996)

Nemoto, N., Matsuzaki, K., Naito, I., Akutsu, T., Ito, H., Matsuda, S. and Nashiyama, I.
An Evaluation of Single-Event Tolerance on Commercial Devices.
The Institute of Electronics, Information and Communication Engineering (Oct. 17-18, 1996)

Ohtsuka, H., Maeta, H., Matsumoto, N., Sugai, H., Saotome, T., Kato, T., Yuya, H. and Motohashi, H.
X-ray Diffuse Scattering Study of Defect Aggromerates in Heavy Ion-irradiated Copper
The 10th Japan Synchrotron Radiation Meeting In Tokyo (January, 10, 1997)

Ohtsuka, H., Maeta, H., Matsumoto, N., Sugai, H., Saotome, T., Kato, T., Yuya, H. and Motohashi, H.
X-ray Diffuse Scattering Study of Defect in Heavy Ion-irradiated Copper
Spring Meetings of Japan Physical Society in Nagoya (March, 28, 1997)

Okayasu, S., Kazumata, Y. and Houjou, K.
Change of Pinning Properties on High-Tc Superconductors with Proton Irradiation
1996 JPS Fall Meeting in Yamaguchi (Oct. 3rd, 1996)

Okayasu, S. and Kazumata, Y.
Proton Irradiation Effects on Effective Activation Energies of QMG-YBCO
9th International Symposium on Superconductivity (Oct. 23, 1996)

Shindo, H., Nemoto, N., Matsuzaki, K., Matsuda, S., Baba, S. and Hirose, T.
Verification of the Efficacy of IDDQ Test as the Estimation Method for Space Application.
The Institute of Electronics, Information and Communication Engineering (Mar. 14, 1997)

Sasaki, Y. and Huang, D.X.
Columnar Defects Produced with B 11MeV Irradiation in $Bi_2Sr_2CaCu_2Ox$ Single Crystal
Meeting on Superconductivity (Japan Atomic Energy Reserch Institute) January 1997

Sasaki, Y., Huang, D.X., Ikuhara, Y. and Houjou, K.
Structures of irradiation defects and the effects on the magnetic property in Bi-2212 superconductor irradiated with high energy ions
Annual Meeting of The Ceramic Society of Japan, March 1997

Sasase, M., Okayasu, S. and Hojou, K.
Effects of Au^{24+} Ion Irradiation on the Superconductivity Properties and Microstructure of EBCO Thin Films.
Asian Science Seminar, Kyushu (March 18, 1997)

Sasase, M., Okayasu, S. and Hojou, K.
Effects of Au^{24+} Ion Irradiation on the Superconductivity Properties and Microstructure of EBCO Thin Films.
Spring Meeting of the Japan Society of Applied Physics, Chiba (March, 30, 1997)

Sataka, M., Imai, M., Yamazaki, Y., Komaki, K., Kanai, Y., Kawatusra, K., Tawara, H., Schltz, D.R. and Reinhold, C.O.
Binary Peak Electrons Observed at O Degree for 0.5-1.0 MeV/u Agq+ and Au8+ Ions in the Collision with a He Target
8Th Int. Conf. on the Physics of Highly Charged Ions (Omiya, Japan)

M., Sataka, M., Kitazawa, S., Komaki, K., Yamazaki, Y., Azuma, T., Shibata, H., Kawatusra, K., Kanai, Y. and Tawara, H.
Differential Cross Section Measurements in the Collisions of Fast Hydrogen Ions and Rare-gas Targets
Fall Meeting of the Physical Society of Japan in Yamaguchi (Octorber, 1996)

Sato, T, Ootsuki, T., Sugai, Maeta, H., Matsumoto, N. Otsuka, H. Iwashita, K. Saotome, T. Haruna, K., Ohhasi, and Ono, F.
Effect of Heavy Ion Irradiation on Electrical Conductivity In B-doped Synthetic Diamond 10th Diamond Symposium in Tokyo (Dec. 2, 1996)

Saotome, T., Maeta, H. Haruna, K., Ohhashi, K. and Ono, F.
Thermal Expansion Coefficient of Ⅱ b Diamond Sigle Crystal at Low Temperature
International Workshop on Hard Electronics in Tsukuba (Feb. 17, 1997)

Sekioka, T., Terasawa, M., Sataka, M., and Kitazawa, S.
Emission of Secondary Ions from a Foil Bombarded with Heavy Ions
Eighth International Conference on the Physics of Highly Charged Ions, Omiya, Saitama, September 23-26 (1996)
Th56 (Sep. 26, 1996)

Sekioka, T., Terasawa, M., Sataka, M., and Kitazawa, S.
Sputtering process in the irradiation of high energy heavy ions
Fall meeting of the Physical society of Japan in Yamaguchi (Oct. 2, 1996)

Sugai, H., Maeta, H., Ohtsuka, H., Matumoto, N., Haruna, K. and Ono, F.
In-situ Measurement of Resistivity of Silicon Semiconductor

Irradiated with Heavy Ions at Low Temperatures
Fall Meeting of the Physical Society of Japan in Yamaguchi (Oct. 2, 1996).

Suzuki, T., Sakai,H., Uritani, A., Mori, C., Yoshida, M., Takahashi, F. and Takahashi, K.
Luminescence Characteristics of Imaging Plate with Heavy Charged Particle
The 33rd Annual Meeting on Radioisotopes in the Physical Sciences and Industries in Tokyo (Jul. 2, 1996)

Suzuki, T., Mori, C., Yoshida, M. and Takahashi, F.
Improvement of Precision in Quantitative Measurement of Radioactivity with Imaging Plate
Annual Meeting of the Atomic Energy Society of Japan in Tokyo (Mar. 26, 1997)

Suzuki, T., Mori, C., Miyahara, H., Uritani, A., Yoshida, M. and Takahashi, F.
Improvement of Precision in Quantitative Measurement of Radioactivity with Imaging Plate
International Committee for Radionuclide Metrology 1997 in Gaithersburg MD USA (May 19, 1997)

Takumi, K., Takase, A., Kuribayashi, M., Kanamaru, T., Katoh, H. and Ishida, K.
X-ray diffraction of nearly perfect crystals whose distortion is given by function of depth
Annu. Meeting of the Physical Society of Japan in Yamaguchi (Oct. 4, 1996)

Terai, T., Ito, Y., Kisio, K., Simoyama, J., Okayasu, S., and Kazumata, Y.
Effect of High-Energy Heavy-Ion Irradiation on the Critical Current Dendity of Bi-2212 Single Crystals
International Symposium on Superconductors 96 (Oct 1996) Japan

Terai, T.
Enhancement in Critical Current Density of High-Tc Superconductor $Bi_{22}Sr_2CaCu_2O7$-Y by Particle Beam Irradiation
International Workshop on Critical Currents in Superconductors for Practical Aplications. (Mar. 6. 1997) China

Terai, T., Kobayashi, T., Y., Kisio, K., Simoyama, J., Okayasu, S., and Kazumata, Y.
Effect of High-Energy Heavy-Ion Irradiation on the Crytical Current Density of Bi-2212 Single Crystals
Materials & Mechanisms of Superconducstivity High-Temperature Superconductors. (Feb. 28, 1997) China

7. Personnel and Commitees

(1) Personeel (FY 1996)

Department of Reactor Engineering

	Yoshio Murao	Director
	Hiroshi Maekawa	Deputy Director
	Takashi Okabe	Administrative Manager

Accelerators Division

Scientific Staff	Tadashi Yoshida*
	Suehiro Takeuch
	Susumu Hanashima
	Makoto Matsuda

Technical Staff

Susumu Kanda
Isao Ohuchi
Tokio Shoji
Katsuzo Horie
Yoshihiro Tsukihashi
Shinichi Abe
Shuhei Kanazawa
Nobuhiro Ishizaki
Hidekazu Tayama

Nuclear Data Center

Akira Hasegawa *
Satoshi Chiba
Tokio Fukahori
Osamu Iwamoto

Fusion Neutronics Laboratory

Yujiro Ikeda*
Yoshitomo Uno
Yoshimi Kasugai

Advanced Science Research Center

Mitsuhiko Ishii

Research Group for Exotic Heavy Nuclei

Hiroshi Ikezoe*
Yasuharu Sugiyama
Masumi Ohshima

* Head

Yoshiaki Tomita
Kazumi Ideno
Yoshimaro Yamanouti
Michiaki Sugita
Tetsuro Ishii
Shingo Hamada
Tomohiko Ikuta
Kazuyoshi Furutaka
Takehito Hayakawa

Research Group for Hadron Transport Theory
Akira Iwamoto*
Yasuaki Nakahara
Toshiki Maruyama
Tomoyuki Maruyama

Research Group for Low-Temperature Radiation Effects
Akihiro Iwase*
Norito Ishikawa
Yasuhiro Chimi

Department of Health Physics
Radiation Control Division Ⅱ
Masayuki Ueno
Katsuya Kawasaki
Tohru Tayama

Radiation Dosimetry Laboratory
Makoto Yoshida
Fumiaki Takahashi

Department of Materials Science and Engineering
Material Innovation Laboratory
Kenji Noda*
Tetsuya Nakazawa
Daijyu Yamaki

Solid State Physics Laboratory
Kiichi Hojou*
Masao Sataka
Satoru Okayasu
Sin-iti Kitazawa

* Head or Leader

Neutron Scattering Laboratory
Hiroshi Tomimitsu
Kazuya Aizawa

Synchrotron Radiation and Solid States Laboratory
Hiroshi Maeta*
Hideo Ohtsuka
Norimasa Matsumoto
Teruo Kato

Fuel Irradiation and Analysis Laboratory
Kousaku Fukuda*
Satoru Kashimura
Kimio Hayashi
Hironobu Kikuchi
Toshiko Ohmichi

Department of Radioisotopes
Isotope Research and Development Division
Nobuo Shinohara
Yuichiro Nagame
Shin-ichi Ichikawa
Yuichi Hatsukawa
Kazuaki Tsukada
Hideki Iimura
Hiroyuki Sugai
Ichiro Nishinaka
Kentaro Hata

Department of High Temperature Engineering
Energy Materials Development Laboratory
Motokuni Eto*
Shintaro Ishiyama
Shin-ichi Baba
Hirokazu Ugachi
Masahiro Ishihara

* Head

(2) Tandem Steering Commitee

(Chirman)	Shinzo	Saito	(Deputy Director General, Tokai Research Establishment)
	Muneyuki	Date	(Director, Advanced Science Research Cen ter)
	Satoru	Funahashi	(Director, Department of Materials Science and Engineering)
	Yoshio	Murao	(Director, Department of Reactor Engineering)
	Michio	Hoshi	(Director, Department of Chemistry and Fuel Research)
	Hisamichi	Yamabayashi	(Director, Department of Radioisotopes)
(Secretary)	Tadashi	Yoshida	(Head, Accelerator Division)
(Secretary)	Tadashi	Okabe	(Administrative Manager, Department of Reac tor Engineering)

(3) Tandem Consultative Committee

(Chairman)	Michio	Ichikawa	(Director General, Tokai Research Establishment)
(Vice Chairman)	Shinzo	Saito	(Deputy Director General, Tokai Research Establishment)
(Vice Chairman)	Yoshio	Murao (Director, Department of Reactor Engineering)	
	Masaharu	Nakazawa	(Professor, University of Tokyo)
	Hiroyasu	Ejiri	(Professor, Osaka University)
	Naohiro	Hirakawa	(Professor, Tohoku University)
	Kenji	Katori	(Professor, Osaka University)
	Jun	Imasato	(Professor, National Laboratory for High Energy Physics)

Masayasu	Ishihara	(Professor, University of Tokyo, Research Scientist, Institute of Physical and Chemical Research)
Yasuo	Ito	(Associate professor, University of Tokyo)
Hisaaki	Kudo	(Associate professor, Niigata University)
Kohzoh	Masuda	(Professor emeritus, University of Tsukuba)
Shunpei	Morinobu	(Professor, Kyushu University)
Hiromichi	Nakahara	(Professor, Tokyo Metropolitan University)
Naoto	Sekimura	(Associate professor, The University of Tokyo)
Akito	Takahashi	(Professor, Osaka University)
Hiroyuki	Tawara	(Associate Professor, Institute of Plasma Physics, Nagoya University)
Hirosuke	Yagi	(Professor, University of Tsukuba)
Sadae	Yomaguchi	(Professor, The Research Institute for Iron Steel and Other Metals, Tohoku University)
Kenji	Morita	(Professor, Nagoya University)
Hiroshi	Maekawa	(Deputy Director, Deportment of Reactor Engineering)
Hiroshi	Ikezoe	(Head, Research Group for Exotic Heavy Nuclei, Advanced Science Research Center)
Akira	Iwamoto	(Head, Research Group for Hadron Transport Theory)
Akihiro	Iwase	(Head, Research Group for Low-Temperature Radiation Effects, Advanced Science Research Center)
Hiroshi	Maeta	(Head, Synchrotron Radiation and Solid State Labratory)

	Kenji	Noda	(Head, Material Innovation Laboratory, Depart ment of Materials Science and Engineering)
	Toshiaki	Sekine	(Department of Radioisotopes)
(Secretary)	Takashi	Okabe	(Adiministrative Manager, Depertment of Reactor Engineering)
(Secretary)	Suehiro	Takeuchi	(Department of Reactor Engineering)
(Secretary)	Tadashi	Yoshida	(Head, Accelerators Division)

8. Cooperative Researches

	Title	Contact person Organization
1.	Study of Unstable Nuclei Produced by Multi-Nucleon Transfer Reactions	Toru NOMURA Institute for Nuclear Study, University of Tokyo
2.	Atomic Collision Research Using Highly Charged Ions	Ken-Ichiro KOMAKI Institute of Physics, College of Arts and Sciences, University of Tokyo
3.	Electromagnetic Properties of Proton-rich Nuclei	Masao OGAWA Tokyo Institute of Technology
4.	Radiation Effects of High Tc Materials	Hiroaki KUMAKURA National Research Institute for Metals
5.	X-Ray Study of Irradiation Defects Caused by MeV Ion Implatation in Si Perfect Crystals.	Kohtaro ISHIDA Faculty of Science, Science University of Tokyo
6.	Study of Multipole Deformed State in Heavy Nuclei II	Hideshige KUSAKARI Faculty of Education, Chiba University
7.	Dependence of Bimodal Fission on Excitation Energy	Hiromichi NAKAHARA Faculty of Science, Tokyo Metropolitan University
8.	Study on Decay Properties of Heavy Nuclei Using JAERI Recoil Mass Separator	Jirota KASAGI Laboratory of Nuclear Science, Tohoku University
9.	Search for Large Nuclear Deformation near N=Z Region	Yasuyuki GONO Faculty of Science, Kyushu University
10.	Radiation Damage of Materials for Environment Resistance Devices	Kazutoshi OHASHI Faculty of Engineering, Tamagawa University

11. Study of Luminescence Characteristics of Photostimulable Phoser with Heavy Charged Particles	Chizuo MORI School of Engineering, Nagoya University
12. Study of Phase Trnasition on Nuclear Fission Phenomenon	Hiroshi BABA Faculty of Science, Osaka University
13. Study of Electromagnetic Properties of Nuclear High-Spin State through Crystal Ball	Kohei FURUNO Tandem Accelerator Center, Tsukuba University
14. Study of Single-Events Induced by High Energy Ions (I)	Sumio MATUDA NASDA
15. Study of Preequibrium Particle Emission in Proton-Induced Reactions	Yukinobu WATANABE Department of Energy Converion Engineering, Graduate School of Engineering Sciences, Kyushu University
16. Research of Coulomb Explosion by Heavy Ions Irradiation	Mititaka TERASAWA Faculty of Engineering, Himeji Institute of Technology
17. Study of the Property and Microstructure on the Oxide Superconductors Irradiated with High Energy Ions	Yukichi SASAKI Japan Fine Ceramics Center
18. Irradiation Effects of Oxide Superconductors	Takayuki TERAI Faculty of Engineering, University of Tokyo
19. α -cluster Structure in Heavy Nuclei	Takashi YAMAYA Faculty of Science Tohoku University

FACSIMILE FORM
(for the JAERI tandem & V.d.G annual report)

TO: Dr. S. TAKEUCHI FAX. +81 29 282 6321

Accelerators Division
Department of
Reactor Engineering
Phone: 029 282 5860

JAPAN ATOMIC ENERGY RESEARCH INSTITUTE
TOKAI RESEARCH ESTABLISHMENT
TOKAI, NAKA, IBARAKI 319-11 JAPAN

I would like to ask you;

☐ to add my name to the mailing list.
☐ to remove my name from the mailing list.
☐ to renew my mailing address.

NAME:_____

INSTITUTION:_____

_____

ADDRESS:_____

_____

_____

PHONE NO.:_____

FAX NO.: _____